Boston University

OpenBU **http://open.bu.edu**

Theses & Dissertations Boston University Theses & Dissertations

2016

Emissions from mobile sources: improved understanding of the drivers of emissions and their spatial patterns

https://hdl.handle.net/2144/14511

Boston University

Boston University

OpenBU **http://open.bu.edu**

Theses & Dissertations Boston University Theses & Dissertations

2016

Emissions from mobile sources: improved understanding of the drivers of emissions and their spatial patterns

https://hdl.handle.net/2144/14511

Boston University

BOSTON UNIVERSITY

GRADUATE SCHOOL OF ARTS AND SCIENCES

Dissertation

EMISSIONS FROM MOBILE SOURCES: IMPROVED UNDERSTANDING OF THE DRIVERS OF EMISSIONS AND THEIR SPATIAL PATTERNS

by

CONOR KENNEDY GATELY

B.A. Wesleyan University, 2002
M.A. Wesleyan University, 2005

Submitted in partial fulfillment of the
requirements for the degree of
Doctor of Philosophy
2016

© Copyright by
CONOR KENNEDY GATELY
2016

Approved by

First Reader _____

Ian Sue Wing, PhD

Associate Professor of Earth and Environment

Second Reader _____

Lucy R. Hutyra, PhD

Associate Professor of Earth and Environment

Third Reader _____

Anthony Janetos, PhD

Associate Professor of Earth and Environment

ACKNOWLEDGEMENTS

I am deeply grateful to the many, many people, without whom this dissertation would not have been possible. My greatest thanks goes to my mother and father, who have raised and guided and encouraged me for so many years, and from whom I still learn something new every day. I would like to thank my advisors Ian Sue Wing and Lucy Hutyra for the countless hours they have dedicated to answering my questions, untangling my confusion and pushing me to improve and explore my potential. The work that you have both put in to help mold me into the scientist and the person that I am today is immense, and I am honored and thankful to have had the opportunity to work under two amazing minds.

I would like to thank the many faculty members of the Earth and Environment Department who have helped shape my time here over the years, who have pondered ideas with me after seminars, shared insight from other fields, and expanded my horizons and curiosity. I owe much to Dana Bauer, who mentored and guided me through the challenging early years of this PhD, and who was always there to listen, encourage and support me and many of my fellow students throughout our time here. Robert, Nathan, Mark, Curtis; you are the names and faces that I will always associate with this fantastic department,

across all of the courses, seminars, coffee breaks and pub nights that have made my experience here more than just an academic one. I am honored to have been a part of this wonderful community.

I must also thank Scott Peterson, Chris Osgood, Nigel Jacob, Vineet Gupta, and the many people at the Boston Metropolitan Planning Office and at the City of Boston who have welcomed me into their world and helped me share and learn and contribute to the affairs of this great city.

I am grateful to the many members of my cohort who have made my time here intellectually stimulating, personally enriching, and most importantly, full to the brim with laughter. A special shout-out to Mike Mann, who kept me sane and well-fed for the first few years, and to Marta, Rachel and Val, who showed me the wisdom of strength in numbers. Thank you to everyone in the Hutyra lab who has helped push, pull and drag me to the finish line over this last year.

And of course, not a single day of this PhD would have ever been possible without the superhuman support of my wife Tricie. She makes everything a possibility, and all the good things a reality. Thanks love.

EMISSIONS FROM MOBILE SOURCES: IMPROVED UNDERSTANDING OF THE DRIVERS OF EMISSIONS AND THEIR SPATIAL PROXIES

(Order No.)

CONOR KENNEDY GATELY

Boston University Graduate School of Arts and Sciences, 2016

Major Professor: Ian Sue Wing, Associate Professor of Earth and Environment

ABSTRACT

Emissions of greenhouse gases from the combustion of fossil fuels, in particular carbon dioxide (CO_2), are a major contributor to global climate change. In the United States 28% of carbon dioxide emissions from fossil fuel combustion are produced by road vehicles. This dissertation reports the results of three studies that improve on our knowledge of the spatial and temporal distribution of vehicle CO_2 emissions in the U.S. over the last 35 years. Using bottom-up data assimilation techniques we produce several new high-resolution inventories of vehicle emissions, and use these new data products to analyze the relationships between emissions, population, employment, traffic congestion, and climate

change at multiple spatial and temporal scales across the U.S. We find that population density has a strong, non-linear effect on vehicle emissions, with increasing emissions in low density areas and decreasing emissions in high density areas. We identify large biases in estimates of vehicle CO_2 emissions by the most commonly used national and global inventories, and highlight the susceptibility of spatially-downscaled inventories to local biases in urban areas. We also quantify emissions of several air pollutants regulated by the U.S. Environment Protection Agency, including carbon monoxide, nitrogen oxides and particulate matter, at hourly and roadway scales for the metropolitan area surrounding Boston, MA. Emissions of these pollutants show high emissions gradients across identifiable spatial hotspots, considerable diurnal and seasonal variations, and a high sensitivity to the presence or absence of heavy-duty truck traffic. We also find that the impact of traffic congestion on air pollution emissions across the region is minimal as a share of the total emissions. We show that policies that combine a reduction in the number of vehicles on the road with a focus on improving traffic speeds have greater success in reducing emissions of air pollutants and greenhouse gases than policies that focus solely on improving traffic speeds. Finally, we estimate that regional emissions of carbon monoxide will increase by 3% in 2050, but with numerous localized increases of 25-50%,

due to an expected rise in mean regional temperatures due to global climate change.

TABLE OF CONTENTS

LIST OF TABLES

LIST OF FIGURES

LIST OF ABBREVIATIONS

AADT	Annualized Average Daily Traffic
CAFÉ	Corporate Average Fuel Economy
CDP	Census Designated Places
CV	Coefficient of Variation
DARTE	Database of Road Transportation Emissions
DEP	Department of Environmental Protection
DOE	Department of Energy
EC	European Commission
EDGAR	Emissions Database for Global Atmospheric Research
EIA	Energy Information Administration
EPA	Environmental Protection Agency
FHWA	Federal Highway Administration
FIPS	Federal Information Processing System
GAM	Generalized Additive Model
GHG	Greenhouse Gas
GIS	Geographic Information System
HPMS	Highway Performance Monitoring System
ISA	Impervious Surface Area

JRC	Joint Research Center
MGGEI	Massachusetts Greenhouse Gas Emissions Inventory
MOVES	Motor Vehicle Emissions Simulator
MPO	Metropolitan Planning Organization
MSA	Metropolitan Statistical Area
MSE	Mean Squared Error
NAD	North American Datum
NCD	National County Database
NEE	Net Ecosystem Exchange
NEI	National Emission Inventory
NRC	National Research Council
PTR	Permanent Traffic Recorder
RGGI	Regional Greenhouse Gas Initiative
SUV	Sport Utility Vehicle
TAZ	Traffic Analysis Zone
VIUS	Vehicle Information and Use Survey
VKT	Vehicle Kilometers Travelled
VMT	Vehicle Miles Travelled

CHAPTER 1 – INTRODUCTION

Emissions of greenhouse gases (GHGs) from the combustion of fossil fuels are a major contributor to global climate change (Solomon et al. 2008). In the United States, emissions of carbon dioxide (CO_2), the major greenhouse gas, comprised over 82% by mass of the total anthropogenic GHG emissions in 2013 (U.S. Environmental Protection Agency 2014a). The dominant sources of CO_2 emissions in the U.S. are coal- and natural gas-fired electric power generation, motor gasoline and diesel combustion for road, rail and air transport, and localized combustion of natural gas and heating oil for residential and commercial space heating (USEPA 2014a). Since 1997 the share of total U.S. carbon emissions from industrial activities has declined as the U.S. economy has shifted away from manufacturing towards a services-oriented economy (Energy Information Administration 2007). In recent years, the rapid domestic expansion of hydraulically fractured natural gas extraction has driven a shift in the fuel profile of electric power generation away from coal towards gas (Lu et al. 2012). The transportation sector has witnessed steady improvements in vehicle fuel economy since the implementation of the Corporate Average Fuel Economy

regulations in 1975 (U.S. Department of Energy 2011). However, while the market penetration of hybrid-electric and full-electric vehicles has progressed at modest rates since the late 1990s, the vast majority of on-road vehicles still consume motor gasoline or diesel fuel. Emissions of carbon dioxide from road vehicles currently account for over 28% of total U.S. CO_2 emissions, and present a major challenge to efforts to reduce greenhouse gas emissions in order to mitigate global climate change. U.S. on-road CO_2 emissions have increased by 16.4% since 1990, and as a share of total U.S. emissions has increased from 30.3% in 1990 to 32.8% in 2013 (USEPA 2014a).

Our understanding of the spatial and temporal patterns and trends of carbon emissions from the on-road sector have improved from early estimates conducted at the national and state levels. Early inventories of U.S. GHG emissions produced estimates of emissions that were aggregated to national scales. These emissions inventories used a bookkeeping approach that quantified the amounts of various fossil fuels consumed by the economy combined with emission factors based on the carbon content and combustion properties of the fuel (USEPA 2014a). While these methods produced relatively accurate estimates of aggregate emissions at the scale of the country as a whole, they did not offer

any insight into how emissions were distributed within the country, region or states. Subsequent efforts to quantify emissions at increasingly finer spatial resolution employed a variety of statistical techniques to combine higher resolution data on the distribution of sources and related spatial proxies (such as population or road density) in order to downscale aggregated emission estimates to gridded data products with resolutions of 50-100 square kilometers (Andres et al. 1996; Brenkert et al. 1998). More recent work has continued to improve the spatial resolution of emissions inventories to provide a basis for local and regional analysis of the underlying drivers of these emissions (Gurney et al. 2009, Gately et al. 2013, Asefi-Najafabady 2014).

Accurately quantifying the location and intensity of carbon emissions at fine spatial scales is also a prerequisite for the design and implementation of emissions mitigation policies, as well as for understanding the underlying drivers that shape patterns and trends in emissions. This dissertation reports the results of several research efforts that have provided substantial improvements to our knowledge and understanding of the processes that drive emissions of carbon dioxide and other GHG and non-GHG pollutants from the on-road sector in the United States. Using a variety of novel and existing datasets in conjunction

with newly developed data assimilation techniques, I have produced a collection of high-resolution, bottom-up inventories of vehicle greenhouse gas and air pollutant emissions. In Chapter 2, I develop a new inventory of Massachusetts on-road CO_2 emissions that spans 1980 through 2008 at a 1 kilometer resolution. In Chapter 3, I extend the methodology from Chapter 2 to produce an inventory of annual on-road CO_2 emissions that spans the coterminous U.S. for every year from 1980 to 2012, also at 1 kilometer spatial resolution. In Chapter 4, I focus on quantifying the localized emissions of both air pollutants and greenhouse gases across eastern Massachusetts for every hour of the year 2012.

With each of these high resolution emissions inventories, I then examine the spatially explicit relationships between emissions and past and future trends in population, employment, transportation and public transit infrastructure, traffic congestion and future climate change at multiple spatial and temporal scales. The research in this dissertation focuses considerably on urban areas in the U.S., which were responsible for over 63% of vehicle CO_2 emissions in 2012 (Gately et al. 2015). Urban areas continue to expand across the U.S. and the globe, and will continue to be a key nexus of the development and implementation of strategies to mitigate carbon emissions, improve local air quality, and adapt to future

climate change. A major contribution of this dissertation is the provision of new, highly detailed data products and urban-scale analyses that are both useful as well as accessible to policymakers at local, state, and national scales.

This dissertation includes three core research articles. The first research chapter, Chapter 2, describes the development of a high-resolution inventory of on-road CO_2 emissions for the state of Massachusetts and its application to the question of how population density influences travel behavior and vehicle emissions at local scales. The second research chapter, Chapter 3, presents an expanded and improved emissions inventory of on-road CO_2 that covers the entire coterminous United States for the years 1980-2012. Analysis using this new inventory revealed large spatial biases in existing inventories, and provided for an expanded analysis of the impact of population, employment and income on the distribution of vehicle CO_2 emissions in and around major urban areas in the U.S. The final research chapter, Chapter 4, consists of a detailed analysis of vehicle travel across the Boston metropolitan area based on cell phone data, and quantifies the impact of traffic congestion, vehicle fleet composition and future climate change on the emission of multiple air pollutants species as well as carbon dioxide. Results of this study indicate that the major sources of regional

air pollution are highly concentrated in space and time, and thus are amenable to targeted mitigation policies. It also quantifies the expected reductions in emissions under several traffic management scenarios aimed to reduce road congestion. Finally, the results of Chapter 4 also comprise a collection of 100m resolution, hourly estimates of vehicle emissions that will also be made publically available for download.

Taken as a whole this dissertation presents a collection of new methodologies and new analytical results that considerably improve on the state of scientific knowledge concerning the spatial and temporal variation in greenhouse gas emissions and air pollutants from vehicle sources. With the high-resolution inventories developed herein, it was possible to perform explicit analyses of the multiple factors that drive trends in emissions across time and space, and to quantify the key relationships between emissions, population, and the built environment that continue to be the target of global, national and local policies to mitigate the contributions to global climate change from the on-road sector.

CHAPTER 2 – A BOTTOM UP APPROACH TO ON-ROAD CO_2 EMISSIONS ESTIMATES: IMPROVED SPATIAL ACCURACY AND APPLICATIONS FOR REGIONAL PLANNING.

On-road transportation is responsible for 28% of all U.S. fossil-fuel CO_2 emissions. Mapping vehicle emissions at regional scales is challenging due to data limitations. Existing emission inventories use spatial proxies such as population and road density to downscale national or state-level data. Such procedures introduce errors where the proxy variables and actual emissions are weakly correlated, and limit analysis of the relationship between emissions and demographic trends at local scales. We develop an on-road emission inventory product for Massachusetts based on roadway-level traffic data obtained from the Highway Performance Monitoring System (HPMS). We provide annual estimates of on-road CO_2 emissions at a 1km x 1km grid scale for the years 1980 through 2008. We compared our results with on-road emissions estimates from the Emissions Database for Global Atmospheric Research (EDGAR), with the Vulcan Product, and with estimates derived from state fuel consumption statistics reported by the Federal Highway Administration (FHWA). Our model

differs from FHWA estimates by less than 8.5% on average, and is within 5% of Vulcan estimates. We found that EDGAR estimates systematically exceed FHWA by an average of 22.8%. Panel regression analysis of per-mile CO_2 emissions on population density at the town scale shows a statistically significant correlation that varies systematically in sign and magnitude as population density increases. Population density has a positive correlation with per-mile CO_2 emissions for densities below 2,000 persons-km^{-2}, above which increasing density correlates negatively with per-mile emissions.

2.1 Introduction

The transportation sector comprises 33% of U.S. greenhouse gas emissions (U.S. Environmental Protection Agency 2011). On-road sources (i.e. excluding aviation and rail) account for 28% of total U.S. CO_2 emissions (USEPA 2011). The largest component of vehicle greenhouse gas (GHG) emissions is CO_2 generated by the combustion of motor gasoline and diesel fuel. CO_2 emissions contribute to global climate change (Solomon et al. 2008), but the United States has yet to formulate a coherent national policy to mitigate domestic emissions of greenhouse gases. In the absence of national policy, states have pursued their

own abatement initiatives such as the Regional Greenhouse Gas Initiative (RGGI) and California's Global Warming Solutions Act (California AB-32 2006). Both policies set emissions reduction targets for power plants and other point sources, but California's also sets future fuel economy standards for vehicles. Regulating transportation sector carbon emissions presents a unique challenge, as sources' mobility results in a change in the spatial distribution of emissions over time. A prerequisite for regulating mobile emissions is therefore accurate, spatially explicit emission inventories which serve to establish the baseline level of GHGs and validate the extent of sources' compliance with abatement targets. This remains incomplete for the on-road sector, and is the contribution of this paper.

In addition to their value for treaty and regulatory compliance, emissions inventories play a vital role in the calibration of general circulation models used to understand and predict global, national and regional climate and ecosystem dynamics. The temporal and spatial distribution of anthropogenic emissions is a fundamental input to most terrestrial carbon cycle models and is typically obtained from emissions inventories developed at a variety of scales using multiple data sources (Peters et al. 2007; Gregg et al. 2009). Reducing uncertainties in emission inventories remains an important challenge, and is

considered essential for improving the accuracy of regional carbon cycle models (Zhou and Gurney 2011; Ciais et al. 2010; Peylin et al. 2011; McKain et al. 2012; National Research Council 2010).

Uncertainty in the spatial and temporal distribution of emissions can produce significant variations in estimates of carbon sequestration in the terrestrial biosphere. Schuh et al. (2012) compared the results of an atmospheric inversion model estimating net ecosystem carbon exchange (NEE) using the 10 km resolution Vulcan emissions product with results from the same model using a 1° resolution emissions product and found differences on the order of 100% in local estimates of NEE between the two models. This is on the same order as the uncertainty associated with CO_2 emissions estimates based on directly measured CO_2 concentrations from sampling towers (NRC 2010), unacceptably high given these models' critical importance. Emissions inventories were initially developed as accounting exercises based on national fossil fuel consumption. Typically, national statistics on fossil fuel consumption are used to estimate carbon emissions and the results are downscaled to higher spatial resolution using proxies to distribute the emissions across a grid. For example, in the Emissions Database for Global Atmospheric Research (EDGAR) (European Commission,

Joint Research Center 2011a) on-road emissions are spatially allocated using road density as a proxy. A key limitation to this approach is its assumption of a fixed relationship between emissions and the proxy, whereas the correlation between road density and actual emissions is likely to vary widely across roadway types and between rural and urban areas. Vehicle miles travelled (VMT) has been observed to vary significantly across roadway types and VMT is highly correlated with CO_2 emissions from vehicles (Federal Highway Administration 1980-2012; USEPA 2011). Thus, while EDGAR offers a time series of emissions spanning 1975 to 2008, trends in its spatial distribution of on-road CO_2 emissions may be biased by trends in the proxy variable that are weakly correlated with the true spatial pattern of vehicle emissions.

The Vulcan Project produced a high-resolution map of hourly U.S. carbon emissions for the year 2002 (Gurney et al. 2009). Its on-road emissions are derived from mostly state-level estimates of VMT, which were downscaled to the county level and allocated to a GIS Road Atlas using a combination of population density and road density. This method allows for broad spatial coverage for the inventory, but does not account for variations in the spatial distribution of travel demand within counties. Using state-level source data greatly improves the

spatial accuracy of on-road emissions relative to EDGAR, but on-road emissions estimates from Vulcan are only available for a single year. Vulcan does report total emissions for the years 1999-2008 at the state/county level but does not break these out by sector. This temporal limitation precludes analysis of trends in the spatial distribution of emissions across time, and requires researchers to use scaling factors to back out emissions in subsequent years.

Several researchers have made improvements to the spatial resolution of emissions estimates by incorporating local data sources. Brondfield et al. (2012) developed a model that used impervious surface area (ISA) and volume-weighted road density to estimate CO_2 emissions for eastern Massachusetts on a 1km grid. They used linear regression to model the relationship between these scaling factors and emissions estimates generated at the scale of Traffic Analysis Zones (TAZ) by the regional Metropolitan Planning Organization. They also modeled emissions estimates from the Vulcan Product, and found that both TAZ and Vulcan emissions could be well represented by ISA and volume-weighted road density. By incorporating locally-sourced data, Brondfield et al. were able to construct a high resolution emissions inventory that avoided using coarser

spatial proxies, but their estimates were still limited by the spatial and temporal extent of both source and proxy data.

Gurney et al. (2012) used a large database of local traffic data to downscale Vulcan on-road emissions for the City of Indianapolis to the level of individual roadways. By combining a high-resolution map of the local road network with traffic counts provided by the local MPO they were able to assign hourly carbon emissions to each road in the city. The use of local data on traffic flows to spatially allocate on-road emissions reduces the uncertainty associated with downscaling county or state level data to such high resolutions. Despite the richness of the local data, the control totals are still drawn from Vulcan's downscaled state-level VMT (Gurney et al. 2012). Our premise is that uncertainty in spatial imputation of on-road emissions due to downscaling can be substantially reduced by using source data for VMT available at roadway scales.

Unlike Vulcan, which uses downscaled state-level VMT from the National County Database (NCD) (Gurney et al. 2010), in this study we make use of roadway-level traffic volumes and road characteristics obtained from archived raw data of the Highway Performance Monitoring System HPMS (Federal Highway Administration 2009). We construct estimates of on-road CO_2

emissions for the state of Massachusetts on a 1km grid for the years 1980-2008. We chose Massachusetts as an initial case study because it has per-capita on-road CO_2 emissions similar to the national average, a recent state-wide greenhouse gas inventory is available for comparison (Massachusetts Department of Environmental Protection 2010), and the state has made freely available a GIS layer of the complete road network for mapping purposes (Massachusetts Department of Transportation 2009).

We also believe Massachusetts is a suitable example to demonstrate our methodology as it contains a wide range of land-use types, population densities and road network densities, all contained within a spatial extent that does not exceed reasonable computational requirements. As our plan is to extend our analysis to other states, we have kept our methodology as simple and as flexible as is reasonably possible, and limited our model's data requirements to publicly available sources. We expect that the only modifications required to extend this work to other states will be the partitioning of the model domain to avoid exceeding available computational resources.

The broad temporal scope of our data permitted the construction of a time series of emissions estimates at high spatial resolution, which allowed us to

analyze trends in on-road emissions across space and time, and to compare our results with other inventories. Since our estimates do not rely on spatial proxies such as population density or road density, we were able to conduct a full cross-section/time-series panel regression of population density on vehicle emissions at the scale of local towns (for Massachusetts, approximately census tracts). Our analysis is valuable in the context of urban planning, as the intensity of emissions is likely to be strongly correlated with characteristics of the built environment such as household and population density, jobs-housing balance and the diversity of land uses (National Research Council 2009; Ewing and Cervero 2010). To accurately quantify the relationship between these variables and emissions it is necessary to characterize vehicle emissions at the same spatial scale as the built environment while minimizing reliance on the variables of interest as proxies for spatially allocating the emissions estimates. By doing this, our method provides the wherewithal to investigate the co-evolution of emissions, population, income, and land uses.

2.2 Methods and Data

We combined data on average daily traffic volumes with the distribution of vehicle miles travelled among different vehicle types to estimate average annual per-mile CO_2 emissions for each roadway section in the state of Massachusetts. We summarize our methodology below. A full description is available in Appendix A.

Our main data source is average daily traffic volumes reported for each road section in the Highway Performance Monitoring System (FHWA 2009). The HPMS is a roadway-scale national database managed by the Federal Highway Administration that contains data on annual average daily traffic volumes (AADT) and centerline mileage for all Federal-Aid roads and most other major and minor roads. For all road sections in the Massachusetts HPMS we calculated annual vehicle miles travelled (VMT) as the product of AADT and road length in miles, multiplied by 365. The AADT values in HPMS have already been adjusted to account for seasonal and day-of-the-week variations as per the submission requirements of HPMS (Federal Highway Administration 2005).

The roadway-scale HPMS data does not include all of the VMT that occurred on local roads. To impute Massachusetts total VMT, it was necessary to use a partial downscaling approach only for local road VMT. We used state-level data

on minor and local road VMT from the Highway Statistics Series (FHWA 1980-2012) and distributed it by county using each county's fraction of total state VMT as calculated from the HPMS roadway-level dataset for each year. HPMS road sections are not explicitly geocoded, but do contain codes for county, urban/rural context and HPMS functional class (FHWA 2009). In order to assign our roadway-level VMT to a spatial location, we were therefore required to aggregate our data to the county level, partitioned by functional class and urban/rural context.

Since vehicle emission rates are a function of fuel type (Energy Information Administration 2007), we estimated diesel and gasoline fuel consumption by functional class and urban/rural context within each county. Our first step was to distribute annual vehicle miles travelled amongst five different vehicle types: passenger cars, passenger trucks (includes SUVs, vans and pickup trucks), buses, single-unit trucks and combination trucks. State-level data on the distribution of VMT among different vehicle types is available for the years 1993 through 1999 and for 2009 and 2010 (FHWA 1980-2012). For model years 1999 through 2008 we interpolated linearly between the state-level distributions for 1999 and 2009; for years prior to 1993, we applied the 1993 distribution for all years. Our vehicle

type distribution accounts for variation in the types of vehicles on different types of roads by assigning different distributions for six different functional classes of road, three rural and three urban (FHWA 1980-2012). This captures the variation in the composition of traffic on different classes of roads and between urban and rural areas.

We used the national average fuel economy for each vehicle type for each year (FHWA 1980-2012) to estimate fuel consumption for each roadway functional class, county and year. Fuel consumption was calculated by dividing distance travelled by average fuel economy. Fuel consumption was converted to CO_2 emissions using the emission factors of 8.91 kg CO_2 per gallon gasoline and 10.15 kg CO_2 per gallon diesel fuel (EIA 2007). Emissions from both fuels were aggregated to obtain total emissions for each functional class of road at the county scale.

Emissions were assigned to a road network using the 2009 GIS Road Inventory provided by the Massachusetts Department of Transportation (2009). We calculated the total centerline mileage of each functional class of road in each county, and then divided our relevant CO_2 emissions by this mileage to generate average per-mile CO_2 emissions. These average per-mile emissions were then

assigned by functional class, urban/rural context and county to the road network for each year in the study period.

For comparability with prior estimates, we aggregated our roadway-scale emissions to multiple scales: a 1km grid, a 0.1 degree grid, and summed to the level of local towns.

2.3 Results and Discussion

Using our HPMS data model, we produced on-road CO_2 emissions estimates at the scale of towns, and at a 1 km and 0.1 degree grid for Massachusetts for the years 1980 through 2008. The 1 km gridded results show the strong influence on emissions of major urban areas as well as both urban and rural interstates and highways (Figure 2.1).

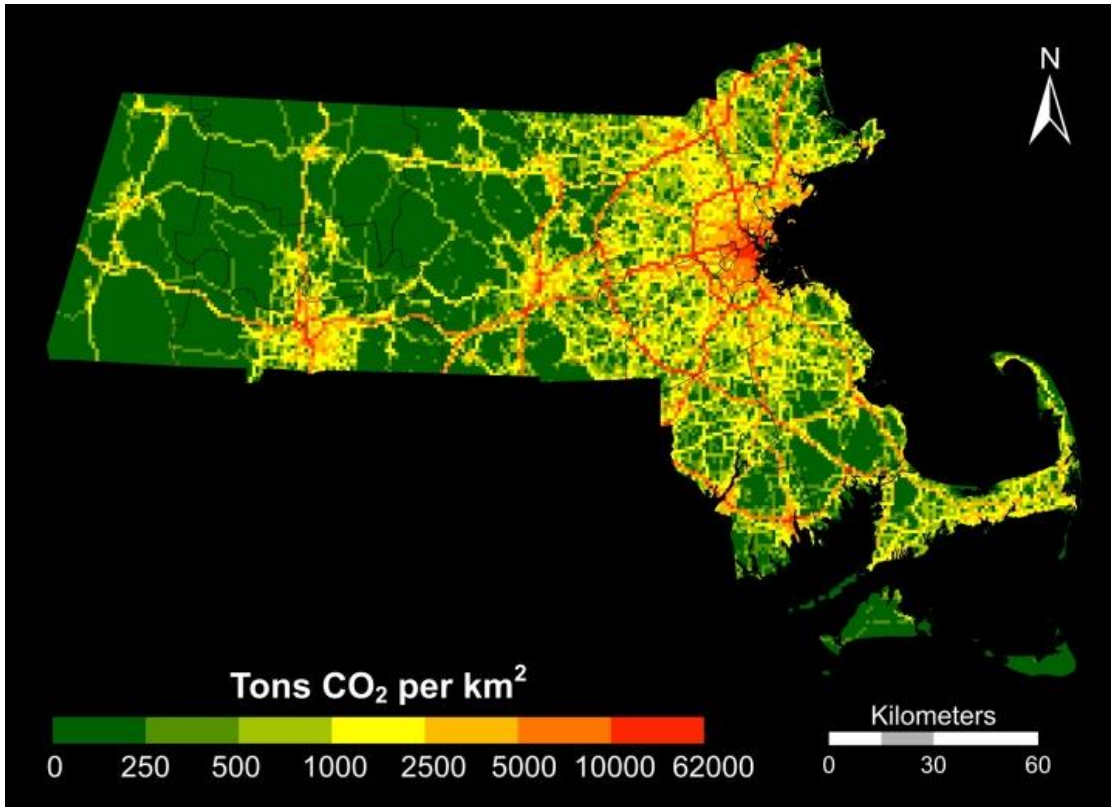

Figure 2.1. 1 km gridded on-road CO_2 emissions (metric tons CO_2) estimated by HPMS-based model for the year 2008.

We compared our total state-wide estimates to the estimates produced by EDGAR, Vulcan, the Massachusetts Greenhouse Gas Emissions Inventory (MGGEI - Massachusetts DEP 2010), the National Emissions Inventory (USEPA 2008), the EPA's Motor Vehicle Emission Simulator (MOVES – USEPA 2010a), and with emissions estimates derived by applying emissions factors (EIA 2007) to statewide fuel consumption reported by FHWA (1980-2012), (Figure 2.2). We

found that EDGAR emissions estimates significantly exceeded FHWA estimates, our model estimates, and most other inventory products. Since we assume the FHWA fuel consumption data to be the closest to actual "ground-truth" for statewide on-road CO_2 emissions, it is of concern that EDGAR estimates exceed these values by as much as 9.3 million tons, or more than 33%, and systematically exceed FHWA estimates by an average of 22.8% across the study period. The EDGAR emissions are closest to the MGGEI. However, the discrepancy may be accounted for by the fact that the MGGEI emissions represent the entire transportation sector (Massachusetts DEP 2010), including emissions associated with rail and air transportation that are absent from other inventories.

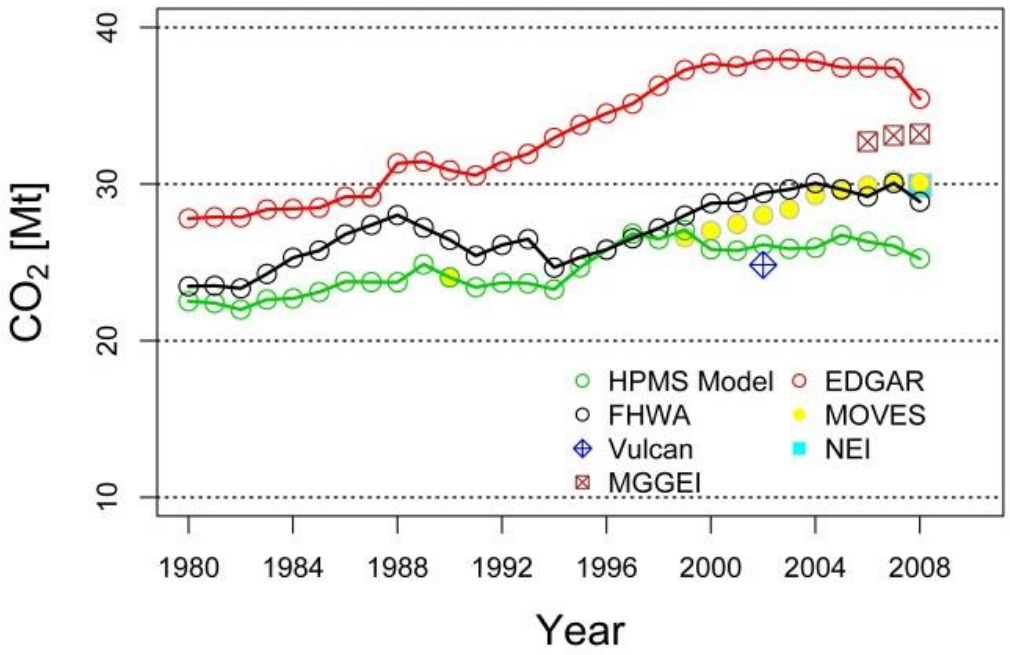

Figure 2.2. Comparison of total Massachusetts on-road CO_2 emissions estimates from our HPMS model with EDGAR, FHWA, MOVES, Vulcan, MGGEI and NEI inventories. Emissions for FHWA estimated using emissions factors for fuel combustion from Energy Information Administration (EIA 2007).

Our HPMS-based model is in better agreement with the FHWA estimates, but does show a systematic under-prediction. The best fit between our model and FHWA data is for the years that we used state-level data for distribution of VMT among vehicle types (1993-1999). In the years that we estimated this distribution, our model show larger deviations from FHWA, which suggests that our estimated distribution may underestimate the miles travelled by lower fuel

economy vehicles during those years. It is also possible that FHWA overestimates the amount of fuel that is consumed by drivers in the state, since state totals are derived from the volumes of fuel sold—but not necessarily consumed—within the state's boundaries. This discrepancy is likely to be larger in states such as Massachusetts, which have both a small areal extent and substantial cross-border traffic flows.

Our model also exhibits generally good agreement with results generated by the EPA MOVES software for 1990 and 1999, but diverges in later years where MOVES estimates are observed to match the trend in FHWA estimates. We ran the MOVES software for the state of Massachusetts using the built-in default values for fleet age and vehicle type distribution. The trend in our estimates matches that in MOVES, which suggests that both models are capturing the same underlying processes that drive changes in emissions.

The divergence of our estimates from EDGAR and FHWA are fundamentally explained by their underlying methodological differences. EDGAR's use of a national emission control total in conjunction with road density as a downscaling proxy (EC/JRC 2011b), combined with the fact that Massachusetts has the third-highest road density of all U.S. states (FHWA 1980-2012), tends to bias its

estimates upward. Symmetrically, for states with lower than average road densities EDGAR will tend to systematically under-predict emissions relative to inventories calibrated to state-level data.

The EDGAR emissions product plays an important role in carbon cycle modeling, as many inverse atmospheric models, such as CarbonTracker (Peters et al. 2007), use EDGAR as an input term in the calculation of terrestrial carbon fluxes. Spatial misallocation of anthropogenic emissions introduces error to these models, and may bias estimates of carbon storage in terrestrial ecosystems (Schuh et al. 2010). A key implication of our results is that out of an abundance of caution, future U.S.-focused regional- or national-scale carbon-cycle modeling studies would be well advised to compare EDGAR's regional estimates to FHWA's state-wide fuel consumption estimates, which are available from 1980 to present, and provide a simple validation of on-road CO_2 emissions at the regional scale.

We next compared our results with on-road CO_2 emissions estimated by Vulcan and the EDGAR inventory (Figure 2.3) for the year 2002, the only year for which all three inventories generate on-road CO_2. When summed to total statewide emissions, we find good agreement between our model and Vulcan: 26,127,254

tons CO_2 for HPMS and 24,838,683 tons CO_2 for Vulcan, a difference of roughly 5%. This is an improvement compared to the EDGAR product, which estimates total emissions of 37,942,510 tons CO_2 in the year 2002, 45% greater than our HPMS estimates and 53% greater than Vulcan. We also calculated cell-by-cell differences between HPMS and Vulcan, which show a mean difference of 6,190 tons. Difference maps and additional details are available in Appendix A.

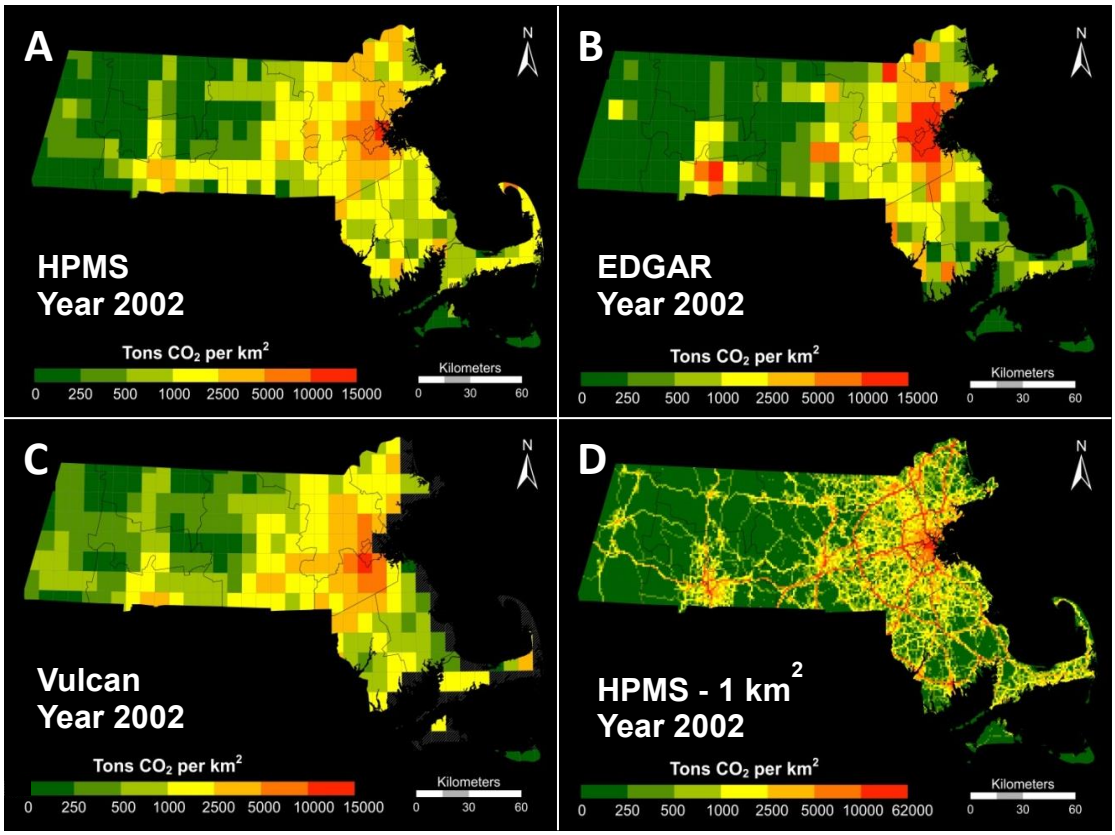

Figure 2.3. Comparison of CO_2 emission inventories for Massachusetts at 0.1 degree grid scale. Panel A shows HPMS-based estimates, Panel B shows EDGAR Product estimates, Panel C shows Vulcan Product estimates. Panel D shows HPMS-based estimates at 1 km grid scale. Note the difference in the highest legend value for the $1km^2$ estimates versus the 0.1 degree estimates. This is a demonstration of how aggregation to the 0.1 degree scale masks the presence and location of the significantly higher emissions intensities that are present in the cores of urban areas.

Despite the good aggregate correspondence between our results and Vulcan, we observed differences between all three models in the spatial allocation of emissions (Figure 2.3). The EDGAR product shows emissions declining relatively

sharply outside the densest urban areas in eastern Massachusetts and the Springfield Urbanized Area in the south-central part of the state. Vulcan shows the most gradual decline in emissions moving from dense urban areas to less dense suburban and rural areas, while our HPMS-based emissions inventory falls between EDGAR's and Vulcan's urban-rural emission gradients. Per our discussion above, EDGAR's spatial distribution of emissions corresponds tightly to the spatial extent of the road network, but, crucially, its estimates do not distinguish either roads' functional classes or their rural-urban context, both of which are predictors of traffic patterns. Vulcan partially addresses this issue by using a combination of population density, road density, and functional class to spatially allocate CO_2 emissions. In urban areas Vulcan emissions correlate well with both our model and with the EDGAR product. However Vulcan distributes rural VMT by roadway class in each county using the county's share of total state rural-area population (Gurney et al. 2010). Given that only five counties comprise nearly all of the predominantly rural western and central parts of Massachusetts, each spatial unit represents a sizeable share of total state rural population. And, since Vulcan assigns rural VMT uniformly across each road type within a county, it is likely that some areas are assigned VMT in excess of that actually occurring

on their constituent local roads. This explanation is consistent with Vulcan's higher emission values in grid cells in the rural western areas of the state compared to non-population based techniques. Our 1km resolution estimates (Figure 2.3D) show clearly the underlying Massachusetts road network and the consequent sparseness of emissions in the western part of the state. For both our model and EDGAR, rural-area emissions only exceed 250 tons CO_2 per km^2 in areas that contain large freeway segments. To recapitulate, it seems likely that Vulcan over-allocates CO_2 emissions to rural roads in Massachusetts, a result which is consistent with other recent findings (Gurney et al. 2009; Shu, Lam, and Reams 2010).

2.4 Sources of Uncertainty

We elaborate on two potentially significant sources of uncertainty in our HPMS model: uncertainty associated with the values of AADT reported by HPMS and uncertainty in our fuel economy estimates of each vehicle type. Uncertainty in the fuel economy of each vehicle type arises from variation in the average travel speed of each vehicle and from variations in vehicle age. Older model-year vehicles tend to have lower fuel economy than newer ones, due to tightening of

the Corporate Average Fuel Economy (CAFE) standards over the period of our sample (U.S. Department of Energy 2011). As well, fuel economy is substantially reduced by travel at lower speeds, as occurs when traffic flow is congested. This effect also varies by vehicle type (West et al. 1999). Our ability to account for local heterogeneity in fuel economy's response to these regulatory changes is limited by our use of a national average fuel economy for each vehicle type, which is averaged across all vehicle ages, all road types, and all travel speeds (FHWA 1980-2012). Therefore to the extent that the age distribution of vehicles or the level of traffic congestion in Massachusetts diverges from the national average, our model's fuel economy values will be biased. Although the uncertainty associated with the vehicle age distribution for Massachusetts is difficult to estimate without access to data on individual vehicle registrations, a recent study by Mendoza et al. (2013) estimated that the impact on fuel economy of variations in vehicle age to be less than 2% for most vehicle types. Data from the most recent Urban Mobility Report (Shrank, Lomax, and Eisele 2011) indicate that the major urban areas in Massachusetts have levels of congestion similar to the national average. However, given that, first, our model does not directly account for the effects of traffic congestion on fuel economy, and, second, we

under-predict FHWA fuel consumption by on average 8.5%, it is reasonable to suspect that some of this difference may be accounted for by this particular uncertainty.

There are two types of uncertainty associated with AADT: uncertainty in actual traffic measurements and uncertainty in estimates of AADT that FHWA impute for roads that are not directly measured. The latter type of uncertainty stems from the practice of using seasonal and geographic factoring to assign AADT from permanent or portable automated traffic recorder stations (ATRs) to similar road links in the network that lack ATR data. Several researchers have used state data to estimate this uncertainty. Ritchie (1986) estimated uncertainties in factored AADT of 7-18 % for Washington State. Gadda et al. (2007) found average uncertainties of 12-14% for Minnesota and Florida roads. The FHWA Guidelines for Data Quality Measurement (Batelle Institute 2004) set uncertainty targets of less than 10% mean absolute error for most road classes in HPMS.

Mendoza et al. (2013) use reported confidence interval and precision estimates from the HPMS Field Manual (FHWA 2005) to estimate one-sigma percent uncertainties for HPMS reported AADT that range from 3.04% to 7.8% depending on functional class. One-sigma uncertainties are roughly equivalent

to a 68.3% confidence interval. To evaluate the impact of AADT uncertainty on our model results, we calculated upper and lower bound estimates of AADT for each road section using both a one-sigma percent difference and a two-sigma percent difference. Two-sigma uncertainties (equivalent to a 95.4% confidence interval) were obtained by doubling the one-sigma values reported by Mendoza et al. (2013) Using these higher and lower AADT values our model generated CO_2 estimates that ranged from ±7.4% to ±7.6% for one-sigma differences in AADT and from ±14.7% to ±15.2% for two-sigma differences, relative to our original estimates. Both ranges are in general agreement with the micro-level studies cited above, and give us additional confidence in the veracity of our estimation procedure. As well, the upper boundary estimates encompass the values for FHWA emissions for most but not all of the years of this study. Further details are included in Appendix A.

2.5 Analysis of On-road CO_2 Emissions and Population Density

A key issue in the debate over how to reduce on-road CO_2 is the nature of the relationships between emissions and VMT, and between VMT and other features of the built environment such as the density of roads, residences and commercial

activity. These issues have been the subject of intensive study for several decades, with recent work focusing on the influence of road infrastructure (Noland 2001; Cervero and Hanson 2002; Duranton and Turner 2011), the effect of fuel prices and vehicle fuel economy (Small and Van Dender 2007; Hymel, Small, and Dender 2010) and the influence of land-use, population density and other demographic factors (Brownstone and Golob 2009; Cervero and Murakami 2010; Glaeser and Kahn 2010; Kim and Brownstone 2013). A 2009 National Research Council investigation found that the majority of studies report an inverse relationship between VMT and population density, with VMT decreasing by 5% to 12% given a doubling of population density (NRC 2009). Quantifying the effect on VMT of changes in population density is important, as it informs policymakers considering planning policies such as infill development or lot-size restrictions that aim to reduce vehicle CO_2 emissions by traffic in and around large urbanized areas.

To accurately characterize the effects of population density on CO_2 emissions, it is necessary to account for trends in these variables across both time and space. As our method for estimating emissions does not rely on population density as a spatial proxy, we were able to use the results of our emissions inventory to

conduct a cross-sectional time-series regression analysis of CO_2 on population density at the scale of local towns. We used population data for each of the 351 Massachusetts towns for the years 1980 through 2008 (Massachusetts Department of Revenue 2012). We aggregated our emissions estimates to the town scale and normalized CO_2 emissions by dividing them by the total length of roads in each town. We ran a panel regression of CO_2 $mile^{-1}$ on population km^{-2}, estimating town and year fixed effects for the whole dataset. The town fixed effects capture heterogeneous unmeasured influences on emissions that are unique to the spatial area covered by each town, such as the spatial structure of the road network or local zoning practices, but which are stable across time. The year fixed effects represent exogenous impacts that affect all towns in the sample but vary over time, such as changing demand for travel and VMT, and trends in unmeasured economic variables such as fuel prices and income. We employ a semi-parametric stratification of our estimates by population density to allow the marginal effect of population density on emissions to vary with different densities. Our model showed excellent goodness-of-fit with an R^2 value of 0.93 and a statistically significant negative correlation between population density and CO_2 emissions per mile of roadway.

To evaluate whether the sign and magnitude of the relationship between emissions and population density changes across different levels of density, we pooled our population density data and used the estimated regression coefficients to predict CO_2 emissions over the range of observed densities. The general functional form of the relationship is characterized as a sequence of linear splines, each with its own confidence interval (Figure 2.4). As the data are pooled across all towns and years, each spline segment represents the common marginal impact of density in a collection of different towns in different years. The shape of the curve in Figure 2.4 reflects the effect of increasing population density on CO_2 emissions, independent of the year- and town-fixed effects.

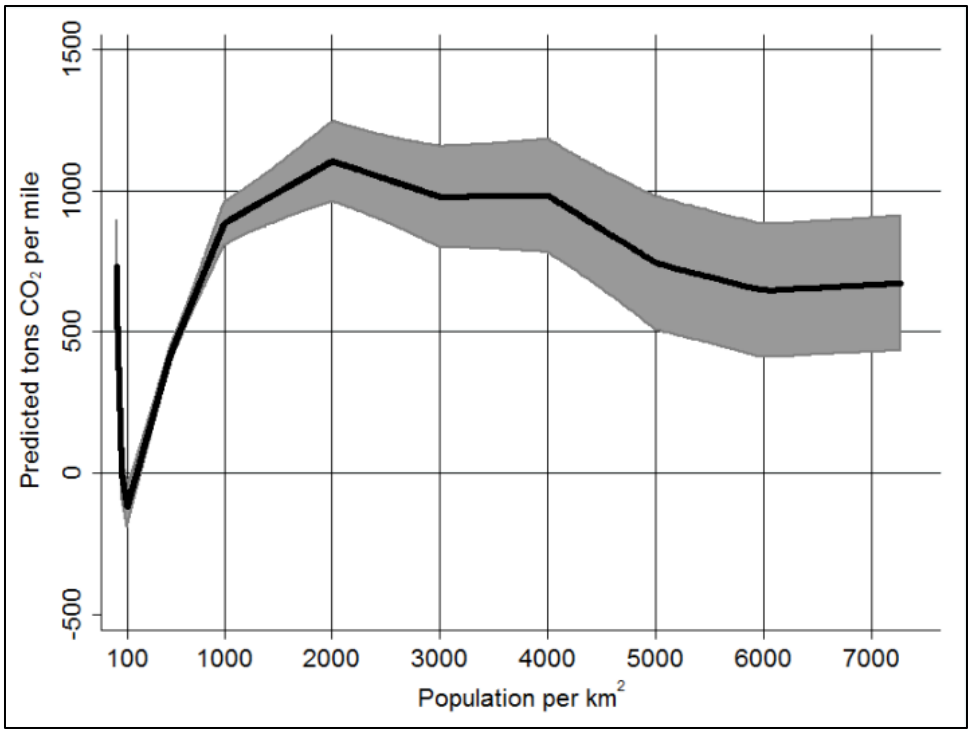

Figure 2.4. Plot of predicted CO_2 emissions per mile vs. population density, with town and year fixed effects excluded. Observations are pooled across all towns and years. Grey area represents extent of 95% confidence intervals.

Population density is positively correlated with vehicle emissions at densities less than 2000 persons-km^{-2}. However, above this level the correlation becomes negative, and emissions decline slowly until densities exceed 4000 persons-km^{-2}, and then more rapidly thereafter. These results suggest that it is only at the higher population densities associated with dense, urban-core towns that we would expect to see on-road emissions decline with rising density. For lower-density towns, increasing population density is more likely to result in an

increase rather than a decrease in vehicle emissions occurring within the town. This result may be a consequence of adding new resident-drivers to the roads, or an indirect effect of denser development drawing more travelers into the area from neighboring towns. Since our emissions estimates only consider the emissions that occur within each town's boundary, we cannot distinguish emissions emitted by residents of the town versus those emitted by drivers from other towns.

Our estimates reflect emissions generated by four different categories of vehicle travel: (1) trips that occur entirely within the given town; (2) trips that originate in the town and terminate outside the town; (3) trips that originate outside the town and terminate within the town; and (4) trips which pass through the town, but start and end elsewhere. We would expect a town's population density to have a stronger direct effect on emissions from categories 1 and 2 and a weaker effect on emissions from categories 3 and 4. That is, higher local population density should reduce per capita vehicle emissions by reducing VMT by the residents of the town, both for trips within the town (category 1) and trips outside the town (category 2). This effect could be generated by increasing the availability of trip destinations such as employment or retail centers or by

induced shifts to alternative modes of travel such as walking, bicycling or public transit.

Density's impact on category-3 trips is less straightforward, as a town with high density may draw vehicle trips from neighboring towns if it contains destinations that attract these trips. Indeed in urban areas the availability of trip destinations has been shown to be a stronger predictor of VMT than population density (Ewing and Cervero 2010, Cervero and Murakami 2009). Across the state, we would expect this effect to vary depending on local relationships between population density and destination availability. Emissions from category-4 trips are probably influenced more strongly by the nature of the road network that transits the town than by the town's population density. We expect this effect to be most pronounced in the rural towns containing sections of interstate highway in the western part of the state, and this is reflected in the higher marginal impact of density close to the origin in Figure 2.4. Disentangling the proportions of total emissions that originate from the four categories listed above requires a far more data-intensive process of conducting a full traffic assignment using origin and destination survey data for the entire road network, which is a task that we leave for future research. Nevertheless, our results still show clearly that population

density influences on-road emissions through a combination of direct and indirect pathways, with high density towns showing a decrease in per-mile CO_2 emissions relative to low density towns. That this decrease is only observed in towns above a relatively high density threshold highlights the potential magnitude of the indirect effects of density described in category 3, and suggests that at low to medium densities, the attraction of vehicle trips from surrounding towns may counteract the decline in per-capita emissions caused by increased local density.

These results highlight the value of using an emissions inventory with high spatial and temporal resolution. At coarser spatial scales, much of the variation in population density and on-road emissions between towns is lost in the aggregation to larger grid cells. By preserving this local variation, and by generating emissions estimates that did not rely on population density as a proxy for spatial allocation, we were able to highlight the shape of the response surface between on-road CO_2 emissions and population density at the scale of local municipalities in Massachusetts. Lastly, our finding of a highly nonlinear relationship between bottom-up emission estimates and a spatially-varying

proxy variable used in prior studies highlights the potential pitfalls of relying on linear predictors in the construction of downscaled emission inventories.

Acknowledgments: We would like to express gratitude to Scott Peterson at the Boston Metropolitan Planning Organization and to Steve Raciti at Boston University for their assistance. This research for Chapter 1 was funded by Boston University and the National Science Foundation Urban Long Term Research Area Exploratory Awards (ULTRA-Ex) program (DEB-0948857). We also gratefully acknowledge support from U.S. Dept. of Energy Office of Science (BER) grant no. DE-SC005171. We also thank the Vulcan Project team for granting us use of Vulcan data.

Appendix A contains detailed methodology, panel regression statistics, and additional figures.

CHAPTER 3 – CITIES, TRAFFIC, AND CO2: A MULTI-DECADAL ASSESSMENT OF TRENDS, DRIVERS, AND SCALING RELATIONSHIPS

Carbon dioxide emissions from road vehicles were 1.57 billion metric tons in 2012, accounting for 28% of U.S. fossil fuel CO_2 emissions, but the spatial distributions of these emissions are highly uncertain. We develop a new emissions inventory, DARTE (Database of Road Transportation Emissions), which estimates CO_2 emitted by U.S. road transport at 1 km resolution annually for 1980-2012. DARTE reveals that urban areas are responsible for 80% of on-road emissions growth since 1980, and 63% of total 2012 emissions. We observe nonlinearities between CO_2 emissions and population density at broad spatial/temporal scales, with total on-road CO_2 increasing non-linearly with population density, rapidly up to 1,650 persons-km^{-2} and slowly thereafter. Per-capita emissions decline as density rises, but at markedly varying rates depending on existing densities.

We make use of DARTE's bottom-up construction to highlight the biases associated with the common practice of using population as a linear proxy for disaggregating national or state-scale emissions. Comparing DARTE with

existing downscaled inventories we find biases of 100% or more in the spatial distribution of urban and rural emissions, largely driven by mismatches between inventory downscaling proxies and the actual spatial patterns of vehicle activity at urban scales. Given cities' dual importance as sources of CO_2 and an emerging nexus of climate mitigation initiatives, high-resolution estimates such as DARTE are critical for both accurately quantifying surface carbon fluxes and for verifying the effectiveness of emissions mitigation efforts at urban scales.

3.1 Significance

We use roadway-level traffic data to construct a 33-year, high-resolution inventory of annual on-road CO_2 emissions for the U.S. that differs markedly from other emissions estimates. We find a highly non-linear relationship between population density and emissions, and identify large biases in local and regional estimates of CO_2 from inventories that rely on population as a linear predictor of vehicle activity. Geographic differences in the density-emissions relationship suggest that 'smart growth' policies to increase urban residential densities will have significantly different effects on emissions depending on local conditions, and may be most effective at low densities. Our results highlight the importance

of cities as sources of CO_2 and the need for improved fine-scale inventories for monitoring and reporting of emissions.

3.2 Introduction

The United States, with 5% of the world's population and 30% of the world's automobiles, emits 45% of global transportation CO_2 emissions (DeCicco, Fung and, An 2006). Nationally, the on-road sector represented 28% of total fossil fuel CO_2 emissions in 2012, and is responsible for almost half of the growth in total U.S. emissions since 1990 (USEPA 2014). Despite being a substantial component of U.S. emissions, on-road CO_2 remains poorly quantified at sub-state and urban scales. Reducing the uncertainty of on-road CO_2 emissions at finer spatial scales is critical to better understanding the determinants of motor vehicle emissions (Gately et al. 2013), constraining carbon budgets (Andres et al. 2012), and supporting greenhouse gas emission monitoring and abatement verification (NRC 2010)—particularly at the scale of cities, which have emerged as hubs of climate change mitigation activity (Rosenzweig et al. 2012).

Carbon cycle models now operate at resolutions much finer than U.S. states, and their reliance on gridded inventories for *a priori* estimates of the spatial

distribution of emissions (Schuh et al. 2010; McKain et al. 2012; Hutyra et al. 2014) means that raw emissions data available at coarse spatial scales must be 'downscaled' to match model grids. Increasing the spatial resolution of emission inventories has been shown to change modeled terrestrial carbon flux estimates by more than 50% (Schuh et al. 2010). The notion that population density is a robust predictor of CO_2 emissions underpins most gridded global emissions estimates. Early studies used maps of population density to distribute national CO_2 emissions on a global 1° grid, assuming uniform per capita emissions within each country (Andres et al. 1996; Brenkert et al. 1998). This assumption was shown to be invalid for the U.S., where per capita emissions vary by an order of magnitude across states (Blasing et al. 2005). Population becomes an even less reliable predictor of total CO_2 emissions at finer scales, where local patterns of concentrated point and line sources dominate more diffuse area sources (Rayner et al. 2010; Gately et al. 2013). Used alone, population may be a valid predictor for residential and commercial sector emissions, but performs poorly when used to model emissions from power stations or the on-road sector (Rayner et al. 2010; Andres et al. 2012; Gately et al. 2013). Recent global inventories such as the Fossil Fuel Data Assimilation System partially correct for this by modeling power plant

emissions directly as point sources, although on-road emissions are still spatially allocated using population and luminosity data (Asefi-Najafabady 2014). The Emissions Database for Global Atmospheric Research (EDGAR v4.2) used a wide variety of sector-specific variables to allocate national CO_2 emissions onto a 0.1° global grid (EC/JRC 2011a), but used only road density to spatially distribute emissions (EC/JRC 2011b). In the U.S. there is substantial variation in the intensity of vehicle activity per mile of roadway, as well as considerable differences in the fleet composition and fuel economy of vehicles that travel on different functional classes of roads (FHWA 1980-2012).

A multivariate regression framework that broadens the number of proxies to incorporate demographic, socioeconomic and built-environment variables appears to improve the spatial accuracy of predicted emissions. Individuals' vehicle travel was found to be best predicted by household income, vehicle ownership and commuting distance, and the estimated relationships have been used to impute on-road emissions at the zip-code level (Jones and Kammen 2014). Directly-measured roadway CO_2 concentrations have also been parsimoniously modeled using only the local fraction of impervious surface and a traffic-volume weighted road density index (Brondfield et al. 2012). In selected

U.S. states and cities local traffic count data and state-level fuel consumption has been used to downscale emissions to a 500 m grid (McDonald et al. 2014).

Most of these studies relied on cross-sectional data, which means that the temporal stability of their results remains untested. This is important for addressing the enduring question in urban sustainability of how trends in urban sprawl and densification affect individuals' travel behavior and related CO_2 emissions over time (Cervero and Kockelman 1999; Bento et al. 2005; Brownstone and Golob 2009). Population density is not thought to directly affect travel behavior, but proxies for less easily measured characteristics of the urban environment (e.g., public transit availability, walkability, amenity access – Cervero and Murakami 2009; Ewing and Cervero 2010), whose impacts on travel have long been a focus of regional and urban planning research. A classic example is the exponential decline in per capita transportation energy use with increasing population density that was observed in a large cross-section of cities worldwide (Newman and Kenworthy 1989). This relationship suggests that urban densification reduces per capita emissions, an idea that has gone on to influence urban development and sustainability initiatives worldwide. Despite recent advances in this area (NRC 2009; Duranton and Turner 2011), there

remains a fundamental simultaneity which confounds inferences about the density-emissions relationship: individuals' travel behavior is affected by the built environment context of their place of residence, but their choice of residential location is simultaneously influenced by their travel preferences (Cao et al. 2009).

To unravel the joint spatial and temporal co-variation between multiple predictors and emissions we constructed a new, dynamic, process-based emissions inventory. DARTE (Database of Road Transportation Emissions) is an annual 1km resolution CO_2 emissions inventory for the U.S. on-road transportation sector, based on archived data of roadway-level vehicle traffic for the years 1980-2012. Raw vehicle activity data was obtained from the Federal Highway Administration's (FHWA's) Highway Performance Monitoring System (HPMS), a database of road-level traffic counts derived from annual reporting by all U.S. state transportation departments (FHWA 2009). The availability of source activity data at this resolution enabled us to directly estimate vehicle emissions at the scale of individual road segments without the need to downscale emissions using spatial predictors. We combined HPMS roadway-level VMT with year- and state-specific emissions factors for five vehicle types to calculate CO_2

emissions from motor gasoline and diesel consumption on six classes of urban and rural roads. We then used DARTE to quantify the spatiotemporally-varying effects of population density, income, employment, and transit usage on on-road CO_2 emissions across the U.S. We also characterize multi-decadal trends in emissions across all rural and urban road types, finding an increasing dominance of urban emissions across the U.S. Finally, we compared DARTE with several existing inventories of on-road CO_2 emissions and identified large relative biases in emissions estimates, with differences that exceed 500% for several major U.S. metropolitan areas.

3.3 Results

DARTE highlights the large spatial variations in on-road CO_2 emissions that exist across the coterminous U.S. (Figure 3.1). The 1km spatial resolution rectifies sharp gradients in emissions around freeways and expressways, particularly in major urban areas. Total U.S. on-road emissions increased by 50% from 1.04 Gt in 1980 to 1.55 Gt in 2012, with 80% of this increase occurring in urban areas. Rural emissions were 556 Mt in 2012, an overall increase of 23% since 1980, but there has been a notable recent decline from the peak of 637 Mt in 2002. Following

2002, trends for diesel and gasoline vehicles diverged, with rural gasoline emissions declining steadily and rural diesel emissions continuing to rise until the global economic recession in 2008 (Figure 3.2). In contrast, urban area gasoline emissions rose steadily throughout the study period, despite the observed decline in overall emissions between 2008 and 2012.

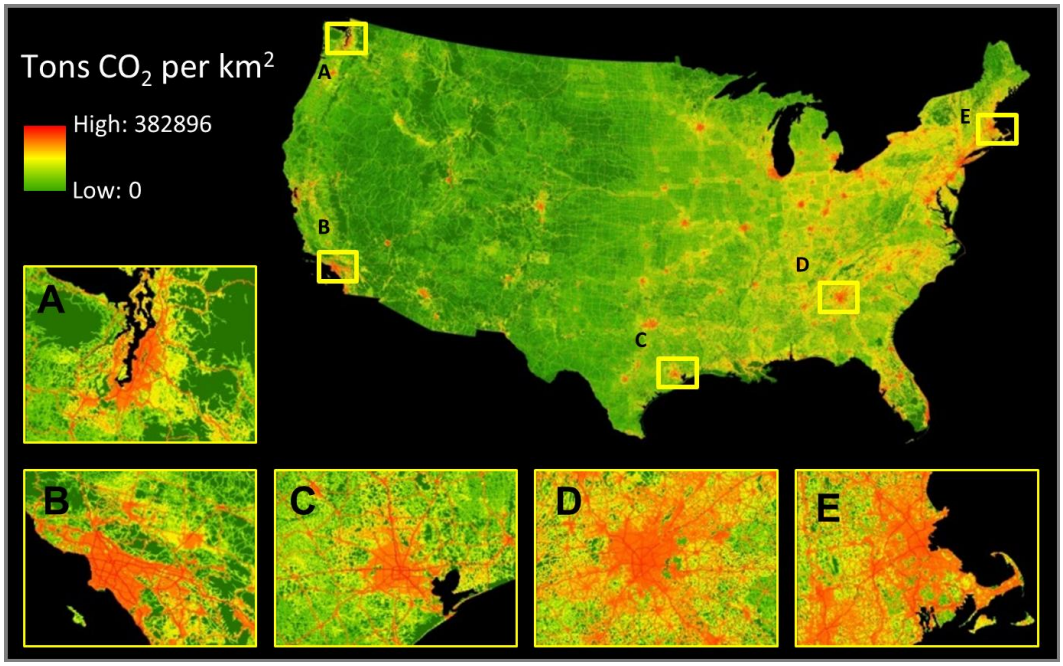

Figure 3.1. Map of 2012 on-road CO_2 emissions for the coterminous U.S. and selected urban areas at 1 km resolution. Inset maps show details of metro areas surrounding: A) Seattle, WA; B) Los Angeles, CA; C) Houston, TX; D) Atlanta, GA; and E) Boston, MA.

Between 1980 and 2010, the U.S. urban population grew by 81 million people, an increase of 49%, while urban per-capita emissions of on-road CO_2 grew by 15% (Figure 3.3). While rural area population declined slightly from 1980 to 2010, rural per-capita emissions rose by 22% over that time. Nationally, per-capita emissions peaked in 2004, although rural and suburban per-capita emissions have begun to rise again since 2009 (Figure 3.3). The sustained decline in urban per-capita emissions is consistent with previous findings on the influence of residential density on vehicle travel (NRC 2009), however it is worth noting that prior to the peak in 2004, urban per-capita emissions rose 19% from 1980 levels, while average urban population density rose 30% over the same time period. This suggests that the future trajectory of per-capita on-road emissions may not be as strongly coupled with trends in urban densification as previously believed.

A confounding factor in analyzing trends in 'urban' variables over time is that definitions of urban boundaries are not stable, as the U.S. Census Bureau revises urbanized area definitions with each decadal census. However, U.S. county boundaries have remained largely unchanged since 1980, as have the designated 'Central' and 'Outlying' counties located at the cores and peripheries, respectively, of most urbanized areas. To avoid any spatio-temporal biases

induced by shifting urbanized area boundaries, we focused our further analysis on emissions at the county scale.

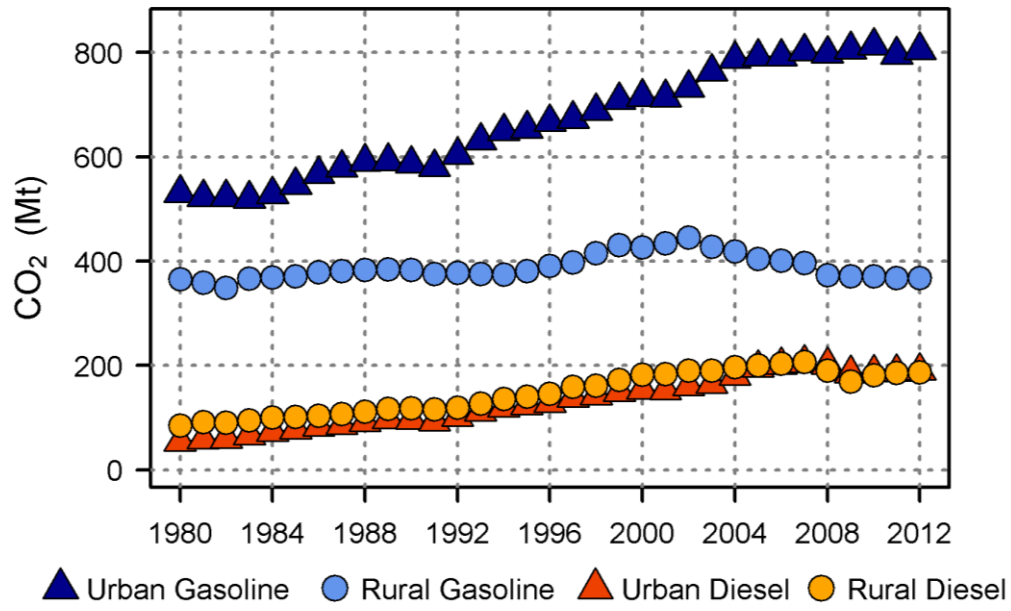

Figure 3.2. Time series of U.S. on-road CO_2 emissions. Urban roads accounted for 80% of total emissions growth since 1980. Rural road emissions have been declining since 2002.

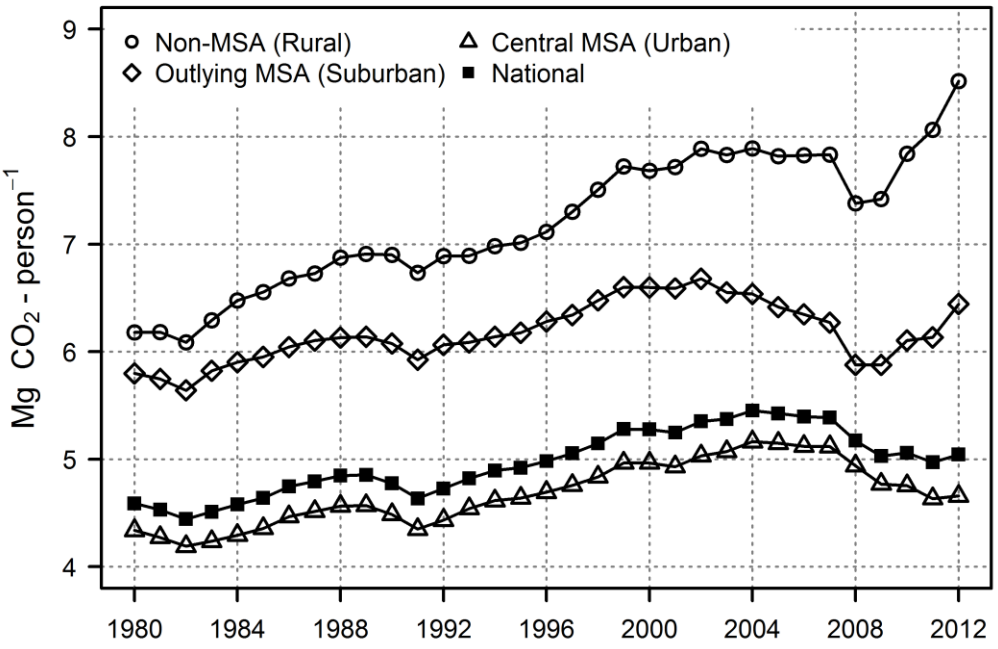

Figure 3.3. Time series of U.S. per-capita on-road CO_2 emissions by county, using Census 2000 Metropolitan Statistical Area (MSA) classification. Per-capita emissions increased from 1980, both in urban and non-urban counties, with brief declines during the 1981-1982, 1990-1991, and 2007-2009 economic recessions. Since 2009 per-capita emissions in Non-MSA (Rural) and Outlying MSA (Suburban) counties have grown rapidly, while Central MSA (Urban) per-capita emissions have continued to decrease.

To elucidate the drivers of on-road emissions we adopted a non-parametric, non-linear modeling approach that characterized the functional forms of the relationships between on-road CO_2, income, employment and population density, while controlling for spatial and temporal fixed effects. A cross-section/time-series generalized additive model (GAM) was used to model CO_2 by

fitting non-parametric splines to population density, per-capita income, retail and non-retail job density, and a lagged population growth term as shown in equation 3.1:

$$\begin{aligned} \mathrm{CO_2}_{\,i,t} = \alpha_i + \tau_t + \Psi_1\left[\begin{pmatrix}\text{Population}\\ \text{density}\end{pmatrix}_{i,t-1}\right] + \Psi_2\left[\begin{pmatrix}\text{Per-capita}\\ \text{income}\end{pmatrix}_{i,t-1}\right] \\ + \Psi_3\left[\begin{pmatrix}\text{Retail jobs}\\ \text{per km}^2\end{pmatrix}_{i,t-1}\right] + \Psi_4\left[\begin{pmatrix}\text{Non-retail jobs}\\ \text{per km}^2\end{pmatrix}_{i,t-1}\right] \\ + \Psi_5\left[(\text{Population})_{i,t-1} - (\text{Population})_{i,t-2}\right] + \varepsilon_{i,t} \end{aligned} \tag{3.1}$$

Here, i and t index counties and years, parameters α and τ represent county fixed effects and year effects, respectively, and ε is a random disturbance term. The terms of interest, Ψ_1-Ψ_5, are non-linear spline functions defined over population density and statistical control variables, lagged one year to reduce simultaneity bias. The same model specification was also used to model per-capita CO_2 emissions. Model diagnostics and summary statistics are included in Appendix B. The adjusted R^2 was 0.98 and 0.88 for the total and per-capita emissions models, respectively. The estimated density-emissions relationship (Ψ_1) shows CO_2 increasing rapidly with population density below 1,650 persons-

km^{-2} before attaining a local maxima (Figure 3.4A_1), consistent with previous findings for Massachusetts towns (3). This corresponds to the relatively slow decline in per-capita emissions with densities between 250 and 1,250 persons-km^{-2}. Per-capita emissions decrease more rapidly with density from 1,250 to 3,500 persons-km^{-2}, which results in a plateau in total emissions at these densities (Figure 3.4A_2). Total emissions begin to rise again as density exceeds 4,000 persons-km^{-2}, and per-capita emissions cease to decline.

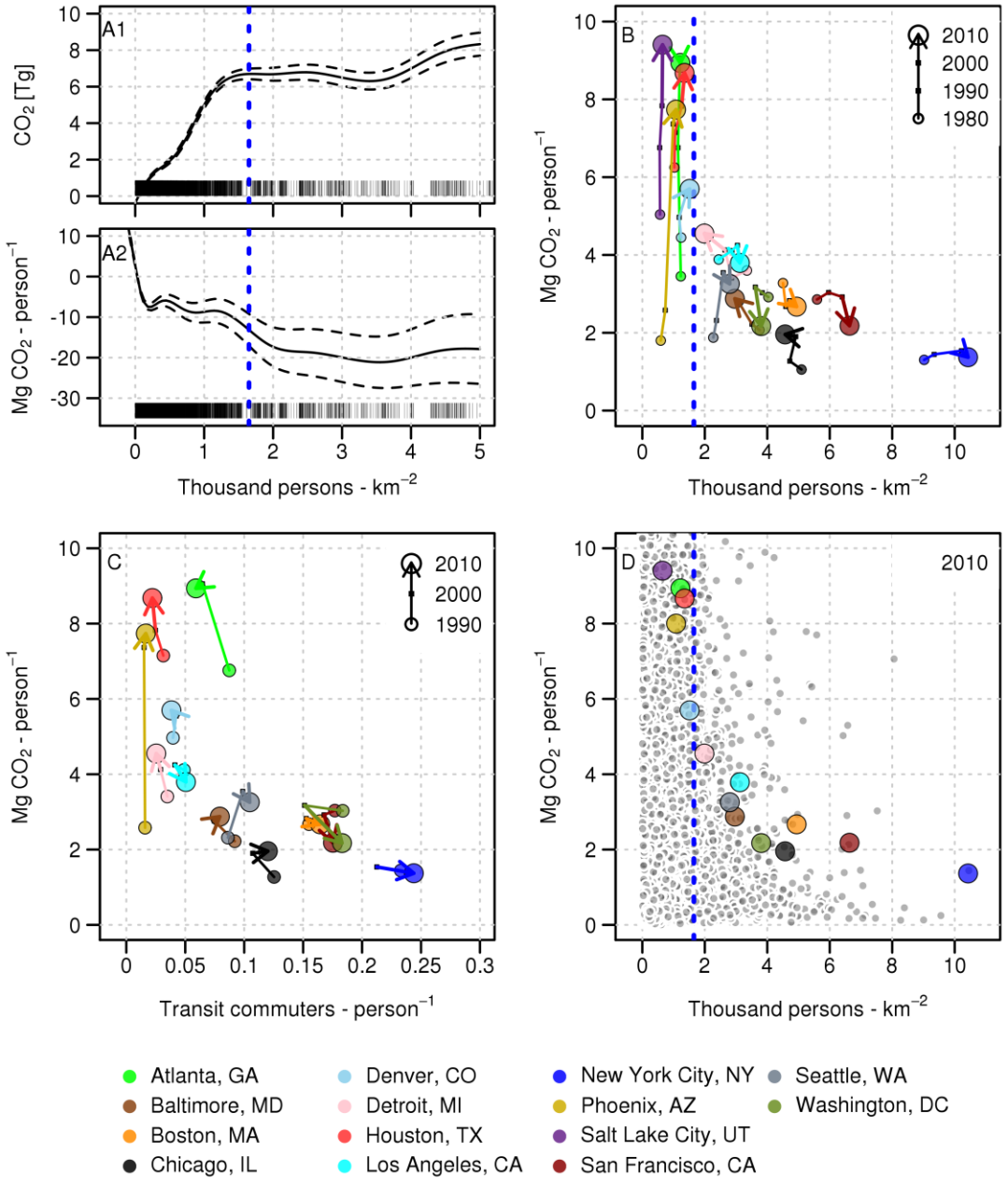

Figure 3.4. Plots of on-road emissions at multiple scales. Panels A_1 and A_2 show the fitted spline Ψ_1 for the partial prediction of total on-road CO_2 and per-capita CO_2, respectively, plotted against county population density. The rug plots in A_1 and A_2 show the distribution of U.S. counties pooled across all years. The values of Ψ_1 are the model-estimated emissions relative to the

conditional mean of each county. Panel B shows decadal per-capita emissions vs. density for 14 U.S. cities. Movement in time is denoted by point size and arrows. Panel C shows per-capita on-road CO_2 plotted vs. the share of residents who commute using public transit. Panel D shows the same cities as Panel B, overlaid on all U.S. Census Designated Places (grey points), for the year 2010. Dashed blue line in Panels A, B, and D identifies first local maxima of Ψ_1 at 1,650 persons-km^{-2}.

The potential for stabilizing on-road CO_2 emissions in the U.S. is limited by the fact that in 2012, only 46 counties (comprising 13% of the U.S. population) had a population density greater than 1,000 persons-km^{-2}. For the remaining 87% of the U.S. population that lives in lower density counties our results indicate that the ongoing urban growth in these counties is likely to produce substantial increases in local on-road emissions, as the reductions in per capita emissions at lower levels of urban density will not be sufficient to stabilize the total emissions growth. Since 2000, the fastest 50 growing counties by population experienced average increases in total on-road emissions of roughly 15%, while their average per-capita emissions fell by only 12%. The average population density of these counties was only 350 persons-km^{-2} in 2012, well below the densities our model indicates are needed to stabilize total on-road emissions on a county scale. Nationally, urban growth and residential densification should continue to reduce total on-road emissions, but in many of the fastest growing urban areas, total on-

road emissions are likely to continue their steady increase. This presents a potential tension between climate change policy at national and regional scales, as the reductions in national emissions provided by urbanization will not necessarily occur in the urban areas that are actually growing denser. From a regional planning perspective, it may make more sense for policy makers to focus on reducing local per-capita emissions, rather than total emissions, as most growing urban areas should expect total on-road emissions to continue to rise with population over the next decades.

To expand our analysis beyond counties, and to test the stability of the density-emissions relationship, we reproduced per-capita emission – density plots for the selection of U.S. cities used by Newman and Kenworthy (1989), but expanded the cross-sectional panel by using DARTE to generate a decadal time-series of emissions estimates for each city (Figure 3.4B,D). We used Census Designated Places (CDP) to define the boundaries of the core city areas, as these are the finest resolution spatial boundaries that have remained unchanged since 1980. We found significantly different trends in the per-capita emissions-density relationship for cities whose densities fall above and below 1,650 persons-km^{-2}. Cities such as Atlanta, Salt Lake City, and Phoenix experienced large increases in per-capita emissions despite minimal changes in population density between

1990 and 2010, while San Francisco and Boston exhibited declining emissions with rising density over the same time period (Figure 3.4B). The divergence of trends in per-capita emissions for cities on either side of 1,650 persons-km^{-2} is consistent with the shape of Ψ_1 in Figure 3.4A$_1$, which shows increasing total emissions at densities below this threshold, and varying trends for densities between 1,650 and 4,000 persons-km^{-2}. The results in Figure 3.4B provide evidence that the emissions-density relationships revealed in Figure 3.4A hold true at the smaller spatial scales.

When the subset of cities in Figure 3.4B is overlaid on data from all other CDPs in the U.S., we see that the sample of major cities used in Newman and Kenworthy (1989) is a poor representation of the underlying emissions-density distribution across all CDPs. We observed very large variation in per-capita emissions across the lower density CDPs, and considerable variation at higher densities as well. While there appears to be a generally decreasing trend between per-capita emissions and density, the spread of the data emphasizes the influence of additional covariates beyond population density on emissions at this spatial scale.

The processes that generate road-sector emissions are influenced by multiple factors, of which population density is only one partial component. We were

unable to directly evaluate the impact of other factors such as public transit usage in our regression model due to the unavailability of transit data through time at county scales. However, by plotting decadal census data on public transit usage for the same sample of cities as in Figure 3.4B we found that cities with large public transit usage shares do tend to have lower per-capita emissions (Figure 3.4C), although these trends were less consistent over time than trends in population density. Cities with high population density also tend to have higher per-capita transit shares. For the cities with lower population density and lower transit shares, we observed higher per-capita emissions in the more recent data (2000 and 2010). As with the plots of population density, the observed rise in per-capita emissions over time in low density cities suggests that public transit ridership has not had a significant effect on emissions trends in these cities since 1990. The only cities that show a clear correlation between increased transit share and decreased emissions are the cities with > 15% transit share of the overall population. San Francisco, Washington, DC and Boston all show noticeable decreases in per-capita CO_2 emissions between 2000 and 2010, concurrent with increases in the transit usage share of their total population. With the limited sample size available, it is difficult to make conclusions about the large number of cities with lower population densities, and presumably lower shares of public

transit usage. The correlations between population density, employment density, income, and lagged population growth estimated by our model suggest that these factors may be sufficient to explain the majority of variance in on-road emissions at the county scale (See Appendix B - Figures B5-B6), but further research into the influence of urban typology and mobility patterns will be vital to understanding emissions trends at city and municipal scales.

3.4 Inventory Bias and Spatial Proxies

External validation of emission inventories is hampered by the lack of independent measurements of source activity (Andres et al. 2012), but it is informative to compare the effects of different model methodologies and proxy performance on the consistency of emissions estimates. Since DARTE estimates were not calculated using population or road density, we were able to evaluate the performance of these variables as spatial predictors by comparing DARTE with other well-known inventories. We aggregated DARTE's roadway-scale emissions to match the native resolutions of EDGAR (EC/JRC 2011a) and the Vulcan Project (Gurney et al. 2009). EDGAR is a 0.1° gridded global emissions inventory product, with annual sector-level CO_2 emissions reported through the year 2008. Vulcan reports hourly sector-level emissions on a 10km grid for the

U.S. for the year 2002. For on-road emissions, EDGAR uses road density as the sole spatial proxy to downscale national-level emissions (EC/JRC 2011b). On-road emissions in Vulcan were derived from VMT from the EPA National County Database (NCD). The NCD contains state-level VMT that has been downscaled to counties using road and population density, with the exception of a small subset (5%) of counties that reported VMT directly (Gurney et al. 2010).

National emission totals of Vulcan and EDGAR were similar to DARTE, but when compared on a cell-by-cell basis, large deviations in emissions were observed. EDGAR exceeded DARTE by as much as 500% in some urban centers, while Vulcan estimates exceeded DARTE by 50% or more in nearly 40% of grid cells (See Appendix B – Figures B1-B4). In contrast to EDGAR however, Vulcan showed large negative biases relative to DARTE in the cores of large cities, and positive biases as high as 100% in surrounding suburban and exurban areas. EDGAR's use of road density as a sole proxy assumes a uniform emission factor per kilometer of road, resulting in over-allocation of emissions to low-traffic roads and under-allocation to high-traffic roads. Although many urban roads carry large amounts of traffic, and hence are responsible for the majority of emissions, urban areas also contain a substantial fraction of local roads which are comparatively lightly travelled. EDGAR's use of a constant emission factor

across road classes with very different activity levels would explain the positive bias in urban core areas with high road density and the negative bias in suburbs with sparser, but still highly travelled roads.

For Vulcan, the relative biases may be explained by how the VMT activity data is downscaled in the NCD. In the NCD, urban non-highway VMT is re-distributed from Census Urbanized Areas to counties using population shares, while rural non-highway VMT is downscaled from state totals, also using population. The results of our regression model (Figure 3.4) indicate that on-road emissions (and by implication VMT) do not vary linearly with population. The use of population to redistribute VMT from Urbanized Areas to counties will produce spatial biases, as population density, and therefore per-capita emissions rates, will vary substantially from the urban core to the suburban periphery (Figure 3.3). The fact that the aggregated emissions estimates of DARTE, EDGAR and Vulcan are in relative concordance, despite local differences of 500% or more for city-scale regions, underscores the risk in presuming that state-level VMT can be accurately downscaled to sub-county scales for the purpose of emissions modeling.

3.5 Uncertainty in On-road Emissions

Uncertainty in the magnitude of on-road emissions at the national level is estimated to be on the order of 3-5% for developed countries (Andres et al. 2012; Mendoza et al. 2013), but at sub-national or state scales existing inventories disagree by as much as 40% (Gately et al. 2013), and at city scales uncertainty can be as large as 50-100% (Rayner et al. 2010). Direct quantification of the uncertainty in U.S. on-road emissions is made impossible by the absence of independent data sources against which to compare government estimates (Andres et al. 2012). Consequently, emissions uncertainty tends to be characterized in terms of the inherent variability of major data inputs to inventory construction: Traffic sensor measurements, spatial imputation of VMT to roads that lack permanent sensors, and emissions factors used to convert VMT to CO_2.

Traffic sensors are widely considered to measure total vehicle volumes with 95%-99% accuracy (Batelle Institute 2004), therefore we focused on estimating the potential uncertainty associated with the spatial imputation of VMT and the emissions factors used by DARTE. We examined the former by calculating within-county coefficients of variation (CV) for VMT in each road class and year, and found that urban and rural freeways and urban non-freeway roads have consistently low variation in VMT, with CVs ranging from 0.4 to 1.1 on average.

Rural non-freeway VMT shows the most sub-county variation, with a mean CV of 2.4, and CVs as high as 14 in a handful of counties (See Appendix B - Figure B9). Rural road segments are typically the least-sampled roads in HPMS, and are held to lower standards of precision (FHWA 2005). Rural non-freeways also account for only 17% of total VMT, so while the spatial uncertainty of emissions from these roads is larger than other functional class roads, their contribution to the total uncertainty is modest. We calculated similar statistics for the within-state, between-county variation of VMT to test the scale-dependence of variation in VMT. The within-state CV of urban VMT ranged from 0.5 to 4.0 across all states and years, while rural VMT ranged more narrowly from 0.75 to 1.75. This larger variation in urban VMT reflects the broader range of urban area sizes at state scales, as small and large cities have very different levels of vehicle activity.

Within-state CVs of emissions intensity (CO_2 / VMT) were found to be small, ranging from 0.1 – 0.2 on average. Low variation in emissions relative to VMT corroborates previous findings that uncertainty in vehicle fleet and fuel economy characteristics are a minor contributor to the overall uncertainty in emissions estimates from the on-road sector (Mendoza et al. 2013). The relatively low variation in roadway-level VMT suggests that the uncertainty associated with spatially aggregating VMT from the roadway to the county scale is relatively

small, so long as stratification by functional class is maintained. Greater variation in between-county urban VMT implies that downscaling VMT from state to county scales may result in a higher uncertainty associated with urban emissions, depending on the distribution of urban area size and local travel trends within the state.

3.6 Implications

Over the past 40 years global urban population rose from 1.51 to 3.91 billion people, and is expected to reach 6.3 billion by 2050 (United Nations 2014). CO_2 emissions from transportation comprised 23% of global fossil fuel carbon emissions in 2010 (Sims et al. 2014), with over 40% of those emissions produced by road travel in urban areas (International Energy Agency 2013). As the first nationally-consistent inventory of U.S. on-road CO_2 emissions built from bottom-up source activity data, DARTE not only establishes a national benchmark for the monitoring, reporting and verification of emissions that are vital to regulating GHGs, it yields novel insights into how key features of urban areas contribute to climate change. DARTE can provide valuable information to local and regional climate change mitigation initiatives (e.g. state and city climate action plans—Rosenzweig 2012; California AB-32 2006; City of Boston 2010) whose success

turns on the ability to accurately assess both city-scale GHG emissions and their responsiveness to policy.

3.7 Methods

Our emissions estimation procedure is based on a comprehensive dataset of roadway-level traffic volumes recently made available by the HPMS. The raw data are average annualized daily traffic (AADT) on more than one million road segments measured annually by state departments of transportation. AADT is a measure of average daily traffic that takes account of seasonal and day-of-the-week variation, such that annual vehicle miles travelled (VMT) for each segment can be directly obtained by multiplying AADT by the length of the segment and the days in the year. We aggregated VMT to by county and functional class of roadway for each year. HPMS records comprise roughly 80% of all VMT, but the records do not contain comprehensive traffic data for most minor and local roads at the roadway level. For these smaller road classes we used state-level VMT by functional class from FHWA's Highway Statistics Series (FHWA 1980-2012) for rural and urban minor collectors and local roads, and allocated this VMT to each county in proportion to the county's share of total state VMT as reported in the HPMS.

The resulting time series of VMT by county and functional class was quality controlled to identify and adjust any outliers or structural breaks. In some cases, an apparent structural break occurred when a county or state reclassified roads to a different functional class, thereby shifting a significant amount of VMT to that new class. In those cases, there was no observed break in the state's time series for total VMT, so we performed no filtering and the data was preserved. To identify data quality issue, our algorithm identified large annual changes in VMT for a given county and functional class where there were no oppositely-signed changes observed in other functional class roads for that county. Where the year-on-year difference between the reported value and both the previous year and following year was larger than twice the mean annual change in VMT for that time series of county and road, the observation was removed and replaced with an imputed value obtained by fitting a lowess curve to the full time series minus the removed value (see Appendix B).

We used VMT to calculate fuel use and associated CO_2 emissions. Fuel consumption per mile travelled varies substantially by type of vehicle, so VMT was partitioned across five vehicle classes and five road functional classes using data from Highway Statistics Series Table VM-4 (FHWA 1980-2012). Table VM-4 provides state-level data on VMT by vehicle class, but the table is only available

for 1993-1997 and 2009-2012. For the remaining years we developed a calibration routine to impute state-level vehicle shares by functional class. We initialized the calibration using data on state-level fuel consumption and average vehicle fuel economy (FHWA 1980-2012), and the shares of gasoline and diesel fuel truck VMT (U.S. Census Bureau 1982-2002). The algorithm adjusted initial vehicle shares and fuel economies such that the calculated state-level gasoline and diesel consumption totals were within 5% of values reported in Highway Statistics Table MF-21. We used the calibrated fuel economies and VMT by vehicle type to calculate gallons of motor gasoline and diesel fuel consumed. Fuel consumption was then converted to CO_2 emissions for each year, county, and road functional class using EPA emissions factors for motor gasoline and diesel (EIA 2007).

We assigned emissions to a GIS layer of the U.S. road network obtained from the 2012 Census TIGER/Line geodatabase (U.S. Census Bureau 2012). To maintain a consistent spatial framework, the road network used is the same for all years. Urban roads were defined as any road link that intersected or was contained within the boundaries of the 2000 Census Urbanized Areas and Urban Clusters shapefile (U.S. Census Bureau 2002). In 2011 the HPMS changed to a GIS-based reporting format, with a subset of AADT now reported in a GIS road network geodatabase. To maintain consistency across all years in our study, we

extracted VMT from the 2011 and 2012 HPMS geodatabase and merged it with our 1980 – 2010 HPMS database. Roadway-level emissions were aggregated to a 1 km grid, a 0.01 degree grid, a 10 km grid, and a 0.1 degree grid for comparison with the Vulcan and EDGAR inventories. The high resolution grids nest smoothly within the lower resolution Vulcan and EDGAR grid systems for ease of comparison and to allow for the combination of DARTE on-road emissions with other sector emissions from either of those inventories.

Acknowledgements: We again thank Robert Rozycki from the FHWA for providing us with access to the HPMS archives. We are also grateful to Steve Wofsy, Ranga Myneni, and Tony Janetos for their feedback on Chapter 3. Funding for Chapter 2 was provided by NASA through awards NNX12AM82G and NNH13CK02C, by NSF through awards 1149471, 1430145, 1038907 and 1240507, and through DOE grants DE-FG02-06ER64204 and DE-SC005171

CHAPTER 4 – IMPACTS OF TRAFFIC CONGESTION ON VEHICLE EMISSIONS OF CRITERIA AIR POLLUTANTS AND GREENHOUSE GASES

4.1 Introduction and Background

Mobile sources are responsible for a large proportion of emissions of toxic air pollutants in the United States. Over 75% of carbon monoxide (CO), and 60% of Nitrogen Oxides (NO_x) emissions in 2012 were from road and non-road vehicles (USEPA 2011b), and in large urban areas as much as 90% of CO emissions may be due to mobile sources (USEPA 2011c). Due to the variable nature of vehicle activity, local meteorology, and urban structure, human exposure to air pollutants is highly heterogeneous. The EPA estimates that over 45 million people, 14% of the U.S. population, currently live within 300 feet of a major road (USEPA 2014b). Ambient pollutant concentrations from mobile sources are highest in close proximity to major roads, and therefore it is those populations living close to roads that are most likely to suffer from the negative health impacts associated with exposure to fine particulate matter ($PM_{2.5}$), CO, and NO_x emissions from vehicles (EPA, 2014). Zhu et al. (2002) found that CO concentrations near a Los Angeles freeway decrease from 2.3ppm at a distance of

17m to 0.4 ppm at a distance of 150m. Zhu et al. also report that black carbon and ultra-fine particle concentrations declined by 60-80% when measured at a distance of 100 meters from the highway. However other pollutant concentrations may be less strongly influenced by the distance from a major road, as Zwack et al. (2011a) found that $PM_{2..5}$ concentrations around two major highways in Brooklyn, NY declined by only 5-10% at a distance of 500 meters, relative to concentrations right at the roadway edge. In urban areas, the presence of large buildings surrounding roads on all sides can also result in 'street canyon' effects wherein the concentrations of ambient pollutants can rise significantly above background concentrations if the emissions from vehicles are not rapidly dispersed by atmospheric mixing (Zwack et al. 2011b).

Ambient air pollution is correlated with several health impacts including chronic obstructive pulmonary disease, acute lower respiratory illness, ischemic heart disease, and lung cancer (Pope et al. 2002; Cohen et al. 2005; Russell and Brunekreef 2009; Gurjar et al. 2010). A recent study by Lelieveld et al. (2015) estimated that globally, outdoor air pollution is responsible for 3.3 million premature deaths per year, with the dominant sources in the U.S. being $PM_{2.5}$ from agriculture, power generation and land transportation. Other recent studies (Tuomisto et al. 2008; Thurston et al. 2013) suggest that the carbonaceous

component of $PM_{2.5}$ is responsible for a much stronger exposure-response than the inorganic components of $PM_{2.5}$. With revised exposure-response functions that weight carbonaceous $PM_{2.5}$ more highly, Lelieveld et al. estimate that 36% of the premature mortality due to outdoor air pollution in the U.S. is due to emissions from the land transportation sector. Thus in order to accurately model the potential exposures of populations living in urban areas with large amounts of vehicle-derived air pollutant emissions, it is critical that emissions estimates be derived at the scale of individual roadways, and not estimated for larger aggregated regions.

Previous inventories of vehicle emissions of air toxics have relied on aggregated estimates of pollutant emissions at the traffic analysis zone (TAZ) or county scale, and were based on either bulk calculations of fuel sales and consumption or on estimates of vehicle miles travelled that were then combined with emissions factors (Harley et al. 2001; Schifter et al. 2005; Zheng et al. 2009; Dallmann and Harley 2010; McDonald et al. 2012). However, the emissions factors are heavily dependent on several related factors including the makes and models of vehicles on the road, their on-board pollution control technologies, the drive-cycle (speed/acceleration profiles) of the vehicles, the composition of the

fuel they burn, ambient weather conditions, and the temporal and spatial variability of the traffic volumes in the area of interest (Parrish 2005).

Quantifying all of these additional variables at high spatial and temporal resolutions is necessary for the accurate estimation of emissions at local scales. Without detailed local data, emissions estimates must be downscaled using generic spatial proxies such as population density or road density (EC/JRC 2011b; Huang et al. 2011). In recent years, the availability of high temporal and spatial resolution data on vehicle activity and emissions has made it possible to accurately estimate vehicle emission fluxes at high resolution (1km or finer) without relying on extensive spatial downscaling (McDonald et al. 2014; Gately et al. 2015). However, roadway-level emissions inventories that are constructed from actual vehicle activity and fleet data are still relatively uncommon, as the large number of detailed, disparate data sources needed to fully capture the variability of vehicle emissions on sub-daily time scales at the level of individual road segments are often unavailable or difficult to obtain in unison for a significant regional extent.

In this study we successfully integrate several novel datasets with existing regional databases to quantify mobile source emissions at an hourly time resolution for hundreds of thousands of individual road segments across the

Greater Boston metropolitan area for the year 2012. We develop a new data assimilation method that integrates multiple large databases of vehicle activity, fleet characteristics, road network characteristics and local meteorology, and use these assimilated data products to quantify emissions for different vehicle types, identify spatial hotspots of emissions, estimate the additional emissions generated solely due to traffic congestion, and quantify potential changes in future emissions under several traffic management policies as well as a forecast future climate scenario.

As emission rates for different pollutants vary depending on the type of vehicle, its travel speed, and the ambient temperature, it is difficult to downscale aggregated emissions estimates without knowing how the local distribution of vehicle types and traffic intensity varies over time and space. Due to the nature of the internal combustion engines used by most vehicles, tailpipe emission rates tend to be much larger at low vehicle speeds than at higher speeds, although for some pollutants the emission factors are also higher when speeds become very high (>65 mph). The result is that on balance, significantly higher emissions fluxes occur when vehicles are in traffic compared to when they are traveling at typical 'freeflow' or cruising speeds (Sjodin et al. 1998; West et al. 1999; Kean et al. 2003). However, for this 'congestion-effect' to generate significant

enhancements in the typical emissions for a given area, the congestion must be both relatively severe and sustained, and must affect a relatively large number of vehicles. Short-lived congestion events will generate brief spikes in emissions fluxes, but in areas such as our study domain of eastern Massachusetts, typical 'background' fluxes of vehicle emissions during non-congested conditions are already rather large.

To quantify both the absolute and the relative impact of travel speeds and congestion on vehicle emissions in our domain, we utilize a very high-resolution dataset on vehicle speeds obtained from the traffic consultant firm INRIX, which aggregates real-time data from mobile phone and GPS sensors in tens of thousands of vehicles across our study domain. This highly detailed information on the actual movement of vehicles on the roads allowed us to the capture hour-to-hour variations in traffic conditions that drive localized variations in emissions of air pollutant species, and it also allowed us to quantify the aggregate impact over the entire year and domain of these congestion-induced emissions from different vehicle types. We were then able to test alternative emissions scenarios by simulating a variety of traffic conditions in the absence of any congestion, in order to quantify the potential emissions improvements that

might be expected if policies to reduce traffic volumes and/or increase speeds were implemented across the region.

This study produced several key results concerning the relationship between emissions, traffic congestion and local meteorology. Most notably, we find that the overall relative contribution of congestion to emissions of air pollutants and greenhouse gases is quite small across eastern Massachusetts. We show that improving vehicle speeds without reducing the number of vehicles on the road will at best reduce emissions by 3-5 % depending on the pollutant. A combination of reduced traffic volumes and reduced congestion can increase the potential emissions reductions to 5-8% below current levels, but only if the reductions in the number of vehicles are targeted specifically at roads with heavy congestion. We also find that for certain pollutants, localized emissions are dominated by the presence or absence of heavy trucks or other diesel vehicles. By identifying the locations of truck-dominated emissions hotspots, our database provides the benchmark data necessary to support targeted emissions reductions focused on specific vehicle corridors and travel patterns. Finally, we evaluate the future impact on vehicle emissions of rising regional temperatures due to global climate change, and show that for certain pollutants, notably carbon monoxide

(CO), warmer mean temperatures are likely to produce localized increases in emissions of 25% or more by the year 2050.

Our results provide strong evidence that emissions of air pollutants and greenhouse gases from road vehicles are unlikely to be reduced in any significant fashion by policies that focus only on improving travel speed and reducing congestion. Even modest reductions in the number of vehicles on the road will not generate the significant improvements in emissions that are necessary to improve local air quality and mitigate the impact of greenhouse gas emissions on global and regional climate change.

4.2 Data and Methods

4.2.1 Input Data

We construct a new database of emissions of CO, SO_2, NOx, $PM_{2.5}$, and CO_2 from vehicles travelling on the roughly 305,000 road segments that make up the public road network of eastern Massachusetts. We integrate several datasets with varying native spatial and temporal resolutions to produce hourly gridded surface fluxes of these emissions at a 100m grid scale. The main datasets used to develop this database are shown on the left and center of Figure 4.1, and include a large set of vehicle speed data purchased from the traffic consultant firm

INRIX, a GIS database of average daily traffic volumes (ADT) for all of the major roads in Massachusetts (Massachusetts Department of Transportation 2013), road network characteristics and vehicle fleet information from the Boston Metropolitan Planning Organization's Travel Demand Model, hourly traffic counts from permanent traffic recorders (Massachusetts Department of Transportation 2014), hourly meteorology (temperature, atmospheric pressure and specific humidity) from the North American Land Data Assimilation System (Xia et al 2012), and vehicle emissions factors calculated by the EPA MOVES model (USEPA 2014b).

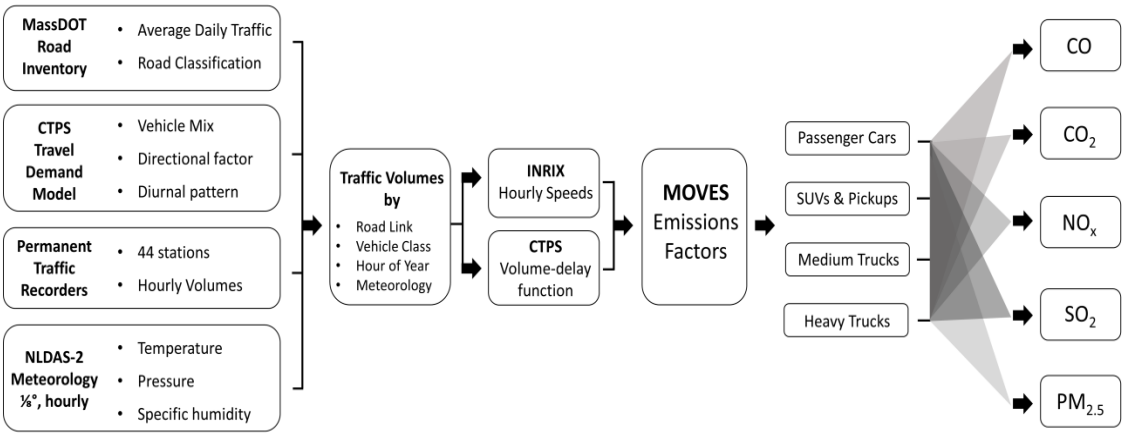

Figure 4.1. Flowchart of data assimilation methodology. The four major input datasets are spatially merged to generate hourly traffic volumes for 4 vehicle types for each of the 305,137 road segments in the domain, coupled to the hourly ambient meteorology for each road. Travel speeds are assigned using INRIX data where available. For non-INRIX segments, speeds are calculated using a volume-delay function that relates speed to road volume and

capacity. Emissions of CO, CO_2, NO_x, SO_2, and $PM_{2.5}$ are calculated using the EPA MOVES2014 model for each vehicle type.

The INRIX speed data is derived from thousands of mobile phone and vehicle GPS devices, which are then aggregated by INRIX to calculate average travel speed on over 60,000 road segments in our study area at a temporal resolution of 5 minutes for the year 2012. The INRIX road network separates vehicle travel on each road segment by the direction of travel, to account for the variation in daily traffic patterns on roads that experience distinct directional patterns of traffic activity depending on the time of day. We joined the INRIX road network shapefile to the Massachusetts Road Inventory shapefile in a GIS using a proximity-based spatial join, as there was no direct crosswalk between the unique IDs of road segments in the two datasets. Manual validation of all major roads in the spatial join was performed by several staff of the Central Transportation Planning Staff (CTPS) of the Boston Metropolitan Planning Orgnization (MPO), and then completed for all remaining road segments by the authors. The Massachusetts Road Inventory road network forms the spatial basis for our emissions model.

4.2.2 Traffic Volumes

The Road Inventory shapefile contains estimates of average daily traffic volumes for each road segment, as well as the number of lanes in the segment and the roadway functional class as defined by FHWA. Some road segments, mostly the local roads, were missing estimates of ADT. However, estimates of total vehicle-miles travelled on local roads in the Boston Urbanized Area are available from the FHWA Highway Statistics Series Table HM-71 (FHWA 1980-2012). We used these aggregate totals to assign a mean ADT to each local road in the Boston Urbanized Area that was missing an ADT value in the Road Inventory file. We first subtract the total VMT from the local roads that do have a reported ADT from the total VMT in Table HM-71, and then divide the remaining VMT by the total length of all the local roads that are missing VMT in the Urbanized Area, and then divide again by 366 days, to get an average daily traffic volume for all local roads.

4.2.3 Travel Demand Model

We next joined the output from the CTPS Travel Demand Model base run for 2012 to the attribute table of the Road Inventory. The CTPS Travel Demand Model is a traditional, four-step traffic assignment model calculated using the TransCAD traffic modeling software, and is continuously updated and

maintained by CTPS for modeling and forecasting of local and regional transportation demand. The first two steps in the model use travel survey data, vehicle fleet data, and demographic information to estimate the number of daily trips taken in the eastern Massachusetts region (trip generation) and then to estimate the likely origins and destinations of each of these trips (trip distribution), aggregated to areas dubbed Traffic Analysis Zones (TAZs). The third and fourth steps in the model are mode choice, where each of the trips in the large origin-destination matrix created in the previous step is assigned to different travel modes (vehicle, public transit, bicycling, walking), followed by the route assignment step, which assigns each of these trips to individual links in the relevant transportation network (roads, heavy/light rail, cycling infrastructure, etc.) using optimization routines.

The output of the model that we utilize consists of estimated vehicle travel for four periods of the day (AM peak from 6am to 10am, mid-day from 10am to 3pm, PM peak from 3pm to 7pm, and night-time from 7pm to 6am), disaggregated by vehicle type and road segment direction. The model is designed to estimate travel on each road segment for an average weekday. The travel demand model also contains additional information on road segment characteristics including the capacity of the segment as well as the alpha (α) and

beta (β) coefficients used to estimate travel speed on the segment using a modified version of the Bureau of Public Roads volume-delay function (Equation 4.1).

$$Speed_{observed} = \frac{Freeflow\ Speed}{1+\alpha\left(\frac{V}{C}\right)^{\beta}} \quad (4.1)$$

For roads that do not have speeds available from the INRIX database, we utilize the relationships captured in Equation 4.1 to estimate vehicle speeds as described later in this section.

We do not directly use the estimated traffic volumes from the CTPS model directly, since the output from the CTPS model does not cover all of the road segments in the Road Inventory file, and many of the local roads are excluded to maintain computational tractability of the traffic assignment calculations. To maintain consistency across the region we use the average daily traffic volumes contained in the Road Inventory file, and use the CTPS model output to disaggregate those volumes by time of day, travel direction, and vehicle type. We first aggregate the vehicle types in the CTPS output to the following five general classes: Passenger Cars, Passenger Trucks (SUVs and pickup trucks), Medium-size Trucks (gasoline-powered), Medium-size Trucks (diesel-powered), and Heavy Trucks (diesel-powered). Both passenger vehicle classes are assumed to

be gasoline-powered. We then divide the CTPS model volume for each vehicle class in each of the four time periods by the total volume for each link (by direction) to get volume shares by vehicle class, direction, and time of day. These shares are then used to disaggregate the ADT volumes from the Road Inventory file. For road segments in the Road Inventory that are not present in the CTPS model, we assign them the characteristics of the nearest CTPS road segment of the same functional class.

4.2.4 Hourly Time Structure

To temporally disaggregate the ADT data from the Road Inventory, we first use a large dataset of hourly traffic volumes obtained from 44 permanent traffic recorders (PTRs) distributed across the study region (Massachusetts Department of Transportation 2014). This data is obtained from inductive loop sensors embedded in the roadway surface that continuously monitor traffic volumes throughout the year. For each PTR station we calculate the aggregate total volume of vehicles for the whole year of 2012, and then divide each hourly volume by this total to get an hourly share. We assign each segment in the Road Inventory the hourly traffic profile of the nearest PTR to that segment. The hourly shares are then used to convert the road segments' ADT values into

hourly traffic volumes by multiplying the segments' ADT by the number of days in the year (366 for the year 2012) and then by the hourly share.

Each hourly volume was then further divided into the respective volumes for each of the vehicle classes using the shares calculated from the CTPS travel demand model output, depending on time of day and travel direction of each road segment. The resulting output is an hourly estimate of traffic volume for each vehicle type on each road segment in the Road Inventory, partitioned by travel direction for the road segments with two-way travel.

4.2.5 Speed Assignment

For all of the road segments that contain a matching INRIX segment, the average hourly speed for each hour of the year is assigned from the INRIX database. Although the raw data from INRIX is at a 5 minute time resolution, the mean speed across each hour was calculated and used in our analysis for the purposes of computational efficiency. For the road segments where INRIX speeds were not available, we used the volume-delay function described in Equation 4.1 to estimate hourly travel speeds on each segment. The main components of Equation 4.1 are the freeflow speed, the hourly volume (v), the hourly capacity (c), and the coefficients α and β. For freeflow speeds we use the

mean 85th percentile speed by functional class from all roads in the INRIX database, and assign these speeds by functional class to the Road Inventory segments that lack INRIX speeds. The hourly capacity and the coefficients α and β are obtained from the CTPS model output.

4.2.6 Emissions Factors

To calculate emissions for each road segment we utilize emissions factors calculated by a customized run of the EPA's Motor Vehicle Emissions Simulator (MOVES) for eastern Massachusetts. MOVES is the successor to the MOBILE model, which was developed by EPA in the late 1970s to support modeling of vehicle emissions at the national, states and local scale. MOBILE was steadily improved and upgraded by EPA until 2010, when it was then overhauled and replaced by MOVES, which is currently the standard for quantifying vehicle emissions of 135 different pollutant species under a wide range of driving conditions. MOVES is widely used by states and regional planning organizations to evaluate compliance with the Clean Air Act, to forecast the air quality impacts of future development, and to quantify the impact of changing vehicle technologies and traffic management practices.

Although the MOVES software contains default values for many of the parameters used to determine emissions rates, EPA strongly recommends that users include as much local data as possible when running the model, so as to minimize biases created by any mismatch between the model default parameters and the actual local parameter values. The spatial resolution of MOVES is limited to county-scale estimates when the model is run in 'inventory' mode. In order to obtain finer resolution estimates of emissions, MOVES also allows the user to run it in 'emission factor' mode, which produces an output table of the emissions of a pollutant in grams per vehicle kilometer travelled (VKT) for the various vehicles and fuel types of interest.

As these emissions factors are highly sensitive to changes in atmospheric conditions, fuel composition, vehicle make, model, and age, and to the average travel speed of the vehicle, the MOVES software requires an array of input files that characterize all of these variables for the domain of interest. Among other responsibilities, the staff of CTPS is responsible for modeling and forecasting the air quality impacts of regional transportation developments, and as such they have developed a customized set of input tables that quantify all of the relevant parameters that are specific to the eastern Massachusetts region. We make only one substitution to the custom MOVES input tables, and include a table that

covers the full range of meteorologic variables observed in the year 2012, as obtained from the NLDAS-2 grid that covers eastern Massachusetts.

4.2.7 Meteorology

The meteorological variables required by MOVES are ambient atmospheric temperature and relative humidity. The NLDAS-2 data product has a spatial resolution of 1/8° (~ 140 km^2 grid cells), and reports hourly values of air temperature, air pressure, and specific humidity at an elevation of 2 meters above the land surface. We use the values of these three variables to calculate the relative humidity for each hour and grid cell using the Clausius-Clapeyron equation (See Appendix C). Each road segment was then assigned the hourly temperature and relative humidity of the NLDAS-2 grid cell within which it was located.

The MOVES model output produced emission factors for CO, CO_2, NO_x, SO_2, and $PM_{2.5}$ in grams emitted per kilometer of vehicle travel, for all combinations of temperature, relative humidity, average vehicle speed, vehicle type, and road functional class. For computational efficiency we rounded all temperatures in both the MOVES data and the NLDAS-2 data to the nearest degree, and we rounded all relative humidity values to the nearest multiple of ten. We then

joined the MOVES output to the Road Inventory dataset, with emission factors assigned by the meteorology, day of week and functional class for each hourly traffic volume. The final output consists of hourly estimates of emissions of the five pollutants of interest for each of the five vehicle types, for each of the ~305,000 road segments in the domain. Emissions were then aggregated to a 100m x 100m grid for further processing and distribution.

4.2.8 Policy Scenarios

Next we estimated emissions under several policy scenarios using our base dataset as a reference. First, we estimated emissions for a scenario that assumes that all vehicle traffic was always traveling at the freeflow speed of the road segment. We use the 85th percentile speed of each road segment as obtained from the INRIX data as an estimate of free-flow speed, as this reduces the influence of high-speed outlier hours, which were observed on some roads during late-night or early morning hours. This scenario does not assume that vehicle volumes were actually reduced to the levels where these speeds would be physically realistic, but rather was designed to explore the consequences of a hypothetical expansion of the road network capacity to accommodate all of the present travel demand. This scenario also assumes that vehicle volumes remain at 2012 levels,

although the literature on 'induced demand' clearly indicates that this would be unlikely given an expansion in road capacity (Cervero and Kockelman 1999; Noland 2001, Cervero and Hansen 2002; Small and Van Dender 2007; Hymel et al. 2010). Nonetheless, this scenario provides an estimate of the fraction of emissions that could be reduced if vehicle traffic was free to travel at freeflow speeds. It also reveals the quantities of both emissions and fuel consumed during congested conditions, and allows us to estimate the monetary cost of traffic congestion with respect to motor fuel wasted.

For a second scenario, we calculate the emissions if vehicle volumes were reduced to the levels required to actually obtain freeflow speeds throughout the road network at all times. To do this, we simply set the hourly traffic volume equal to the capacity of the road segment, for all of the hours where the actual 2012 volumes exceeded the road segment's capacity. For the hours where the hourly volume was below the capacity of the road segment, we make no changes. This scenario reflects the expected outcome of a policy that reduces the demand for vehicle travel on the roadways to the levels required to alleviate all traffic congestion on every road in the study area. The results of this scenario allow us to examine the marginal reductions in emissions with respect to

marginal reductions in vehicle traffic, and to quantify the total expected emissions benefits from a congestion-focused travel demand reduction strategy.

4.2.9 Future Climate Scenario

We simulate an additional scenario that calculates the changes to vehicle emissions due to future climate change, by running our model using the mean meteorological conditions forecast for the year 2050 under the SRES A2 scenario (IPCC 2000). We use the National Center for Atmospheric Research (NCAR) Community Climate System Model (CCSM) ensemble means of monthly mean air temperature, downscaled to a 4.5 km resolution grid for North America. For this scenario we make no adjustments to the relative humidity values in our 2012 meteorology, but adjust each hourly temperature value in a given month by the difference between the forecast mean monthly temperature in 2050 and the mean monthly temperature in 2012 from NLDAS-2. We make no alterations to the vehicle activity part of the dataset, and calculate revised emission estimates using the appropriate MOVES emissions factors under the altered temperature conditions.

4.2.10 Vehicle Cold-Starts

For the base scenario and for the climate change scenario we also estimate the emissions of all five pollutants of interest that occur due to passenger vehicle starts. While the majority of emissions from vehicles occur during running operations, a large amount of emissions also occur when a vehicle is started from a cold engine. To calculate the number of passenger vehicle starts per day, we use data from the 2010 Massachusetts Travel Survey (Massachusetts Department of Transportation 2012) combined with U.S. Census population and housing data for eastern Massachusetts (US Census Bureau 2010). Table MAPC-56 in the Travel Survey provides estimates of the mean number of vehicle trips per person and per household for the Metropolitan Area Planning Council Domain, which is essentially identical to the domain of our study. Table MAPC-57 further disaggregates trip rates per household as a function of household size.

We use estimates of the population and number of households at the census block level to estimate the mean household size in each census block. The number of daily trips per block is then calculated using the values from Table MAPC-57 for all grid cells where the mean population per household was greater than one or less than 11. For census blocks with a population density greater than 10 per household, we use the average rate for individuals of 4.1 trips per day from Table MAPC-56. We then convert the total number of trips per day

into vehicle trips per day using the average mode share of trips by private vehicle of 57.9% reported in Table MAPC-60 of the Travel Survey. Total vehicle trips per census block were then scaled to our 100m x 100m grid and aggregated to annual trips.

To estimate vehicle starts emissions from the trips in each grid cell, we used emission factors derived from the same runs of the MOVES2014 model that were used to generate running emissions factors, as MOVES also calculates the emissions per start for each vehicle type. Emission factors are again partitioned by vehicle type and ambient meteorology, and we assume that each personal vehicle trip in the domain includes one vehicle cold start located at the residence of the traveler. Due to the lack of information on trip destinations, we are unable to calculate the location of cold starts that may occur at the destination as part of the return leg for each trip. Thus our estimates of starts emissions from passenger vehicles should be considered a lower bound. We assume a passenger vehicle distribution that is 62.9% passenger cars and 37.1% SUVs/pickup trucks/vans, using values from Table MAPC-47 on vehicle ownership by vehicle body type.

For ambient meteorology we use the mean values for temperature and relative humidity calculated for the hours between 6AM and 9PM on each day for each NLDAS-2 grid cell, under the assumption that the majority of trips and

vehicle starts occur between these hours. Annual emissions of the pollutants of interest are then calculated by multiplying the relevant emissions factors by the number of trips in each grid cell per day and then multiplying by 366 days. Figure C1 in Appendix C shows the results from our model of emissions from cold starts.

4.3 Results and Discussion

4.3.1 Spatial Patterns of Emissions

We estimate total annual emissions for the domain of 139.9 Gg CO, 0.314 Gg SO_2, 71.6 Gg NO_x, 2.83 Gg $PM_{2.5}$, and 22.21 Tg CO_2 from running vehicle exhaust. Emissions from passenger vehicle starts were: 72.9 Gg CO, 0.012 Gg SO_2, 5.53 Gg NO_x, 0.12 Gg $PM_{2.5}$, and 0.65 Tg CO_2. With running and starts emissions combined, the mean fluxes for the domain are 14.54 g-m^{-2} CO, 0.02 g-m^{-2} SO_2, 5.27 g-m^{-2} NO_x, 0.20 g-m^{-2} $PM_{2.5}$, and 1561.8 g-m^{-2} CO_2. For most pollutants the share of total emissions that arise from cold starts is relatively low (2% for CO_2, 4% for $PM_{2.5}$, 7% for NO_x, and 3% for SO_2). However, CO emissions from cold starts comprise just over 52% of total CO emissions in the domain, despite not including cold start emissions from non-passenger vehicles. CO emissions are high during cold starts and the early running phases of exhaust because low

temperatures of the oxidative catalyst in the vehicle's catalytic converter significantly reduce the catalyst's ability to oxidize CO. Once running temperatures have increased, the catalytic converter then begins to operate in its ideal temperature window and the CO emission rate declines significantly (USEPA 2010b). The high relative shares of CO from cold starts is a function of the large number of trips by passenger cars in our domain, and the short average trip distance due to the dense nature of the Boston metropolitan area.

We compared our model results for CO_2 with the output from DARTE for the same domain and found strong agreement between the two models (Figure 4.2). This is an encouraging finding, as the emissions estimates in DARTE rely on a much coarser dataset of vehicle type distribution, as well as using state-average fuel economies that were not directly tuned to account for the impacts of vehicle speeds and congestion. The main differences in the spatial distribution we see when comparing our current model to DARTE is the differences in the intensity of emissions in urban and rural areas. DARTE emissions in the urban core are higher on average than our current model, while the opposite is true for rural emissions. This is likely due to the nature of the data sources that underlie DARTE emissions estimates. The ADT data from HPMS that forms the basis for DARTE emissions was disaggregated from the county level by functional class.

As a result, there is a 'smearing' of emissions across the all of the roads in the urban counties with large amounts of vehicle traffic. In our current model, we are more likely to be capturing the actual spatial variation within each county, and within each functional class of road, since every road segment except for the local roads that we imputed data for, has a unique value for ADT that was estimated from local traffic counts. As a result, our 100m resolution inventory of CO_2 emissions more accurately reflects the true spatial variability of emissions at a road-segment scale.

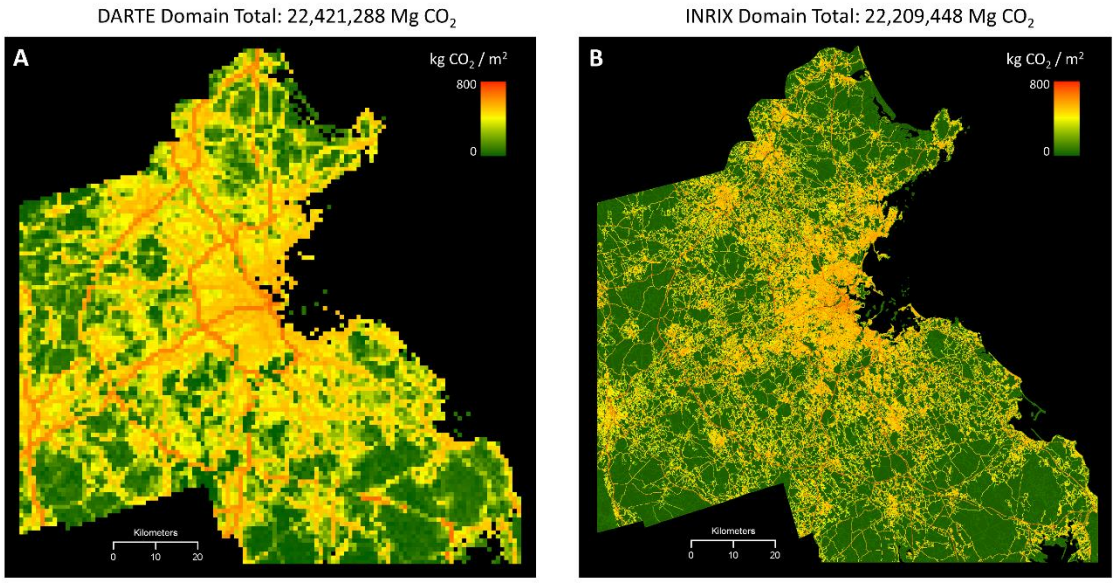

Figure 4.2. Comparison of on-road CO_2 running emissions between DARTE and our INRIX-based model for the year 2012. The spatial resolution of DARTE (left panel) is 1km x 1km. The spatial resolution of the INRIX-based model is 100m x 100m. The total estimates for annual CO_2 emissions are very similar, suggesting that DARTE captures the overall intensity of on-road emissions well, despite not directly accounting for variations in vehicle speeds.

4.3.2 Local Influence of Vehicle Types

We next examine the spatial variation in emissions by looking at four subsets of the broader domain that represent a range of land use and road network characteristics. We summarize emissions of each pollutant, partitioned by vehicle type, for a square kilometer area over Arlington town center, a largely residential area with some small commercial activities on a main street-type road, an area in the town of Chelsea that contains a mix of residential, industrial and commercial activities surrounding two relatively large and busy arterial roads, an area over Kenmore square and Fenway Park in the Back Bay neighborhood of Boston, which contains residential and commercial buildings, the Fenway park stadium, several major arterial roads and a stretch of Interstate 90 that runs below grade through the area. The final area we examine is a square kilometer in the town of Milton, just south of Boston, which is wholly residential, but contains a long stretch of Interstate 93, one of the most heavily traveled and congested roads in the entire domain. We selected these four areal subsets to represent a range of urban and suburban forms of the built environment, in order to explore how localized variations in the types and intensities of vehicle traffic can influence overall emissions of different pollutants.

Emissions of different pollutants are influenced by the dominance of different vehicle types in a clearly observable way (Figure 4.3). NO_x and $PM_{2.5}$ emissions are dominated by heavy truck emissions, as diesel-burning engines produce much higher levels of these pollutants in their exhaust. Conversely, CO and SO_2 emissions are more strongly driven by passenger car and passenger truck activities, as can be seen in all four areas (Figure 4.3). The pie chart insets in each panel of Figure 4.3 show the overall share of emissions by vehicle type calculated for a reduced area of the full domain that is bounded as shown in the upper left panel of the figure. We observe a broadly similar distribution of source apportionment by vehicle type across this moderate subset of the domain as we observe in each of the four smaller subset areas, which suggests that on average it is the overall intensity of vehicle traffic of each type of vehicle that determines the amount of emissions in a given location.

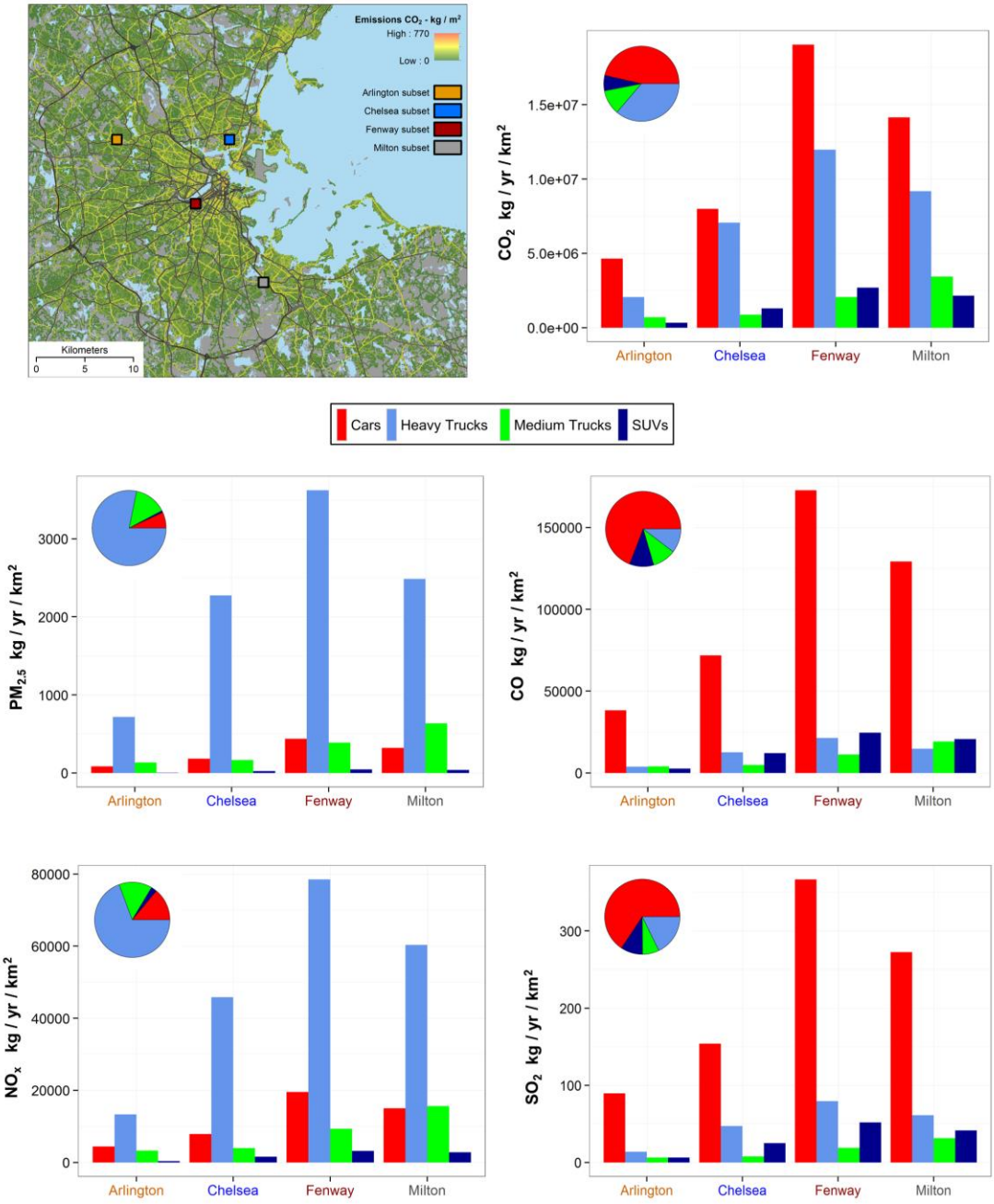

Figure 4.3. Spatial variation in the emissions of CO_2, $PM_{2.5}$, CO, NO_x, and SO_2 for four sample locations in the Boston metro area, disaggregated by vehicle type. There is a strong influence of heavy trucks on the emissions of $PM_{2.5}$ and NO_x, while passenger cars dominate emissions of SO_2 and CO. The pie chart insets

show the vehicle shares of emissions for each pollutant with respect to the total emissions aggregated over the reduced domain shown in the upper left panel.

4.3.3 Impact of Congestion on Emissions

We simulate two hypothetical policy scenarios to explore the influence of traffic congestion, and the associated reductions in vehicle speeds, on running emissions. In the first scenario we assume that all traffic is able to flow at freeflow speeds at all times, without any changes to the number of vehicles on the road. This scenario represents a hypothetical expansion of road capacities to accommodate the current demand, but ignores any feedbacks to the demand such as increases in traffic volumes induced by the reduction in traffic and travel time. The difference between emissions in this scenario and actual emissions can be interpreted as the 'surplus' of emissions that occur solely due to traffic congestion. Although the aggregate totals that we calculate for these surplus emissions seem large in absolute terms, as a relative share of total emissions across the domain they are quite small. For CO, SO_2, NO_x, and $PM_{2.5}$ the percent reduction in emissions under freeflow conditions are 2.1%, 5.1%, 3.2%, and 5.5%, respectively. For CO_2 the reduction is 4.8%. We also calculate the volume of additional fuel burned by using the CO_2 emissions to estimate gasoline and diesel consumption using the same emissions factors as in Chapters 2 and 3 (EIA

2007). We estimate that traffic congestion was responsible for 80.97 million gallons of gasoline and 32.84 million gallons of diesel fuel wasted in 2012. When aggregated to just the Boston Urbanized Area, our estimate of total fuel wasted is 61 million gallons, which is similar to the estimate of 70 million gallons from the 2012 Urban Mobility Report (Shrank, Lomax, and Eiselle 2012). At the average 2012 prices for gasoline and diesel in Massachusetts of $3.53 / gallon and $3.93 / gallon, respectively, our estimate of the total volume of wasted fuel due to traffic congestion is equivalent to an additional $414,900,000 spent on vehicle fuel by drivers in our study domain over the year.

Although the total amounts of fuel wasted and surplus emissions emitted seem very large in absolute terms, the relative amounts are modest. In 2012 the state of Massachusetts consumed over 3.2 billion gallons of fuel for use in motor vehicles. The wasted fuel due to traffic congestion in the eastern half of the state that is our study area was equivalent to roughly 3.5% of that statewide fuel consumption. So although policies that target congestion reduction through speed improvements may be able to make modest contributions to reducing the overall emissions of greenhouse gases from the on-road sector, the ceiling on these reductions appears to be rather low. We do observe larger relative reductions in emissions under this scenario in two particular locations: The

Interstate 90 toll plaza and on-ramp / off-ramp complex in the Allston neighborhood of Boston and the Interstate 93 corridor south of downtown Boston. Overall, a reduction in congestion sufficient to achieve freeflow speeds at the Allston tolls corridor would reduce emissions of CO_2 by 35%, of CO by 34%, of SO_2 by 37%, of NO_x by 35% and of $PM_{2.5}$ by 43% relative to current levels over the course of the whole year. Congestion reductions where Interstate 93 meets State Route 3A could produce as much as 56% reductions in NO_x, 52% reductions in CO, and 65% reductions in $PM_{2.5}$ emissions relative to 2012 levels on that corridor.

However, to actually achieve the traffic conditions necessary for travel speeds to remain at or near freeflow conditions on these heavily used roads would be challenging, if not impossible, considering the strict limitations on capacity expansions that exist due to the densely developed urban environment that surrounds these busy roads. Adding or widening lanes in these locations would be an expensive and potentially controversial prospect, especially in light of an extensive body of research showing that capacity expansions are typically followed by increased traffic volumes (Small and Van Dender 2007; Hymel et al. 2010). Consequently, generating a sustainable reduction in congestion in these locations will ultimately require reductions in the volume of vehicles, in

particular during peak morning and evening periods when the majority of traffic congestion occurs.

4.3.4 Impact of Reduced Traffic Volumes on Emissions

To evaluate the impacts on emissions of a scenario where vehicle travel is reduced sufficiently for all roads to experience freeflow conditions at all times, we adjusted the hourly traffic volumes on each road segment during the hours when volumes exceeded capacity in our original model. With the maximum volume set at the level of each road segment's capacity, the total amount of annual vehicle kilometers travelled would be reduced by 3.7% across the domain. This reduction would result in an annual decrease in emissions of CO, SO_2, NO_x, and $PM_{2.5}$ of 5.7%, 8.5%, 6.5%, and 8.6% respectively, and a reduction of 8.1% in CO_2 emissions.

For each road segment where we adjusted hourly volumes such that the travel speed did not drop below freeflow speed, we compare the percent change in annual vehicle kilometers travelled that resulted from the sum of all of those volume reductions with the percent change in annual emissions on that road segment (Figures 4.4-4.8, upper panels). We fit a linear model to each plot using Ordinary Least Squares, and report the estimated parameters as in inset in each

figure. On average, there is a 1.02 – 1.13 percent reduction in pollutant emission for every one percent reduction in VKT on a road segment. This result does not reflect the maximum possible elasticity of emissions to VKT reductions, as we designed this scenario to prioritize congestion mitigation when adjusting traffic volumes downwards on each road segment. For certain road segments, and for certain pollutants, the relative reductions in emissions could be much larger if the VKT reductions were designed to target these goals. For example, for the same domain-wide reduction in VKT, a focus on reducing VMT on roads with heavy truck traffic would result in considerably higher reductions in total $PM_{2.5}$ and NO_x, as these emissions of these pollutants are dominated by truck sources. One drawback to targeted interventions to reduce VKT in certain areas is that spillover effects may occur if drivers simply adjust their routes to alternative routes, leaving the overall level of vehicle travel unchanged. However, deliberate re-routing, in particular for heavy trucks, can be beneficial if the vehicles are redirected to higher speed roads or away from densely populated neighborhoods. For $PM_{2.5}$ emissions in particular, the distance between the sources and potential exposure is highly variable over relatively small distances (Zwack et al. 2011a; 2011b). Since our model resolves emissions at such fine spatial scales, the output from our base scenario can provide local public health

and transportation policy makers with the specific data needed to develop targeted mitigation policies, as well as the ability to simulate the potential outcomes of multiple policy options.

With the output from the VKT-reduction scenario we also evaluated the cumulative reduction in emissions as a function of the cumulative reduction in VKT across the whole domain (Figures 4.4-4.8, lower panels). Of note is that at very low reductions in VKT, we actually observe an increase in the emissions of CO, as the emission rate of CO is sensitive to increases in vehicle speeds at higher speed profiles. For the set of roadways where only small reductions in VKT are needed to allow vehicles to travel at freeflow speeds, there is thus an initial increase in total CO, despite the concurrent reduction in volumes. As the reduction in volumes increases (with the assumption being that travel speed does not continue to increase beyond the freeflow speed), the decreased VKT eventually produces reductions in total CO emissions (Figure 4.4).

For all other pollutants, initial reductions in VKT produce relatively large reductions in emissions, followed by steady decreases thereafter. For CO, cumulative emissions reductions do not become positive until VKT reductions exceed ~ 300 million VKT, which is less than 0.5% of total 2012 VKT for the domain. When the VKT decrease reaches 1 billion VKT (1.6% cumulative

reduction), total CO emissions have decreased by 2.1 Gg, a reduction of roughly 1.5% of total CO for the domain. However, once total VKT has been reduced by 2 billion VKT (3.2% cumulative reduction), CO reductions exceed 6 Gg, equivalent to a 4.3 reduction in total CO.

For NO_x, reductions in total VKT of 1 and 2 billion result in decreases of 1.6 Gg and 3.7 Gg, respectively. In relative terms, this means that reductions in VKT of 1.6% and 3.2% result in decreases of 2.2% and 5.2% in NO_x emissions. For other pollutants, the effects are similar. For SO_2 the same reductions in VKT result in decreases of 10 Mg and 21 Mg, respectively, equivalent to 3.2% and 6.7%, for $PM_{2.5}$ the same reductions in VKT result in decreases of 116 Mg and 205 Mg, respectively, equivalent to 4.1% and 7.2%, and for CO_2 the same reductions in VKT result in decreases of 678 Gg and 1,428 Gg, respectively, equivalent to 3.1% and 6.4%.

For CO_2, SO_2, and $PM_{2.5}$ our results show that the reductions in emissions that arise from reduced VKT are roughly double the VKT reductions on a relative basis. For CO and NO_x the relative effect is lower, but is still greater than a one-to-one ratio. This can be largely explained by the design of the VKT reduction scenario, which focuses on reducing traffic congestion and improving vehicle speeds. With the initial exception of CO, which is more sensitive to high-

speed travel, improved vehicle speeds combined with reduced vehicle volumes considerably reduces the rate of emissions for the remaining vehicles on the roads, and results in higher relative reductions for a given decrease in VKT than if the VKT reductions were assigned randomly.

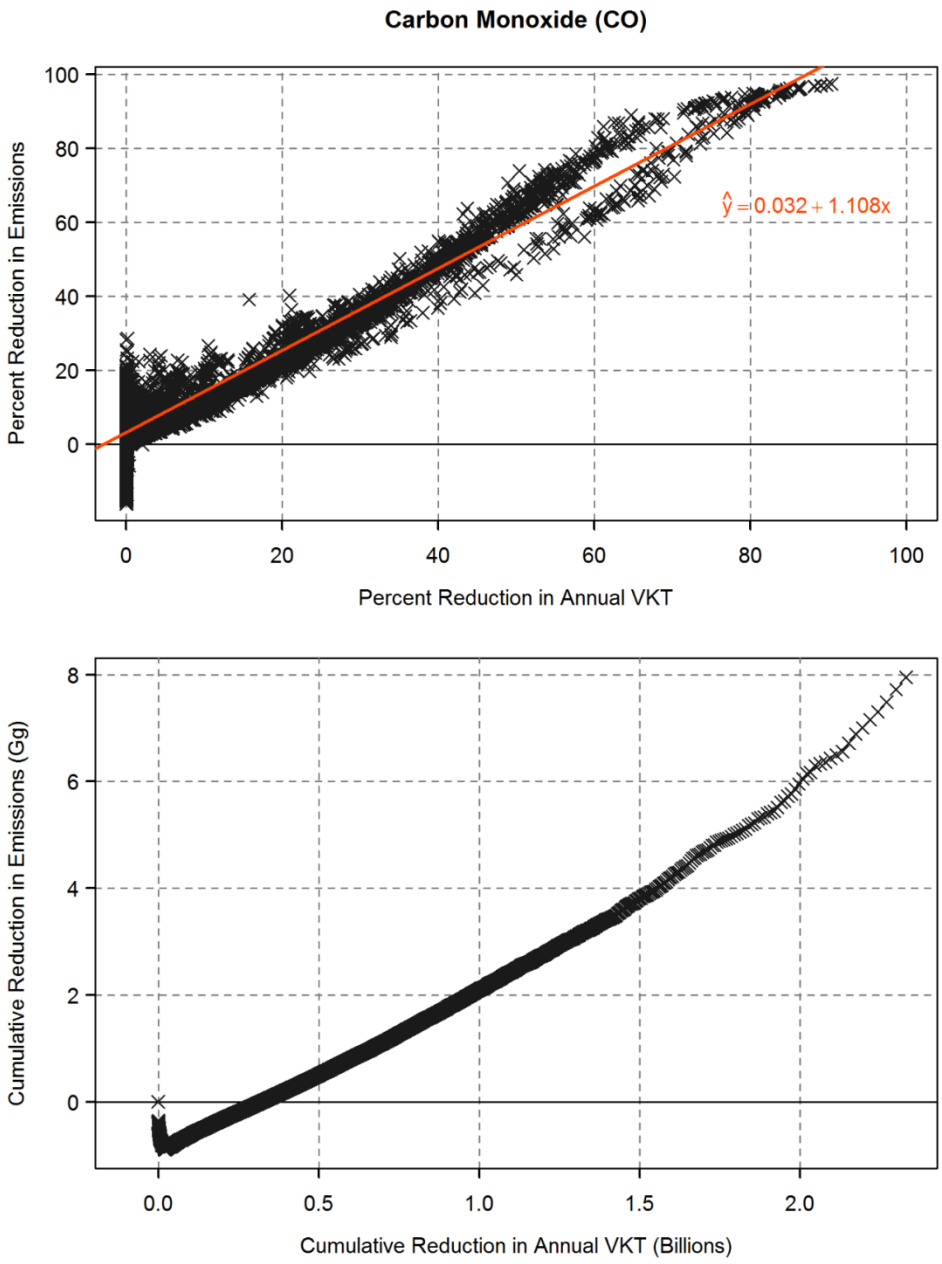

Figure 4.4. Estimated reduction in CO emissions in response to VKT reductions on congested road segments. Upper panel shows percent reduction in annual emissions of CO for each road segment versus the percent reduction in the road segment's annual VKT required to maintain freeflow travel speeds at all times. Lower panel shows cumulative reduction in total emissions over the entire domain relative to the cumulative reduction in annual VKT for the domain.

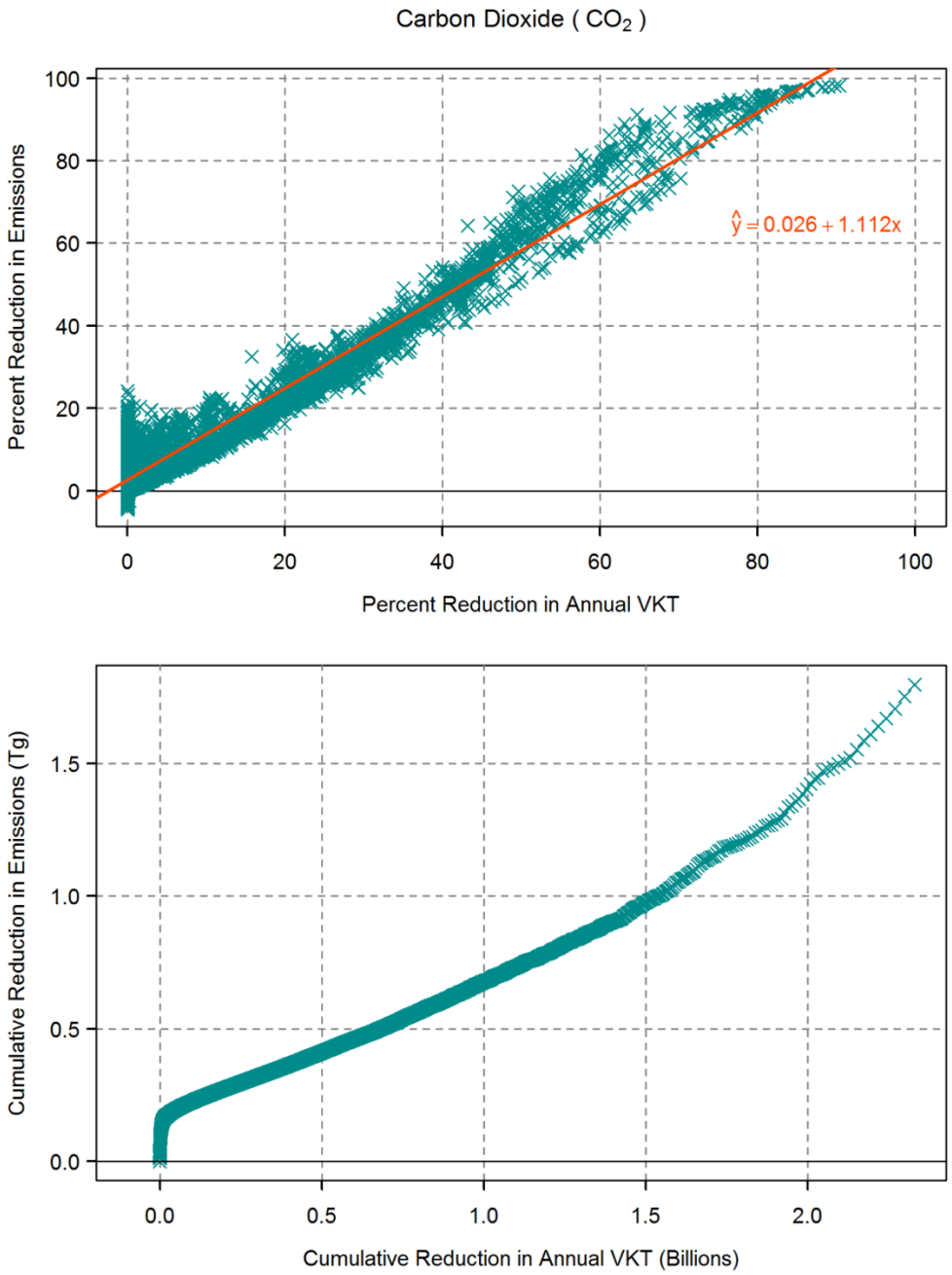

Figure 4.5. Estimated reduction in CO_2 emissions in response to VKT reductions on congested road segments. Upper panel shows percent reduction in annual emissions of CO_2 for each road segment versus the percent reduction in the road segment's annual VKT required to maintain freeflow travel speeds at all times. Lower panel shows cumulative reduction in total emissions over the entire domain relative to the cumulative reduction in annual VKT for the domain.

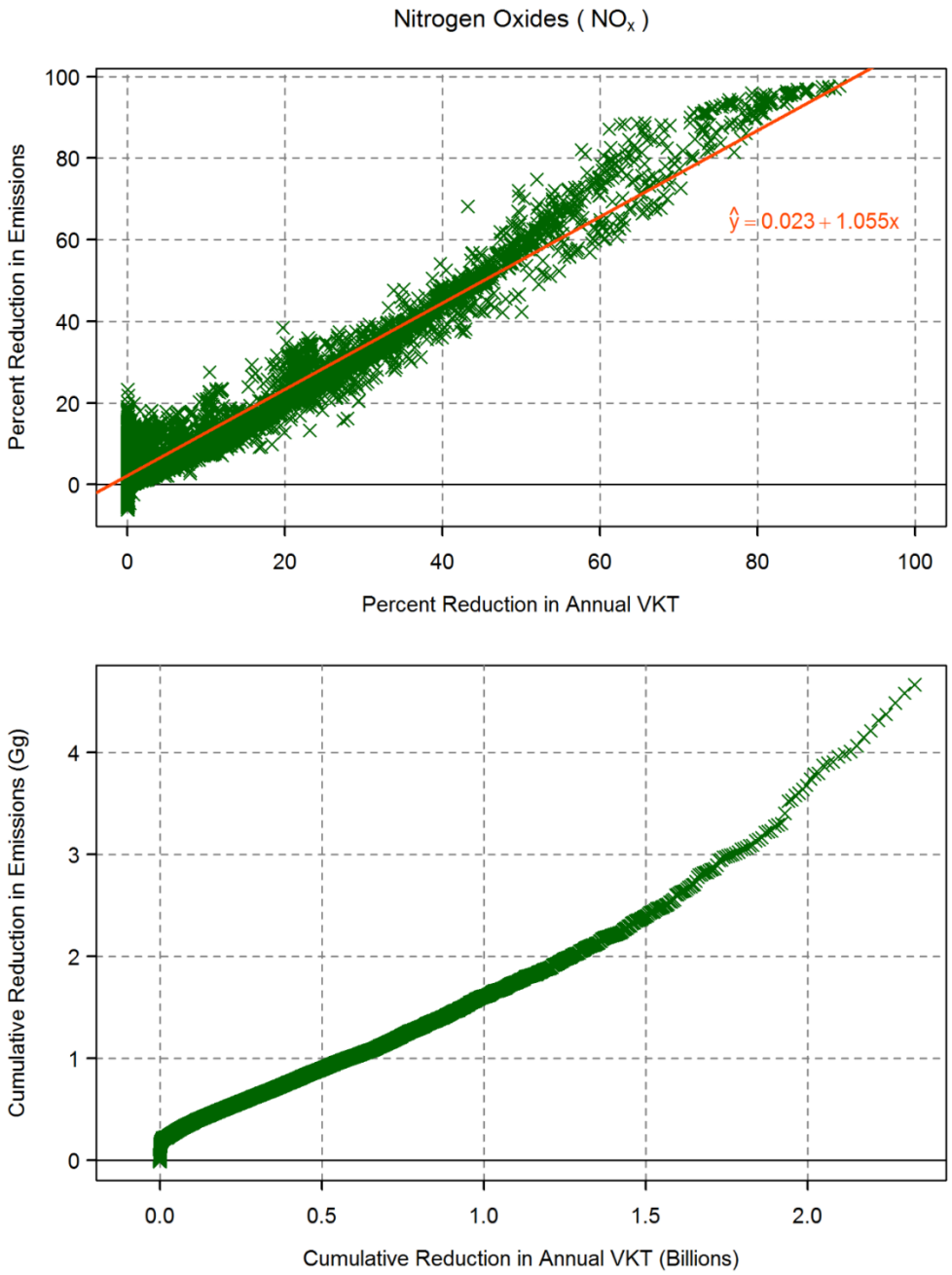

Figure 4.6. Estimated reduction in NO_x emissions in response to VKT reductions on congested road segments. Upper panel shows percent reduction in annual emissions of NO_x for each road segment versus the percent reduction in the road segment's annual VKT required to maintain freeflow travel speeds at all times. Lower panel shows cumulative reduction in total emissions over the entire domain relative to the cumulative reduction in annual VKT for the domain.

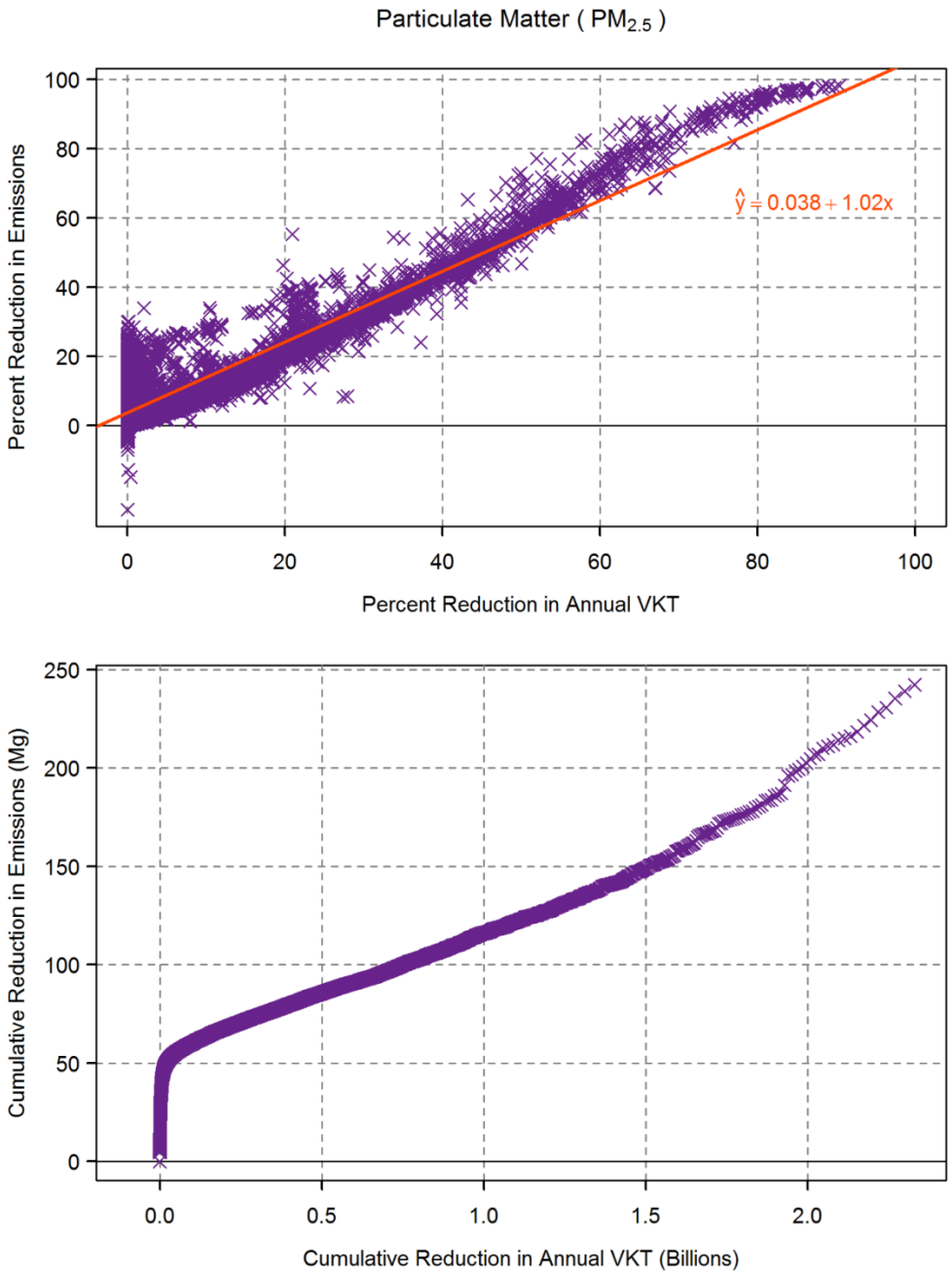

Figure 4.7. Estimated reduction in $PM_{2.5}$ emissions in response to VKT reductions on congested road segments. Upper panel shows percent reduction in annual emissions of $PM_{2.5}$ for each road segment versus the percent reduction in the road segment's annual VKT required to maintain freeflow travel speeds at all times. Lower panel shows cumulative reduction in total emissions over the entire domain relative to the cumulative reduction in annual VKT for the domain.

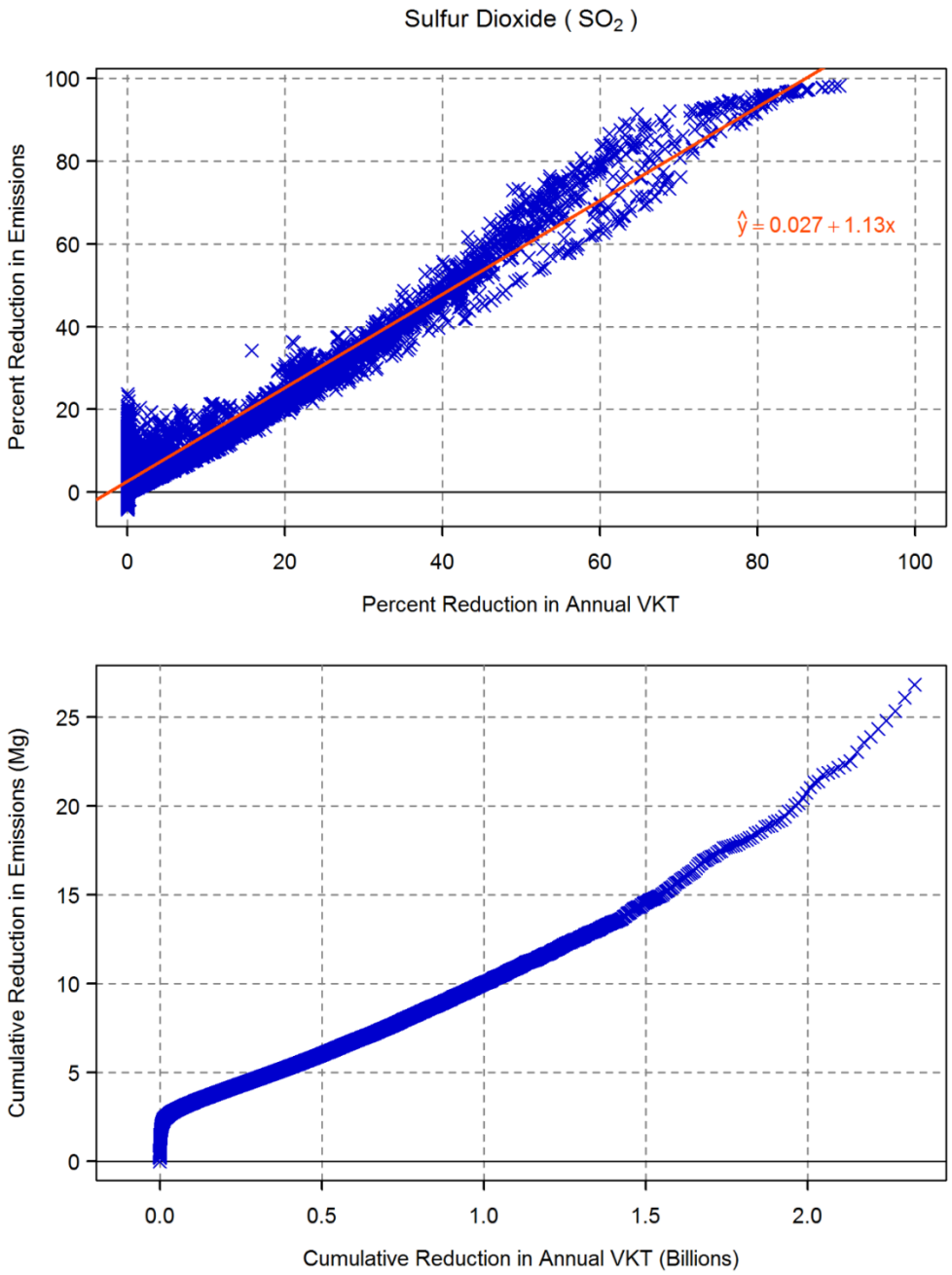

Figure 4.8. Estimated reduction in SO_2 emissions in response to VKT reductions on congested road segments. Upper panel shows percent reduction in annual emissions of SO_2 for each road segment versus the percent reduction in the road segment's annual VKT required to maintain freeflow travel speeds at all times. Lower panel shows cumulative reduction in total emissions over the entire domain relative to the cumulative reduction in annual VKT for the domain.

4.3.5 Impact of Future Climate Change on Emissions

For our final alternative scenario we examined the impact of rising mean air temperature on vehicle running emissions across the domain. We use forecast monthly mean temperatures for eastern Massachusetts in the year 2050 to adjust the 2012 hourly temperatures as described in the methods section of this chapter. VKT and all other parameters were unchanged in this scenario.

The changes to emissions of SO_2, NO_x, and CO_2 from both running and starts was found to be very small (<1% for most grid cells in the domain). For CO and for $PM_{2.5}$ we observed larger changes in specific locations. Overall, CO emissions from running vehicles increased by 2.4% across the domain, with local increases of >25% in many locations (Figure 4.9). For $PM_{2.5}$ the overall change in emissions is negative but small under the 2050 conditions, decreasing by 0.6% for the whole domain, although there are several hotspots where emissions increase by 2.5 – 5% or more (Figure 4.10).

The MOVES model does not adjust emissions rates from combustion for running exhaust for temperatures above 75 F (USEPA 2011b). However, it does account for the additional fuel consumption required to run the vehicle's air conditioning system, and automatically includes the additional emissions

associated with this when temperatures and relative humidity are high. CO emissions are the most sensitive to this 'air-conditioning' effect in the MOVES model, increasing by a factor of 2 when the vehicle is accelerating or cruising, and by 13% when the vehicle is idling. These considerable increases in the emissions rate for CO under 'air-conditioning conditions' likely account for the majority of the increases in CO emissions predicted by our model for 2050.

For $PM_{2.5}$, there is a strong negative correlation between emission rates and temperature. Running exhaust emissions of $PM_{2.5}$ increase by a factor of 3.5 – 5 at 20F relative to 70F (USEPA 2011b), and cold starts $PM_{2.5}$ emissions are higher by a factor of 7 to 11 times at 20F relative to 70F. As forecast changes in mean monthly temperature under SERS A2 are broadly positive across all months and across our whole domain, we expect to see the observed declines in $PM_{2.5}$ emissions from both cold starts and running exhaust as the higher temperatures are less conducive to the production of particulate matter precursors.

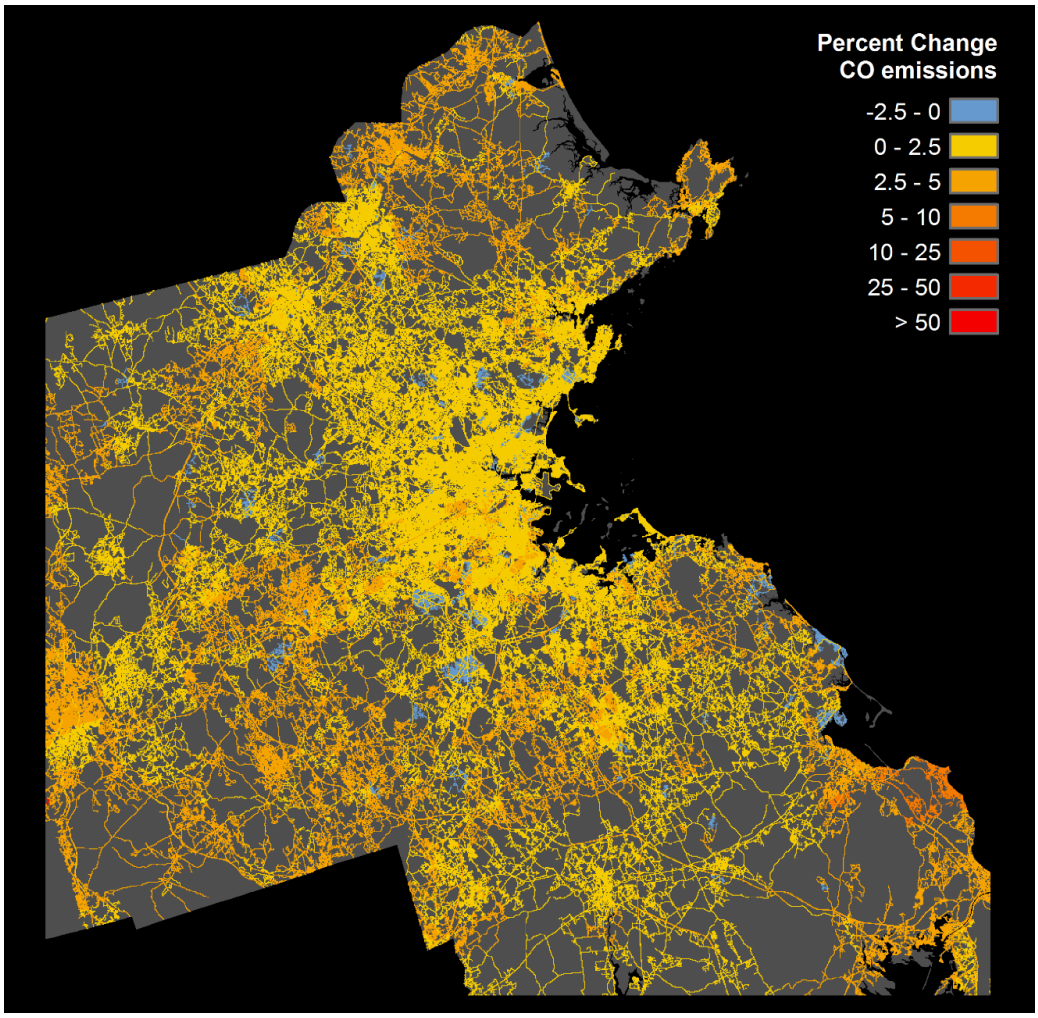

Figure 4.9. Change in emissions of CO due to change in atmospheric temperature forecast under the SRES A2 climate change scenario for the year 2050. On a relative scale, modest increases of 2.5 – 5% are predicted to occur broadly over the study area. Larger increases of 10 – 25 % or more are predicted to occur in a large number of localized areas, and broadly in the more northern parts of the domain. Small areas are predicted to experience modest decreases in CO emissions of ~1-2%.

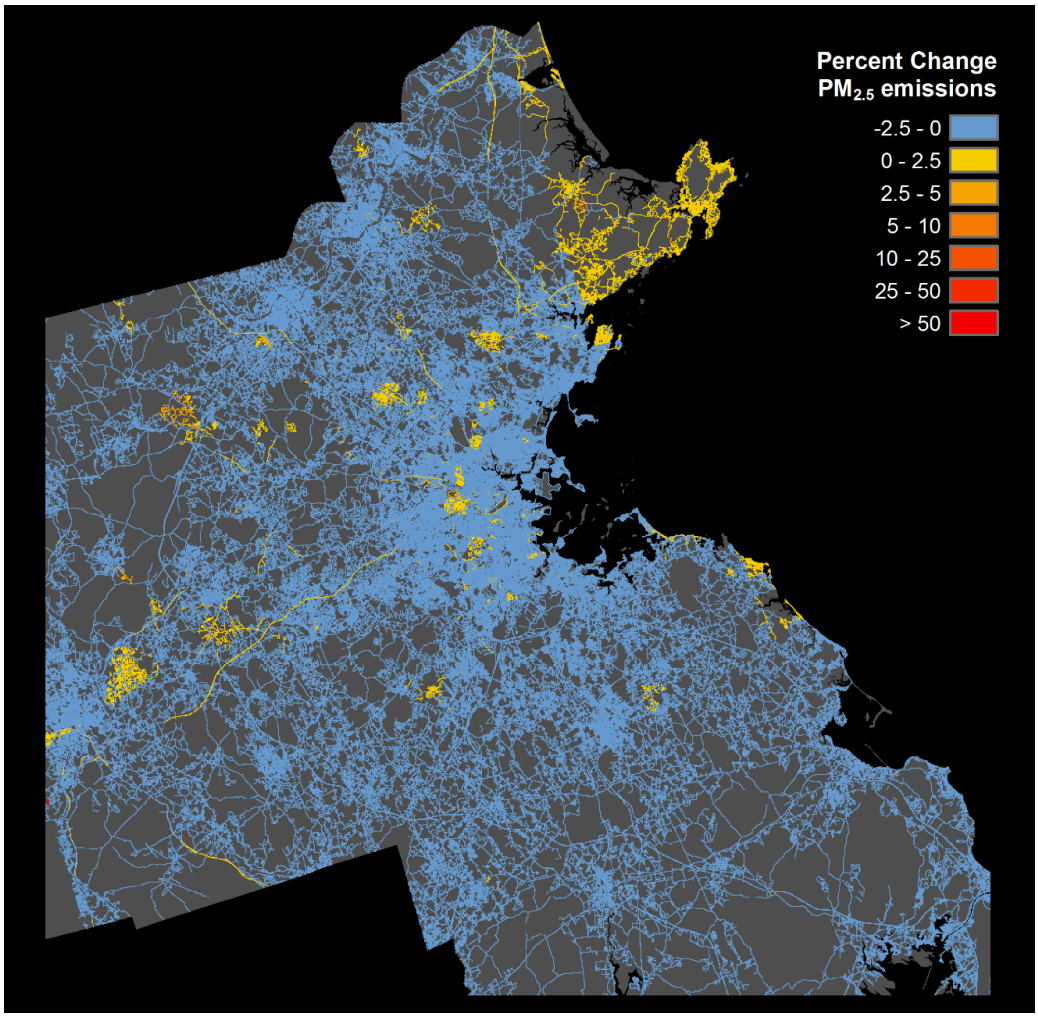

Figure 4.10. Change in emissions of $PM_{2.5}$ due to change in atmospheric temperature forecast under the SRES A2 climate change scenario for the year 2050. Our model predicts modest declines of 0 - 2.5% across most of the study area. $PM_{2.5}$ emissions tend to be higher in cold conditions, so the predicted warming trend for 2050 tends to have a positive impact on emissions from a public health perspective. However we do predict localized large increases of 10 – 25 % or more for a number of areas in the domain, in particular the northeast, where future temperature increases may be more variable.

4.4 Conclusion

In this study we utilize a unique collection of highly detailed datasets to produce a high-resolution inventory of vehicle tailpipe emissions for eastern Massachusetts. Our approach merges data on vehicle speeds and volumes with detailed model outputs from EPA MOVES and the Central Transportation Planning Staff's Travel Demand Model to estimate emissions of five major pollutants at the level of individual roads for every hour of the year 2012. Our emissions estimates fully incorporate data on actual travel speeds to quantify the impact of traffic congestion on emissions, and to separate the influence of different vehicle types on overall emissions profiles at different locations throughout the study area. We integrate data on ambient atmospheric conditions to control for variations in temperature across time and space, and to evaluate the sensitivity of emission rates of certain pollutants to changes in local climate over annual and multi-decadal scales.

Our results identify spatial hotspots of CO_2 emissions, highlight the dominant influence of heavy and medium diesel-powered trucks in driving NO_x and $PM_{2.5}$ emissions, and quantify the elasticity of emissions to reductions in VKT across the domain. We find that the impact of congestion on emissions is relatively small when considered in the context of the very large amount of emissions that

are occurring in the domain even in the absence of congestion. It is clear that the sheer volume of vehicle traffic that travels the roads of eastern Massachusetts on a daily basis presents the major scaling driver of total emissions. The magnitude of total emissions is so large, that while traffic congestion can indeed generate localized, high-intensity emissions events, the potential contribution of any congestion-focused policy to reducing regional air pollution emissions is extremely limited. However, we do find that modest reductions in emissions can be achieved when vehicle volumes are reduced on roads that currently suffer heavy congestion, and that emission reductions of 5-8% can be achieved with traffic reductions of only 3.5%. While the regional reductions of 5-8% that we predict are relatively modest on an annual scale, the potential for targeted reductions that focus on key spatial and temporal hotspots or on heavy-duty vehicle corridors have the potential to produce much larger improvements in emissions and air quality, as we demonstrate in two areas near the core of the Boston metro area.

Finally, in this study we also predict changes in future emissions in 2050 that would occur due to increasing regional temperatures from global climate change. We show that increases in vehicle air-conditioning usage due to rising summer temperatures is expected to increased fuel consumption as well as CO emissions

across the whole domain. However, we also find that warming winter temperatures are likely to result in small reductions in emissions of $PM_{2.5}$ from both cold starts and running exhaust, although we observe numerous localized exceptions to this trend. Future research will continue to explore the spatial and temporal variability in emissions, with a focus on identifying the times and places where human exposure to air pollutant emissions is high due to the colocation of dense residential or commercial areas with high-intensity road segments, and the sensitivity of emissions intensity to variations in local meteorology on multiple time scales.

Additional work is also ongoing to validate these new emissions inventories using direct- and remotely-sensed measurements of ambient concentrations of these pollutants. The influence of ambient meteorology on not only emission rates, but also on the production of additional pollutants due to secondary reactions in the atmosphere continues to be a focus of research, as future global climate change is expected to produce considerable increases in local temperatures for most parts of the world over this coming century. The impacts of rising temperatures on the secondary chemistry associated with production of low-level ozone and other respiratory irritants may add another harmful

consequence to the many others already predicted to arise due to global climate change (Steiner et al. 2006; Kinney 2008; Jacob and Winner 2009).

Additional validation is currently underway in conjunction with the recently launched Orbital Carbon Observatory (OCO-2), the first space-based global-coverage satellite dedicated to direct measurements of atmospheric CO_2 concentrations. The high-resolution emissions inventories produced in this dissertation will play a key role in validating the directly measured estimates of CO_2 reported by OCO-2 and other ground-based sensors. By combining new sources of data on directly measured concentrations with local-scale emissions inventories, it will be possible to quantify temporal and spatial variations in emissions more accurately than ever before. With future improvements to the spatial and temporal resolution of DARTE and the other inventories described above, we can continue to improve on emissions benchmarking that supports the monitoring and mitigation of emissions across all scales, from small metropolitan areas, to megacities such as New York and Los Angeles.

CHAPTER 5 – CONCLUSION

This dissertation reports on the results of several studies designed to improve the understanding of greenhouse gas emissions and other air pollutants from on-road vehicle activity in the United States. The motivating goal of this research was to improve on the existing emissions inventory products that underpin much of the current research into the origins and impacts of fossil fuel CO_2 emissions. The development and implementation of the new, highly detailed inventories published herein has supported the analytical frameworks required to explore the relationships between emissions and the multitude of spatially and temporally correlated variables that contribute to the patterns and trends in fossil fuel CO_2 emissions that we observe. The quantification of these relationships is vital to support policies for monitoring, reporting and verifying future emissions reductions under all types of policy frameworks – from the municipal climate action plans of Boston and New York, to state and regional legislation such as California's AB-32, to the ongoing and future negotiations over the U.S. Climate Action Plan and international negotiations for a comprehensive global treaty.

The development of new data assimilation techniques and the production and public sharing of the novel, high-resolution, spatially explicit data products

that made it possible to conduct the analyses in these studies are also a major contribution to the emissions research and carbon-cycle modeling communities. Current and future research will build on the methods and analyses presented above, and will aim to continue to improve our understanding of the coupled human and natural systems that comprise our world, to support development of sustainable and environmentally sensitive practices to address the impacts of global climate change, and to improve access to scientific data products and analysis for the academic community, the government and non-governmental sectors and the general public at large.

With the recent launch of the Orbital Carbon Observatory (OCO-2), the first space-based global-coverage satellite dedicated to measuring concentrations of atmospheric CO_2, the types of bottom-up, high-resolution emissions inventories produced in dissertation are now taking on a much more prominent role in the monitoring, reporting, and validation of emissions of greenhouse gases at larger scales. The combination of directly measured concentrations with source-based emissions inventories will allow us to understand the temporal and spatial variations in emissions more accurately than ever before. High resolution emissions inventories will continue to play a key role in the attribution of observed atmospheric CO_2 to the wide variety of emissions sources. An accurate

and precise understanding of source attribution is a necessity for both the development of sector-specific emissions mitigation policies, and for monitoring the efficacy of those policies over time. An expansion of the work described in this dissertation to other types of emissions sources, and to other nations and regions across the globe will continue to be a critical avenue of research over the next decade, if we are to successfully inform and support the national and international policy frameworks necessary to deal with the impending impacts of global climate change.

APPENDIX A

All figures and spatial data were projected using the NAD1983 State Plane Massachusetts Mainland FIPS 2001 Lambert Conformal Conic Projection.

1. Detailed Methodology of HPMS-based on-road CO_2 emissions model

Calculate VMT by functional class and county

The Highway Performance Management System (HPMS) is a national database managed by the Federal Highway Administration (FHWA) that contains data on annual average daily traffic volumes (AADT) and centerline mileage for all Federal-Aid roads and most other major and minor roads. We obtained annual VMT for each road section in the HPMS by multiplying the average daily traffic volume by the length of the road section in miles and then multiplied by 365 days. The FHWA requires that the AADT values submitted by each state be adjusted prior to submission to take into account both weekday/weekend and seasonal variations in traffic volumes on the road section. Thus the AADT reported in the HPMS reflects an average daily traffic volume for any day in the calendar year, independent of day of the week or month of the year. While this

limits the use of the data for analyses at shorter time scales, it allows for a straightforward estimation of annual statistics for each road section without having to account for weekly and monthly variations.

The road sections in the HPMS are not geo-coded, and consequently we were not able to assign our annual VMT estimates directly to a map of the road network. However, functional class and county were available for each road section, with each functional class identified as urban or rural depending on if the road section passes through a Census Bureau Urbanized Area or Urban Cluster. Therefore we chose to aggregate our roadway-scale VMT to the county scale, stratified by the 12 HPMS functional classes (FHWA 2005). Since our roadway-scale HPMS data does not include all of the VMT that occurred on local roads it was necessary to use a downscaling approach to account for emissions from these roads. We allocated state-level data from FHWA on VMT for Rural Minor Collectors and Rural and Urban Local roads to each county using the county's fraction of total state VMT as calculated from the HPMS dataset for each year (FHWA 1980-2011; FHWA 2009).

Disaggregate VMT by Vehicle Type

As on-road CO_2 emissions are a product of fuel combustion, and the rate of emissions is a function of fuel type (EIA 2007), our intermediate goal was to estimate diesel and motor gasoline fuel consumption for each functional class and county. First we partitioned annual vehicle miles travelled amongst five different vehicle types: passenger cars, passenger trucks (which includes SUVs, vans and pickup trucks), buses, single-unit trucks and combination trucks. State-level data on the distribution of VMT among different vehicle types is available for the years 1993 through 1999 and for 2009 and 2010 (FHWA 1980-2011). A comparable national average distribution for the years 1980 to present exists as well. However, when we compared the state and national distributions for 1993 through 1999 we observed that Massachusetts had significantly lower fractions of passenger truck and heavy truck VMT across all road types relative to the national average (FHWA 1980-2011). Since this difference would strongly affect our fuel estimates, we chose to use the state-level data for the available years and to estimate values for the years prior to 1993 and after 1999. For our model years 1999 through 2008 we interpolated linearly between the state-level distributions for 1999 and 2009; for years prior to 1993, we applied the 1993 distribution for all years.

Estimate fuel consumption by vehicle type, functional class, and county.

We used the national average fuel economy for each vehicle type for each year (FHWA 1980-2011) to estimate fuel consumption for each roadway functional class, county and year. Fuel consumption was calculated as the quotient of distance travelled and average fuel economy. We assumed all fuel consumption by passenger cars and passenger trucks was motor gasoline, all fuel consumption by buses and combination trucks was diesel fuel, and that fuel consumption for single-unit trucks was 23% motor gasoline and 77% diesel fuel. The fuel shares for single-unit trucks were taken as an average value across the study period using reported fuel consumption by medium and heavy vehicles obtained from the 2010 Transportation Energy Data Book (USDOE 2011).

Calculate CO_2 emissions by functional class and county

We used emissions factors to estimate the CO_2 emissions produced by the fuel consumption for each vehicle type. Fuel consumption was converted to CO_2 emissions using the emission factors of 8.91 kg CO_2 per gallon gasoline and 10.15 kg CO_2 per gallon diesel fuel (EIA 2007). We then aggregated CO_2 emissions from both fuels to obtain total emissions for each functional class of road at the county scale.

Assign emissions to road network

To assign emissions to a map of the road network we used the 2009 GIS Road Inventory (Massachusetts Department of Transportation 2009) which provides the length and functional class of almost every road section in the state. We recognize that the road network has changed in extent since 1980, but FHWA records for Massachusetts indicate that total centerline mileage increased only 6.9%, from 33,777 in 1980 to 36,105 in 2008 (FHWA 1980-2011). We decided to use the Road Inventory for our analysis, as it is the only geo-referenced dataset that covers all Massachusetts roads. However, we note that the use of this dataset might introduce potential errors due to the allocation of historical emissions across the contemporary road network.

To assign CO_2 emissions to each road we calculated the total centerline mileage of each functional class of road in each county, and then divided our relevant CO_2 emissions by this mileage to generate average per-mile CO_2 emissions. These average per-mile emissions were then assigned by functional class and county to the road network for each year in the study period.

Aggregate road-level emissions to other spatial scales

For comparability with other CO_2 emissions inventories, we aggregated our roadway-scale emissions to multiple scales: a 1km x 1km grid, a 0.1 x 0.1 degree grid, and summed to the level of local towns. The 1km grid cells provided a high-resolution display of the emissions data in a gridded format. The 0.1 degree grid aggregation provided for a direct comparison with the EDGAR and Vulcan inventory products. The town level data was used in regression analysis of the spatial and temporal correlations between emissions and population density, as population data for the full time series was only available at the town scale. All figures and spatial data were projected in ESRI ArcGIS 10.0, using the NAD1983 State Plane Massachusetts Mainland FIPS 2001 Lambert Conformal Conic Projection.

2. Cell-by-cell comparison of HPMS and Vulcan emissions for 2002

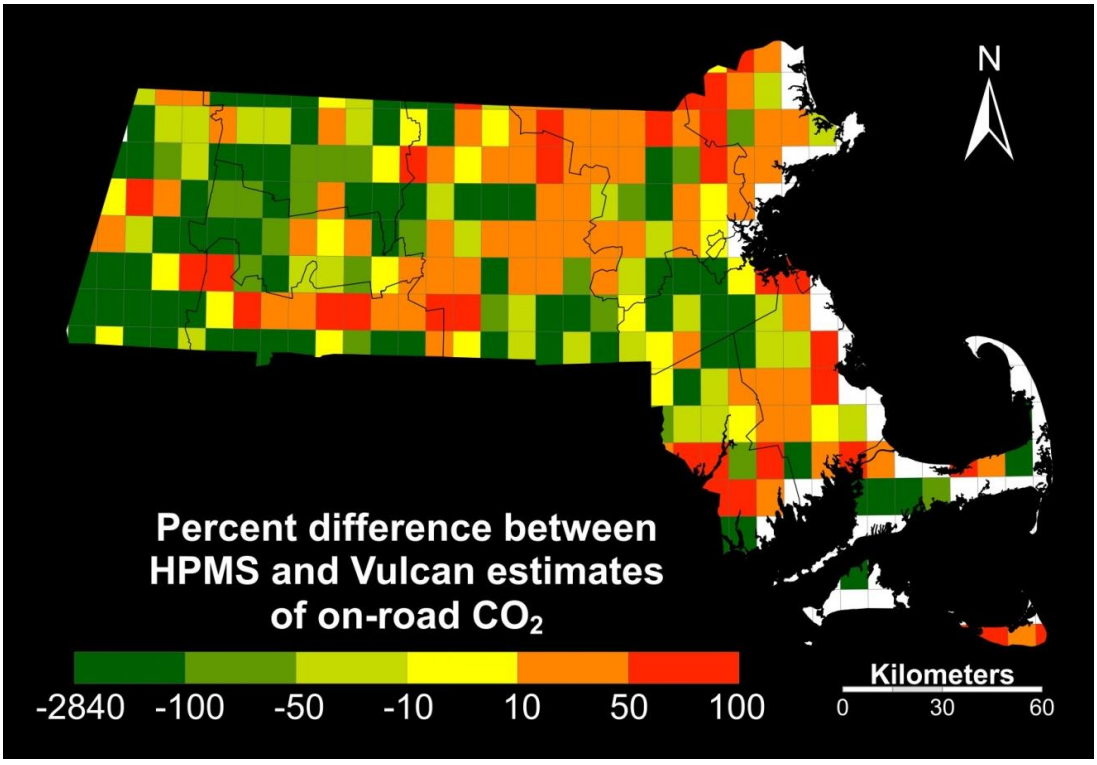

Figure A1. Percent differences between HPMS model CO_2 estimates and Vulcan Product estimates for the year 2002, at 0.1 degree grid scale. Values calculated as: (HPMS – Vulcan) / HPMS *100; positive values indicate grid cells where HPMS estimates exceed Vulcan estimates. White grid cells indicate cells where Vulcan reports zero emissions. This is a result of the re-gridding process used by Vulcan to transform the original 10km^2 gridded results to the 0.1 degree grid (Gurney et al. 2010). Note that the HPMS model produces higher emissions estimates than Vulcan in urban areas, whereas the opposite is true in more rural or less populated areas.

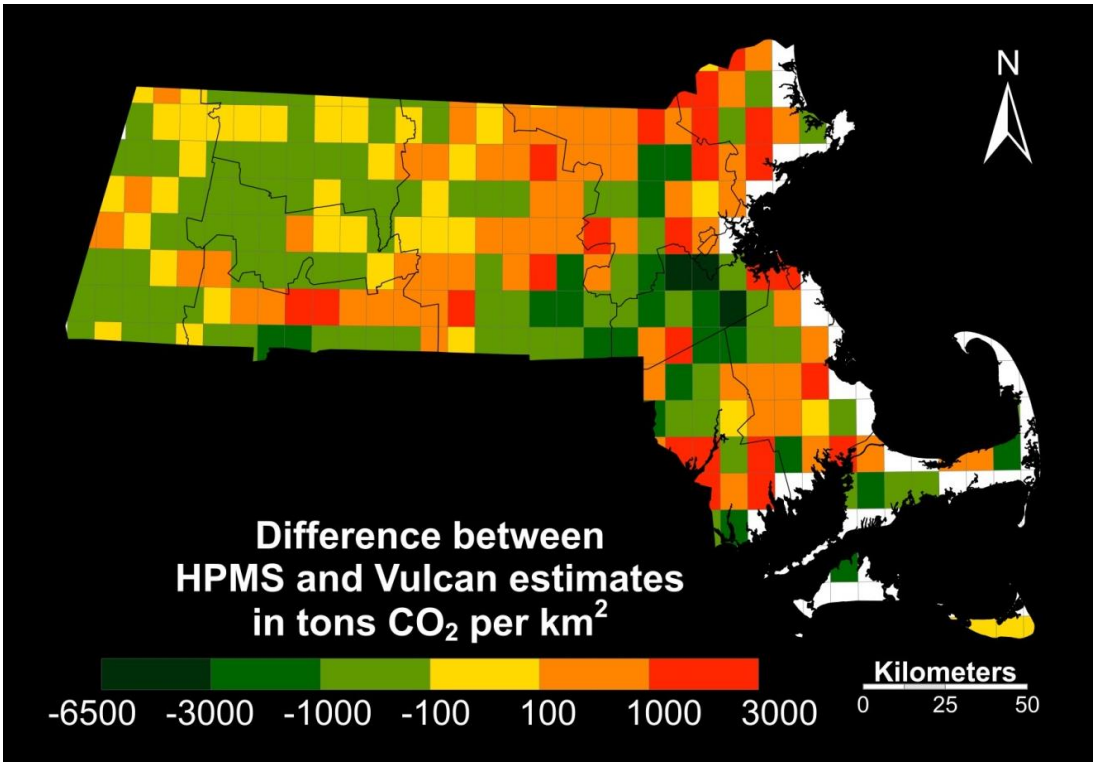

Figure A2. Absolute difference in estimates of tons CO2 per square kilometer between HPMS and Vulcan. Positive values indicate cells where our HPMS model predicts higher CO2 emissions than the Vulcan Product. The spatial distribution of raw difference between the two models is similar to that of the percent difference, with HPMS producing higher estimates in urban areas relative to Vulcan (north central, north eastern and south eastern areas), and Vulcan producing higher emissions estimates in rural areas (western regions and parts of south central and south eastern areas).

Uncertainty Estimates

The uncertainty associated with annual average daily traffic (AADT) values reported in HPMS is characterized by the confidence intervals and precision levels reported in Chapter 6 of the HPMS Field Manual (FHWA 2005). These confidence intervals vary by functional class, and take the form of a

combined confidence interval and precision level in the form of A-B, where is A is the probability that the value falls within B percent of the true value. For example a reported uncertainty of 90-10 would mean that 90 percent of the time the reported value will be within 10% of the true value.

However, as each functional class of road has a different confidence interval and precision level associated with its AADT estimates, these cannot be directly combined into an overall estimate of the uncertainty in AADT for the whole HPMS data set. To standardize this uncertainty, Mendoza et al. (2013) converted each HPMS confidence interval / precision level into one-sigma percent uncertainties as quoted below:

"…the stated confidence interval and precision level were combined into a single estimate of uncertainty as follows:

$U_x = V_x / S_x$

Where U_x is the uncertainty percent value associated with road type; V_x is the percent variation from the true value for road type (10 for 90-10); and S_x is the number of standard deviations within a normal distribution that is within variation of the true value for road type ("90" for 90-10)."

Source: Mendoza et al. 2013

Using this method Mendoza et al. estimate one-sigma percent uncertainties for Rural Interstates and Rural Principal Arterials of ±3.04%, for Rural Minor Arterials of ±6.08%, and for all other functional classes of road of ±7.8%. These are one standard deviation percent uncertainties, which represent roughly a 68.3% confidence interval. To estimate a broader confidence interval we also calculated a two-sigma uncertainty, equivalent to a 95.4% confidence interval. To do this, we doubled the one-sigma percent uncertainties reported in Mendoza et al. 2013. We used both the one-sigma and two-sigma percent differences to calculate upper and lower estimates of AADT for each road in our dataset. We then ran our model using these values to produce upper and lower estimates of CO_2 emissions for each road section. The one-sigma shifted AADT produced emissions estimates that ranged from ±7.4% to ±7.6% relative to our original CO_2 estimates. The two-sigma shifted AADT produced emissions estimates that ranged from ±14.7% to ±15.2% relative to our original estimates. Both of these ranges correspond well with the empirical estimates of AADT uncertainty by Ritchie (1986) and Gadda et al. (2007), and suggest that the FHWA confidence/precision levels provide a reasonable basis for assessing the uncertainty of CO_2 emission estimates generated from the AADT values reported

by HPMS. We report the upper and lower bound estimates of CO_2 emissions from our HPMS model in Figure A3.

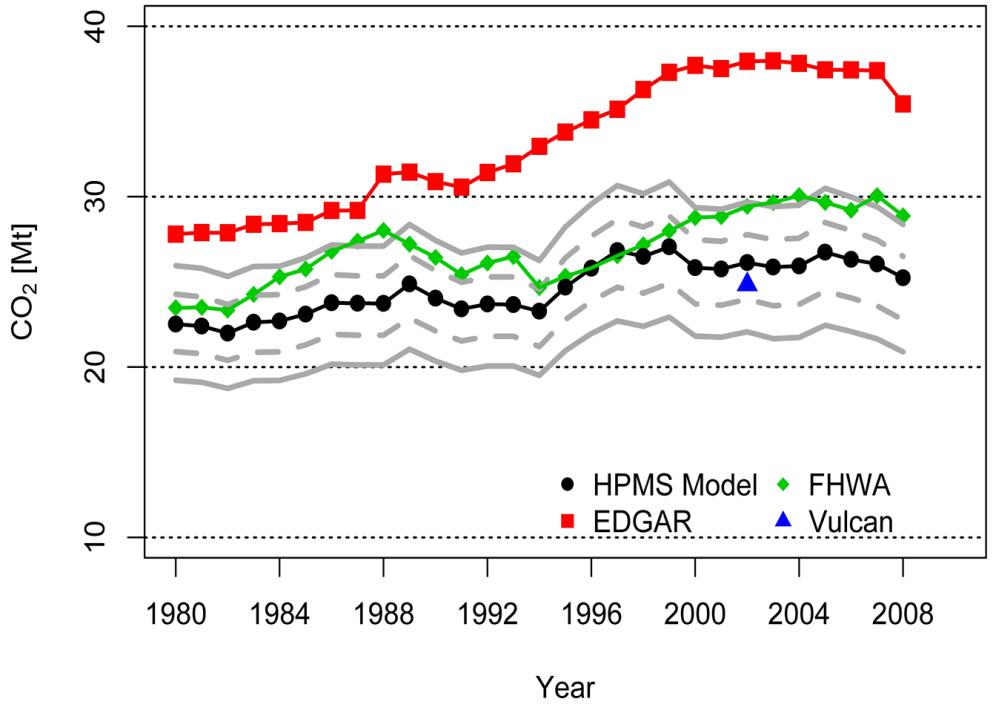

Figure A3. Plot of CO_2 estimates from HPMS, FHWA, EDGAR and Vulcan. Solid gray line shows upper and lower estimates from HPMS model run with two-sigma percent changes in AADT. Dashed gray line shows upper and lower estimates from one-sigma percent change in AADT.

Results of panel regression.

Number of obs.	10150		
F(389, 9760)	1513.35	R-squared	0.933
Prob. > F	0.0000	Root MSE	104.29
Variable	**Coefficient**	**Standard Error**	**t**
pop / km^2	-26.684	2.971	-8.980
pop / km^2 > 10	13.842	3.296	4.200
pop / km^2 > 50	10.577	1.531	6.910
pop / km^2 > 100	3.580	0.463	7.740
pop / km^2 > 200	0.036	0.197	0.180
pop / km^2 > 500	-0.418	0.100	-4.170
pop / km^2 > 1000	-0.713	0.095	-7.530
pop / km^2 > 2000	-0.346	0.082	-4.200
pop / km^2 > 3000	0.130	0.060	2.170
pop / km^2 > 4000	-0.243	0.073	-3.340
pop / km^2 > 5000	0.140	0.073	1.900
pop / km^2 > 6000	0.120	0.031	3.880
constant	775.924	85.122	9.120

Table A1. Results of panel regression analysis. Dependent variable is tons of CO_2 emissions per mile of road. Town and year fixed effects not shown.

APPENDIX B

DARTE is available for download at http://dx.doi.org/10.3334/ORNLDAAC/1285 or at dx.doi.org/10.7910/DVN/28999

Data Sources and Methodology

The Highway Performance Monitoring System (HPMS) is a traffic monitoring program overseen by the Federal Highway Administration. All U.S. states and the District of Columbia are required to submit annual estimates for a wide variety of traffic and highway condition data to HPMS in compliance with federal statute. This data has been archived in a digital tabular format since 1980, and was made available to us upon request. The data format is described in detail in the HPMS Field Manual (FHWA 2005), which has been published and revised on a roughly 5 year cycle since 1977. The HPMS underwent significant revisions in 2010, with the most notable change being the requirement that states submit data in a GIS shapefile format. The HPMS dataset used to generate the 1980 – 2009 emissions estimates in DARTE is based on the old format of HPMS data, which is well described in the archived versions of the HPMS Field Manual (FHWA 2005). The raw HPMS data is unavailable for year 2010 due to issues

associated with the transition to the GIS format. We imputed this data using the HPMS data from neighboring years as described below. For 2011 and 2012 we obtained the new GIS shapefile formatted HPMS data from FHWA and extracted the feature data into a tabular format compatible with the 1980 – 2009 data series. Data from all years was then merged into a single database.

The core data features of the HPMS are individual road segments that are defined by the state transportation departments. For each road segment HPMS reports the center-line length in miles, annual average daily traffic (AADT), functional class, urban/rural context, and county. AADT is a measure of the number of vehicles that traverse the road segment on an average day, adjusted for seasonal and day-of-week variation. Measurements of AADT are obtained from roads with permanent traffic recorders (PTRs) and from repeated short-term (48-72 hour) traffic counts performed throughout the year on other roads in the network. Data from PTRs is used to develop monthly, weekly, and day-of-week scaling factors that are then applied to short-term count data to obtain AADT values for neighboring roads that lack PTRs.

We calculated annual vehicle miles travelled (VMT) on each road segment in HPMS by multiplying AADT by the length of the road segment and then by 365 days. Since the individual road segments in HPMS were not explicitly geocoded

until 2011, we aggregated road-segment VMT to the lowest common level of geography. There are 12 roadway functional classes included in HPMS (Table B1), six for urban roads and six for rural roads. Urban roads are defined as any road segment that falls partially or entirely within the boundaries of a Census Urbanized Area or Urban Cluster. We aggregated the HPMS data to counties by using the reported functional classes and a geocoded road network for the U.S. that is also partitioned by these functional classes.

Code	Description	Code	Description
RURAL		URBAN	
1	Principal Arterial - Interstate	11	Principal Arterial - Interstate
2	Principal Arterial - Other	12	Principal Arterial-Other Freeways & Expressways
6	Minor Arterial	14	Principal Arterial - Other
7	Major Collector	16	Minor Arterial
8	Minor Collector	17	Collector
9	Local	19	Local

Table B1. Highway Performance Monitoring System – Table of Roadway Functional Classification Definitions (FHWA 2005).

Although road segments in the 2011 and 2012 HPMS are individually geocoded, we chose to preserve the consistency and continuity of our emissions time series by performing the same aggregation by functional class and county and then merging all years of data into a uniformly formatted database. With the transition of HPMS to the GIS submission model, a subset of states submitted

their 2009 HPMS data in the new GIS format. We performed a similar aggregation by functional class and county to this VMT, as was done with the 2011 and 2012 data. For 2010, there was no archived data from HPMS available; we linearly interpolate VMT between the 2009 and 2011 values of the HPMS raw data for each combination of county and urban/rural functional class.

The HPMS database does not include roadway-level data for many minor and local roads, as it was originally conceived as a highway-focused database. However, the archived data contains 'Summary Files' wherein states report VMT for rural and urban minor collectors, as well as urban local roads. State-level VMT for rural local roads is reported separately in Highway Statistics Table VM-2 (FHWA 1980-2012). We integrate this state-level local road VMT data into our county-level database by allocating state totals by functional class to each county as shown in equations A.1 and A.2:

$$VMT_{c,f_{urban\ minor/local}} = VMT^{summary}_{s,f_{urban\ minor/local}} \times \frac{\sum_{f_{urban}} VMT^{hpms}_{c,f}}{\sum_{f_{urban}} VMT^{hpms}_{s,f}} \quad \text{(A.1)}$$

$$VMT_{c,f_{rural\ minor/local}} = VMT^{summary}_{s,f_{rural\ minor/local}} \times \frac{\sum_{f_{rural}} VMT^{hpms}_{c,f}}{\sum_{f_{rural}} VMT^{hpms}_{s,f}} \quad \text{(A.2)}$$

Where:

- $VMT_{s,f_{urban\ minor/local}}^{summary}$ is the total VMT for urban minor collectors or local roads in state $\boldsymbol{S}$ reported in the HPMS Summary Files
- $\sum_{f_{urban}} VMT_{c,f}^{hpms}$ is the sum of all urban road VMT reported to HPMS for county $\boldsymbol{C}$
- $\sum_{f_{urban}} VMT_{s,f}^{hpms}$ is the sum of all urban road VMT reported to HPMS for state $\boldsymbol{S}$ that contains county $\boldsymbol{C}$
- $VMT_{s,f_{rural\ minor/local}}^{summary}$ is the total VMT for rural minor collectors or local roads in state $\boldsymbol{S}$ reported in the HPMS Summary Files or Highway Statistics Series Table VM-2, respectively
- $\sum_{f_{rural}} VMT_{c,f}^{hpms}$ is the sum of all rural road VMT reported to HPMS for county $\boldsymbol{C}$
- $\sum_{f_{rural}} VMT_{s,f}^{hpms}$ is the sum of all rural road VMT reported to HPMS for state $\boldsymbol{S}$ that contains county $\boldsymbol{C}$

The resulting database contains a complete VMT time series for every functional class of road present in each county for the years 1980 – 2012.

Data Quality Assurance & Control

We inspected the complete time series of VMT by county and functional class to identify potential outliers or structural breaks in the dataset. We developed a filtering algorithm that flagged any observation in an individual county/functional class time series if the magnitude of the year-on-year difference between an observation and adjacent years was greater than two standard deviations from the mean year-on-year difference of that time series. For these single points that deviated significantly from the trend of the series, we removed the value and replaced it with an imputed value obtained by fitting a lowess curve to the full time series minus the removed value.

In some cases, we observed apparent structural breaks in a county/functional class time series when a county or state reclassified roads to a different functional class, thereby shifting a significant amount of VMT to that new class. This occurred most often in the years following a Decennial Census, when the boundaries of Urbanized Areas were revised and roads that were previously classified as rural were shifted to the urban equivalent of their previous functional class. In those cases, there was no observed break in the state's time series for total VMT, and our algorithm did not generate a flag. However, visual inspection of the data noted the presence of a small number of genuine structural

breaks that could not be explained by road reclassification. These cases tended to be similar in style to the single outlier observations described above, but instead of a single errant observation we observed small clusters of 2-4 observations that were bookended by large, oppositely signed deviations from the main trend of the time series. The filtering algorithm identified these in the same manner as the single outliers, with the similar condition that no concurrent and complementary deviations were present on any other road classes in that county. These observations were similarly dropped and imputed using values from a lowess fit to the series minus the outlying cluster. Of the 761,759 observations in the dataset, roughly 10% were flagged and replaced by our filtering procedure.

Partitioning VMT by vehicle type

For each year, county, and functional class, we partitioned annual VMT from HPMS into the five vehicle types used by the Highway Statistics Series Table VM-4 (FHWA 1980-2012): Passenger cars, passenger trucks (SUV, pickups, mini-vans), buses, single-unit trucks, and combination trucks. Motorcycle VMT was included with passenger cars. The values in Table VM-4 were estimated by state transportation departments based on vehicle classification studies, transit agency data, the number of registered vehicles of each type in the state, and data on

interstate freight travel. These vehicle type estimates can be used to calculate the total volume of fuel consumed by each vehicle class by dividing VMT by vehicle fuel economy. However, using the reported vehicle shares and the average fuel economies for each vehicle type (FHWA 1980-2012) produced gasoline and diesel consumption totals that did not match the values reported in Highway Statistics Table MF-21 (FHWA 1980-2012) for most states. As Table MF-21 is based on state tax revenue from fuel sales, we considered it to be the most reliable estimate of fuel consumption at the state level. To correct for this mismatch, we developed a calibration routine to make small adjustments to the reported vehicle shares and fuel economies for each state, such that the resulting calculations of gasoline and diesel consumption for each state were within ± 5% of the values reported in Table MF-21. This routine was developed and performed using the CONOPT optimization routine in the software package GAMS.

Vehicle shares calibration routine

The calibration routine is initialized using the reported values for vehicle shares taken from the Highway Statistics Series Table VM-4. For years prior to 1993, initial values for vehicle shares of VMT are assigned the values reported in the 1993 Table VM-4, the first year that this table was published. Attempts were

made to initialize the model using national average vehicle shares reported in Highway Statistics Series Table VM-1, which are available for 1980-1993, but model convergence and calculations of fuel consumption was found to be extremely poor. Our review of state-level vehicle shares in Table VM-4 showed that there is significant variation about the national mean for vehicle shares, and therefore the national average is not a sufficiently precise representation of local vehicle fleet VMT distributions. We used the 1993 Table VM-4 values for each state for the years prior to 1993. For the years 1993-1997, we used vehicle shares reported in each year's Table VM-4. For the years 1998-2008, publication of Table VM-4 was temporarily suspended. Publication was then resumed in the year 2009. For each state and functional class, we linearly interpolated vehicles shares between the 1997 and the 2009 and used those values to initialize the model for the intervening years. For years after 2009 we use the published VM-4 shares.

National average fuel economies for each vehicle type were obtained from Highway Statistics Series Table VM-1 (FHWA 1980-2012). For passenger cars and passenger trucks we assumed all fuel consumption is motor gasoline. For buses and combination trucks we assumed all fuel consumption is diesel fuel. Single-unit truck VMT was split into diesel and gasoline shares using data from the Vehicle Inventory and Use Survey (VIUS) conducted in the years 1982, 1987,

1992, 1997 and 2002 (U.S. Census Bureau 1982-2002). For the years prior to 1982, the 1982 share was used. For years between 1982 and 2002, we interpolated the shares linearly between each VIUS. Since VIUS was discontinued in 2002, for years after 2002 we used the value from the 2002 VIUS.

Optimization of vehicle shares and fuel economies was performed annually, starting with 1980. The initial values for each year were provided as described above. The calibration routine used this initial data to calculate gasoline and diesel consumption for each vehicle type in each functional class for each state. Gas and diesel consumption was then summed to the state level for each year. For each year the model minimized the sums of squared deviations between initial and optimized values for vehicle fuel economies, gasoline and diesel consumption, and single-unit truck gas/diesel share, subject to the following constraints:

1. Final calculated state totals of gas and diesel consumption must be within 5% of state totals published in Highway Statistics Series Table MF-21.
2. Fuel economy for each vehicle type must be within 3 miles per gallon of national average for that vehicle type.

3. Year-on-year changes to the share of VMT for any given vehicle type could not be more or less than 10% of previous year's share for that vehicle type.
4. Total VMT by functional class in each state must match exactly the reported values from Highway Statistics Series Table VM-2.

Fuel economies, vehicle shares, and single-unit truck gas/diesel split for each functional class of road in each state were adjusted from initial values by the routine, subject to the above constraints. State totals of VMT by functional class were not altered. This routine's output included calibrated values for the vehicle shares of VMT for each functional class and state, the fuel economies for each vehicle type by functional class and state, and the single-unit truck gas/diesel split by state. We then applied these values to our full HPMS dataset of VMT at the county/functional class level.

The HPMS dataset partitions VMT across 12 functional classes of road, but vehicle shares in Table VM-4 were reported only for a more aggregated set of 5 functional classes. The output of the calibration routine was similarly partitioned by these 5 functional classes, and we used a crosswalk table (Table B2) to assign the calibrated vehicle shares and fuel economies to all county/functional class

pairs in the HPMS database. All counties within a state were assigned the same state-level vehicle shares and fuel economies by functional class for a given year.

Highway Statistics Series			Highway Performance Monitoring System	
Code	*Description*		*Code*	*Description*
1	Rural Interstates and Freeways		1	Rural Principal Arterial - Interstate
2	Rural Principal Arterials		2	Rural Principal Arterial - Other
3	Rural Other Arterials		6	Rural Minor Arterial
3	Rural Other Arterials		7	Rural Major Collector
3	Rural Other Arterials		8	Rural Minor Collector
3	Rural Other Arterials		9	Rural Local Road
4	Urban Interstates and Freeways		11	Urban Principal Arterial - Interstate
4	Urban Interstates and Freeways		12	Urban Arterial - Other Freeways & Expressways
5	Urban Other Arterials		14	Urban Principal Arterial - Other
5	Urban Other Arterials		16	Urban Minor Arterial
5	Urban Other Arterials		17	Urban Collector
5	Urban Other Arterials		19	Urban Local Road

Table B2. Crosswalk table between functional classifications used for roads in Highway Statistics Series Tables VM-1 and VM-4 and the functional classifications system used in the Highway Performance Monitoring System.

VMT for each county / functional class was partitioned across the five vehicle types, and motor gasoline and diesel fuel consumption was calculated using the fuel economies for each vehicle type. Single-unit truck VMT was further partitioned into gasoline and diesel shares, with fuel consumption calculated separately. The same fuel economy was used for both gasoline and diesel single-unit trucks in a given state and functional class of road. Total gasoline and diesel consumption for each county and functional class was converted to emissions of

CO_2 using emissions factors of 8.91 kg CO_2 $gallon^{-1}$ gasoline and 10.15 kg CO_2 $gallon^{-1}$ diesel (EIA 2007). Emissions from gasoline and diesel consumption were summed by county and functional class for assignment to the GIS road network.

We used 2012 Census TIGER/Line road shapefiles for all states in the coterminous U.S. The TIGER road network classifies roads using only 3 functional classes, and does not distinguish between urban and rural roads. We therefore intersected the TIGER road shapefile with a polygon shapefile of the Census 2000 Urbanized Areas and Urban Clusters to add an urban/rural classification to each TIGER road segment. Next we aggregated our HPMS-based emissions to the 3 urban and 3 rural functional classes of the TIGER road network as shown in Table B3.

MFCC Code	*Description*		*Code*	*Description*
S1100	Primary Road		1	Rural Principal Arterial - Interstate
S1100	Primary Road		2	Rural Principal Arterial - Other
S1200	Secondary Road		6	Rural Minor Arterial
S1200	Secondary Road		7	Rural Major Collector
S1400	Local Road		8	Rural Minor Collector
S1400	Local Road		9	Rural Local Road
S1100	Primary Road		11	Urban Principal Arterial - Interstate
S1100	Primary Road		12	Urban Arterial - Other Freeways & Expressways
S1100	Primary Road		14	Urban Principal Arterial - Other
S1200	Secondary Road		16	Urban Minor Arterial
S1200	Secondary Road		17	Urban Collector
S1400	Local Road		19	Urban Local Road

Table B3. Crosswalk table between functional classification systems of Census TIGER/Line road network and HPMS.

We calculated the total length in kilometers of each functional class of road in each county in the TIGER network, and divided our CO_2 emissions by this length to obtain per-kilometer emissions for each year/county/functional class. These per-km emissions were then assigned to all segments in the TIGER road network. The road network was intersected with a 1 x 1 km grid and a 0.01 x 0.01 degree grid, and the new lengths of the road segments within each grid cell were calculated. Total emissions for each grid cell were obtained by multiplying the new road segment lengths by the per-kilometer emissions assigned to each segment and then summing by grid cell.

Both the 1km and 0.01 degree DARTE grids were based on the grids used by the Vulcan (Gurney et al. 2009) and EDGAR (EC/JRC 2011a) emission inventories, respectively. The 1km grid has the same datum and geographic projection as the Vulcan grid, and is an even division of the Vulcan 10km grid cells, such that all cell boundaries overlap exactly. The same is the case with the 0.01 degree grid with respect to the EDGAR 0.1 degree grid. This was done so that DARTE can be easily compared and combined with Vulcan and EDGAR emissions from other sectors without the need for re-gridding.

Comparison of DARTE with EDGAR and Vulcan inventories

National on-road CO_2 emissions totals for DARTE, the EDGAR and Vulcan inventories, the EPA national greenhouse gas inventory (USEPA 2014), and emissions calculated from FHWA state-level fuel consumption data (FHWA 1980-2012) show broadly consistent patterns in time (Figure B1). DARTE emissions are within 3% of EPA and FHWA values, while EDGAR emissions are systematically lower than DARTE, EPA, and FHWA, with an average annual deviation of 8%.

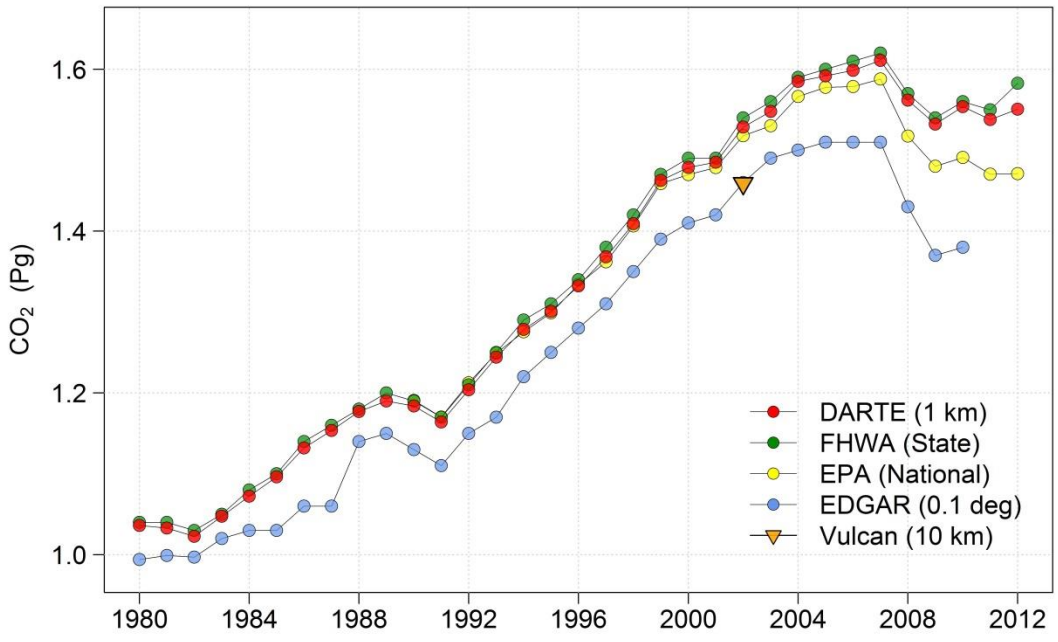

Figure B1. Comparison of total national on-road CO_2 emissions reported by DARTE with the EDGAR and Vulcan Inventories, the EPA national greenhouse gas inventory and emissions calculated from FHWA state-level

fuel consumption data. The spatial resolution of each inventory is shown parenthetically in the legend.

To examine the sub-national differences between EDGAR and DARTE emissions, DARTE was aggregated to the 0.1 degree EDGAR grid, and grid cells were classified based on the fraction of each cell's overlap with the U.S. Census 2000 Urbanized Areas and Urban Clusters. Although national emission totals were similar for DARTE and EDGAR (Figure B1), when they were compared on a cell-by-cell basis large deviations in emissions were observed, with EDGAR exceeding DARTE by as much as 500% in some locations (Figure B2). There was a systematic positive bias of EDGAR emissions in urban areas relative to DARTE, with over 30% of cells in the 75% urban category having EDGAR emissions that exceeded DARTE by more than 50%. For a full 25% of all grid cells EDGAR emissions exceeded DARTE by greater than 50%. The relative biases in EDGAR emissions for rural cells were similarly large, but less systematic: 40% of rural cells had EDGAR emissions 50% lower than DARTE and 29% of rural cells had EDGAR emissions 50% higher than DARTE.

EDGAR's use of road density as a sole proxy assumes a uniform emission factor per kilometer of road, which causes CO_2 to be over-allocated to low-traffic roads and under-allocated to high-traffic roads. This is most clearly visible across

the Midwest and the rural Southeast (Figure B3), where EDGAR emissions showed a large negative bias relative to DARTE in grid cells containing major interstate highways (green), and a positive bias in grid cells dominated by local rural roads (orange). These deviations demonstrate the mismatch between road extent and vehicle activity that occurs at this scale. Symmetrically, in large urban areas EDGAR's estimates significantly exceeded DARTE in city centers while underestimating at the suburban and exurban fringes. Although many urban roads carry large amounts of traffic, and hence are responsible for the majority of emissions, urban areas also contain a large number of local roads which are comparatively lightly travelled. EDGAR's use of a constant emission factor across road classes with very different activity levels is likely the main source of the large spatial biases we observed relative to DARTE. Overall, the spatial structure of EDGAR on-road emissions does not appear to be consistent with the spatial patterns of the underlying emission-generating source activity.

Aggregating DARTE's 2002 CO_2 estimates to Vulcan's 10km grid revealed similarly large spatial differences in emissions, with Vulcan estimates exceeding DARTE by 50% or greater in nearly 40% of grid cells. However, in contrast to EDGAR, we found that Vulcan emissions showed large negative biases relative to DARTE in the cores of large cities, and large positive biases in the surrounding

suburban and exurban areas (Figure B2). Vulcan emissions in rural areas of the western United States show good agreement with DARTE on average, however, as with EDGAR, Vulcan displayed a large negative bias relative to DARTE on most of the rural interstate highway network (Figure B4). The differences between Vulcan and DARTE are most likely explained by how the VMT used by Vulcan to estimate on-road emissions was spatially downscaled from state and Urbanized Areas to counties in the NCD (see discussion in main text of Chapter 2).

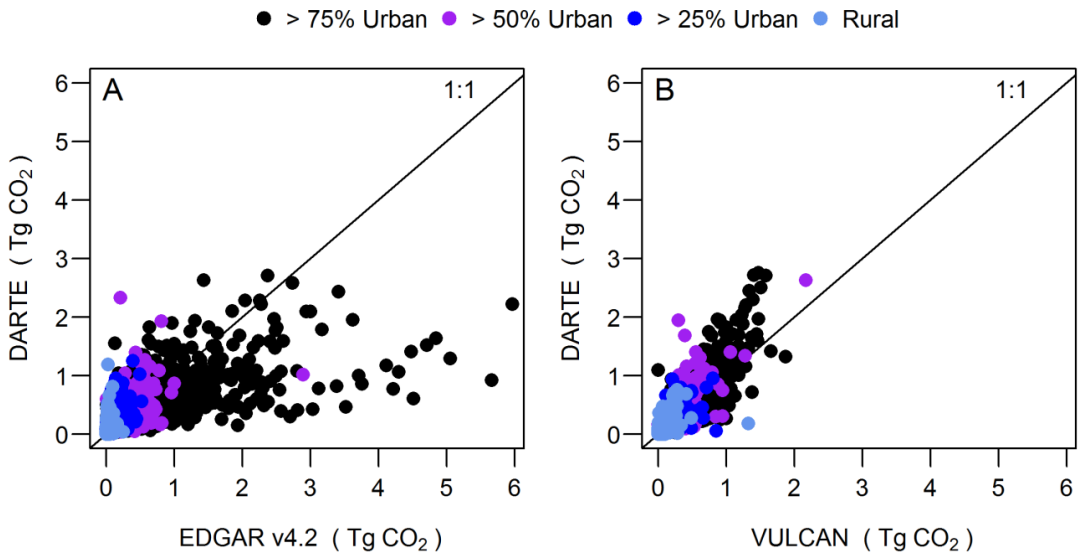

Figure B2. Cell-by-cell comparison of DARTE with EDGAR v4.2 (0.1° grid) and Vulcan (10 km grid). Grid cells were classified by their percent area of overlap with U.S. Census Urbanized Areas or Urban Clusters. DARTE – EDGAR comparison is for year 2008 emissions. DARTE – Vulcan comparison is for year 2002 emissions.

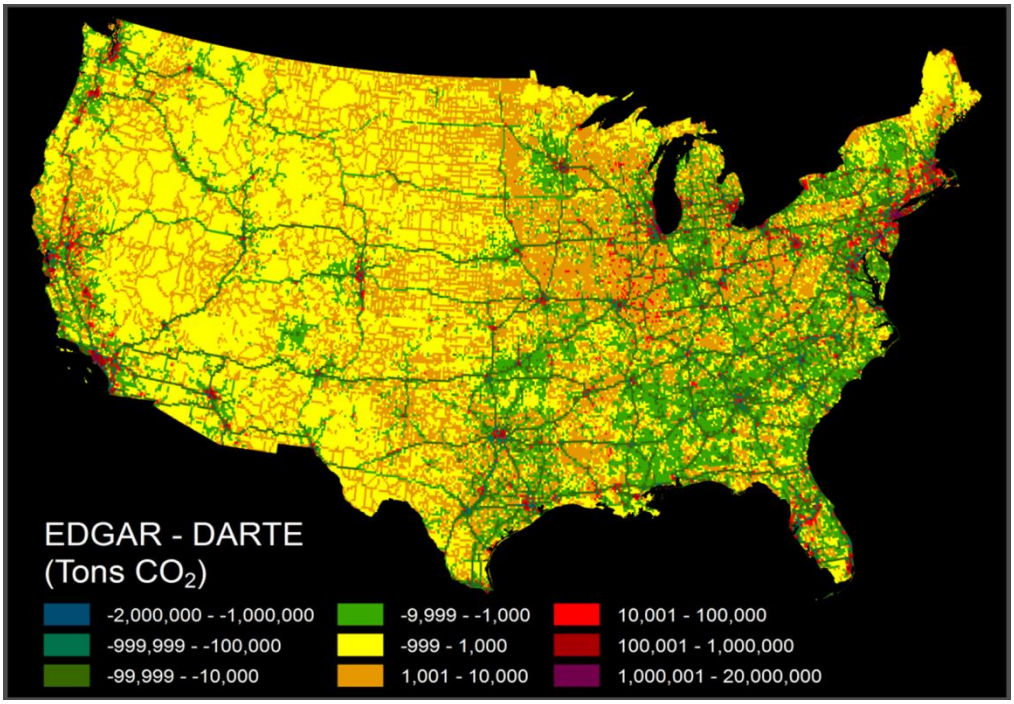

Figure B3. Cell-by-cell difference between EDGAR and DARTE for the year 2008; 2008 is the most recent year for which EDGAR v4.2 estimates are available. Resolution is 0.1^{o} x 0.1^{o} on the native EDGAR grid. Green areas indicate cells where EDGAR showed a negative bias relative to DARTE; orange and red areas show cells with a positive bias relative to DARTE. Differences are largest in the major urban areas.

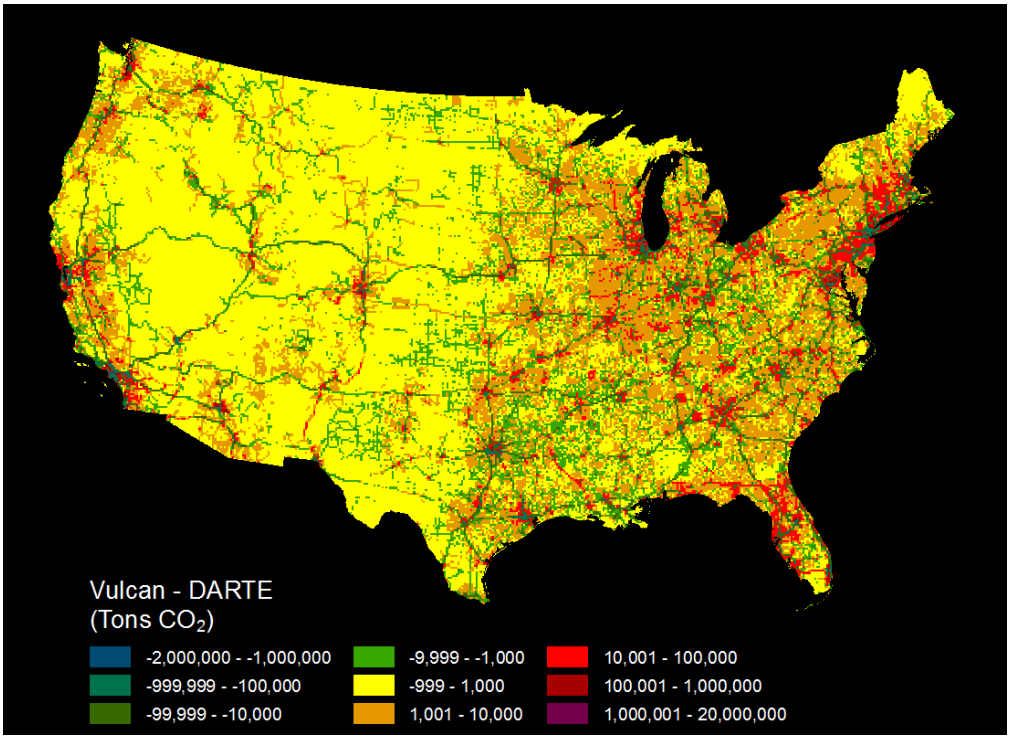

Figure B4. Cell-by-cell difference between Vulcan and DARTE for the year 2002. Green areas indicate cells where Vulcan under-allocated emissions relative to DARTE, orange and red cells show where Vulcan over-allocated emissions relative to DARTE.

Generalized Additive Model

We estimated two generalized additive models using on-road CO_2 emissions from DARTE. In the first model, **GAM$_1$,** we regressed total county-level on-road CO_2 emissions on lagged values of population density, per-capita income (in constant 2009 dollars), retail job density, non-retail job density and annual change in population (the last term being defined as the county population in the previous year minus the population in the year before that). The second model,

GAM$_2$, we regressed per-capita on-road CO_2 emissions on the same variables. Non-retail jobs were calculated as the sum of all jobs in a county not classified as retail. All employment and income data were obtained from the Bureau of Economic Affairs Regional Data Tables (http://www.bea.gov/iTable/index_regional.cfm).

GAM$_1$:

$$\mathrm{CO}_{2\ i,t} = \alpha_i + \tau_t + \Psi_1\left[\begin{pmatrix}\text{Population}\\ \text{density}\end{pmatrix}_{i,t-1}\right] + \Psi_2\left[\begin{pmatrix}\text{Per-capita}\\ \text{income}\end{pmatrix}_{i,t-1}\right] + \Psi_3\left[\begin{pmatrix}\text{Retail jobs}\\ \text{per km}^2\end{pmatrix}_{i,t-1}\right] + \Psi_4\left[\begin{pmatrix}\text{Non-retail jobs}\\ \text{per km}^2\end{pmatrix}_{i,t-1}\right] + \Psi_5\left[(\text{Population})_{i,t-1} - (\text{Population})_{i,t-2}\right] + \varepsilon_{i,t}$$

GAM$_2$:

$$\text{Per-capita } \mathrm{CO}_{2\ i,t} = \alpha_i + \tau_t + \Psi_1\left[\begin{pmatrix}\text{Population}\\ \text{density}\end{pmatrix}_{i,t-1}\right] + \Psi_2\left[\begin{pmatrix}\text{Per-capita}\\ \text{income}\end{pmatrix}_{i,t-1}\right] + \Psi_3\left[\begin{pmatrix}\text{Retail jobs}\\ \text{per km}^2\end{pmatrix}_{i,t-1}\right] + \Psi_4\left[\begin{pmatrix}\text{Non-retail jobs}\\ \text{per km}^2\end{pmatrix}_{i,t-1}\right] + \Psi_5\left[(\text{Population})_{i,t-1} - (\text{Population})_{i,t-2}\right] + \varepsilon_{i,t}$$

The fitted splines for the lagged population density component from each model across the full range of U.S. county population densities are shown in Figure B5. The fitted splines for the other independent variables in both models (Figure B6) and the summary statistics (Table B4) for each model are reported. The estimated splines are non-parametric estimates of the partial component of emissions explained by each independent variable, relative to the conditional mean. The shape of each spline describes the average within-county effect of the independent variable on total or per-capita emissions across all counties and years in the dataset. For total CO_2 emissions we find that retail employment density is negatively correlated with emissions, and that non-retail employment density is positively correlated with emissions in all counties except New York City.. Non-retail employment and population density are the two largest contributors to total emissions as estimated by our model. Per-capita income has a small positive contribution to total emissions for incomes between $30,000 and $60,000, and a negative contribution at incomes greater than $60,000. The lagged annual population growth term shows a minimal influence on total emissions for most counties, but for fast-growing counties the effect is positive with lagged annual growth of 50,000 – 125,000, then becomes negative at higher levels. For

per-capita emissions, per-capita income initially has a negative effect at low incomes and then becomes a positive effect for incomes above $30,000. Retail employment density is positively associated with per-capita emissions, but the effect plateaus at ~400 retail jobs per km^2. Non-retail employment density has a negative association with per-capita emissions, although the effect is largely stable across most counties at ~ -5 Tg-person^{-1}-km^{-2}. Lagged population growth had no statistically significant effect on per-capita emissions.

The rug plots along the x-axis in each panel in Figure B5 reveal the heavily skewed distribution of population density for U.S. counties. Despite increasing growth of large urban areas, in 2012, over 87% of the U.S. population still lived in counties with densities of less than 1,000 persons-km^{-2}, a share that has not changed significantly since 1980 (Figure B7). Our results show that increasing density is associated with an increase in total county emissions of on-road CO_2 until densities exceed 1,650 persons-km^{-2}, while the decreasing trend in per-capita emissions with density appears to level out and stabilize once densities exceed 1,200 persons-km^{-2}. Only at the high densities of the largest cities in the U.S. (2,000 – 4,000 persons-km^{-2}) do we observe decreases in per-capita emissions large enough to offset increasing total CO_2 emissions. For low-density towns and counties that are attempting to reduce future on-road emissions by increasing

population densities in their urban areas, our results offer the caution that the per-capita decreases associated with densification may not provide the reductions in total vehicle travel that earlier research on this topic seemed to promise (Newman and Kenworthy 1989).

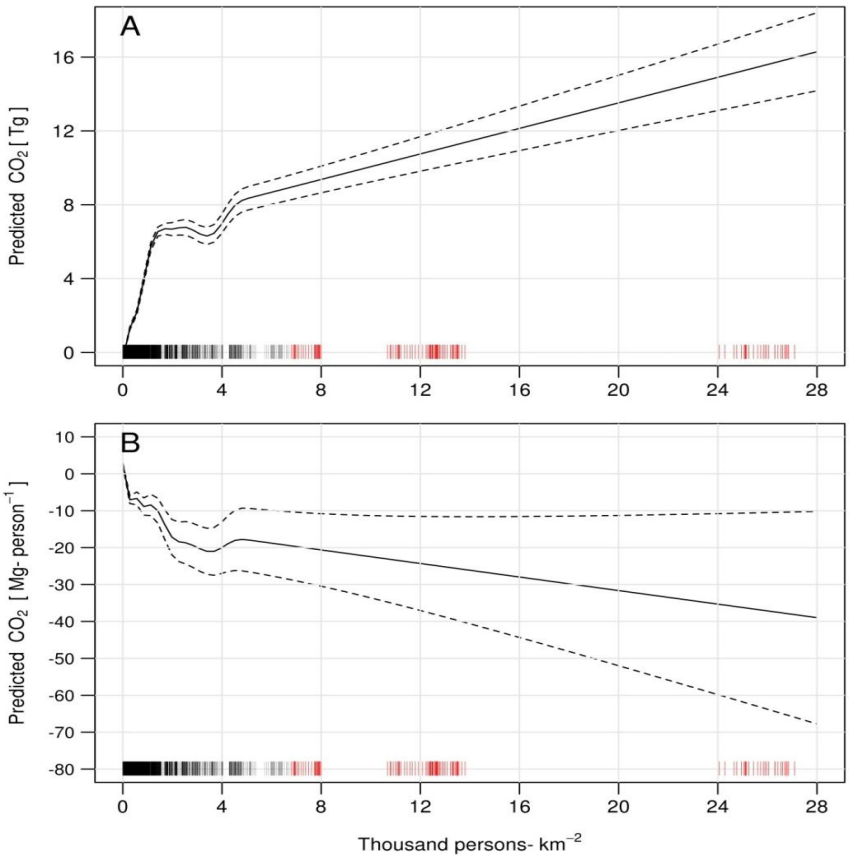

Figure B5. Comparison of fitted splines for total emissions versus population density (Panel A) and per-capita emissions versus population density (Panel B), as estimated by the generalized additive models described in the main text. The increase in total emissions with density begins to plateau at 1,650 persons-km^{-2}, before rising sharply again at 4,000 persons-km^{-2}. Per-capita emissions decrease rapidly for densities less than 250 persons-km^{-2}, but then

decrease much more slowly between 250 and 1,200 persons-km^{-2}. The rapid decrease resumes at 1,200 persons-km^{-2} and continues before flattening slightly at 2,000 persons-km^{-2} and then plateauing until 8,000 persons-km^{-2}. The rug plot at the base of both graphs shows the pooled distribution of population density across all U.S. counties and years covered by DARTE. The red ticks in the rug plots denote counties that comprise parts of New York City, NY.

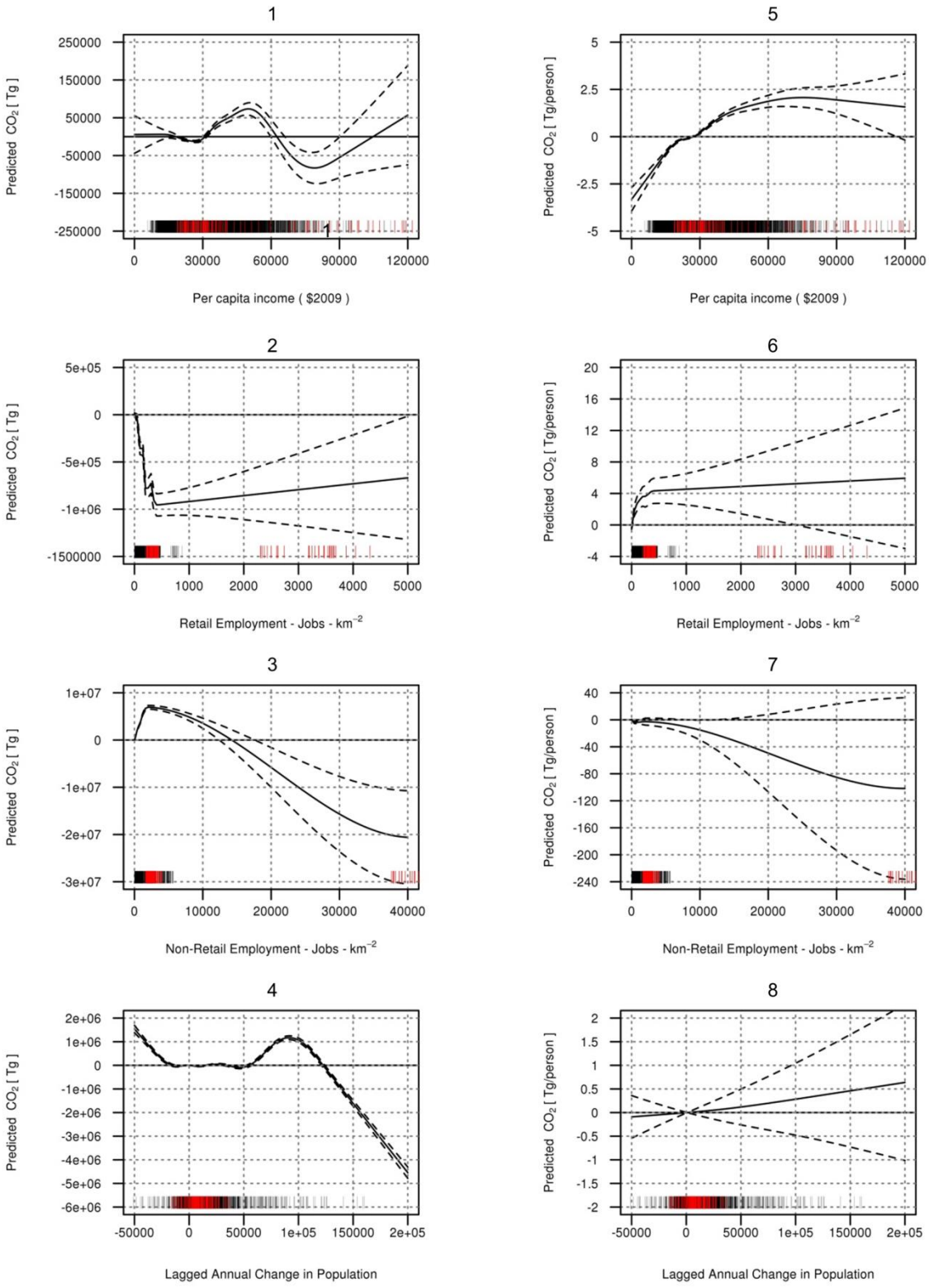
1
Predicted CO_2 [Tg]
250000
150000
50000
-50000
-150000
-250000
0
30000
60000
90000
120000
Per capita income ($2009)
5
Predicted CO_2 [Tg/person]
5
2.5
0
-2.5
-5
0
30000
60000
90000
120000
Per capita income ($2009)
2
Predicted CO_2 [Tg]
5e+05
0
-5e+05
-1e+06
-1500000
0
1000
2000
3000
4000
5000
Retail Employment - Jobs - km^{-2}
6
Predicted CO_2 [Tg/person]
20
16
12
8
4
0
-4
0
1000
2000
3000
4000
5000
Retail Employment - Jobs - km^{-2}
3
Predicted CO_2 [Tg]
1e+07
0
-1e+07
-2e+07
-3e+07
0
10000
20000
30000
40000
Non-Retail Employment - Jobs - km^{-2}
7
Predicted CO_2 [Tg/person]
40
0
-40
-80
-120
-160
-200
-240
0
10000
20000
30000
40000
Non-Retail Employment - Jobs - km^{-2}
4
Predicted CO_2 [Tg]
2e+06
1e+06
0
-1e+06
-2e+06
-3e+06
-4e+06
-5e+06
-6e+06
-50000
0
50000
1e+05
150000
2e+05
Lagged Annual Change in Population
8
Predicted CO_2 [Tg/person]
2
1.5
1
0.5
0
-0.5
-1
-1.5
-2
-50000
0
50000
1e+05
150000
2e+05
Lagged Annual Change in Population

Figure B6. Plot of smooth terms (Ψ_2-Ψ_5) in GAM_1 (total emissions - left column, Panels 1-4), and GAM_2 (per-capita emissions - right column, Panels 5-8). Rug plots show distribution of county values for each independent variable, pooled over all years. Red tick marks in the rug plots represent the counties that comprise New York City, NY.

GAM_1	*Effective Degrees of Freedom*	*Reference Degrees of Freedom*	*p-value*	GAM_2	*Effective Degrees of Freedom*	*Reference Degrees of Freedom*	*p-value*
Ψ_1	8.987	9.000	< 2E-16	Ψ_1	9.000	9.000	< 2E-16
Ψ_2	8.562	8.947	< 2E-16	Ψ_2	7.792	8.640	< 2E-16
Ψ_3	8.881	8.994	< 2E-16	Ψ_3	8.892	8.994	3.36E-13
Ψ_4	8.981	9.000	< 2E-16	Ψ_4	8.048	8.710	4.73E-07
Ψ_5	8.929	8.999	< 2E-16	Ψ_5	1.160	1.306	0.707
Adj-R^2 = 0.98	Generalized Cross Validation (GCV) = 3.29E10			Adj-R^2 = 0.88	Generalized Cross Validation (GCV) = 6.16		

Table B4. Summary statistics for the smooth terms in each GAM model.

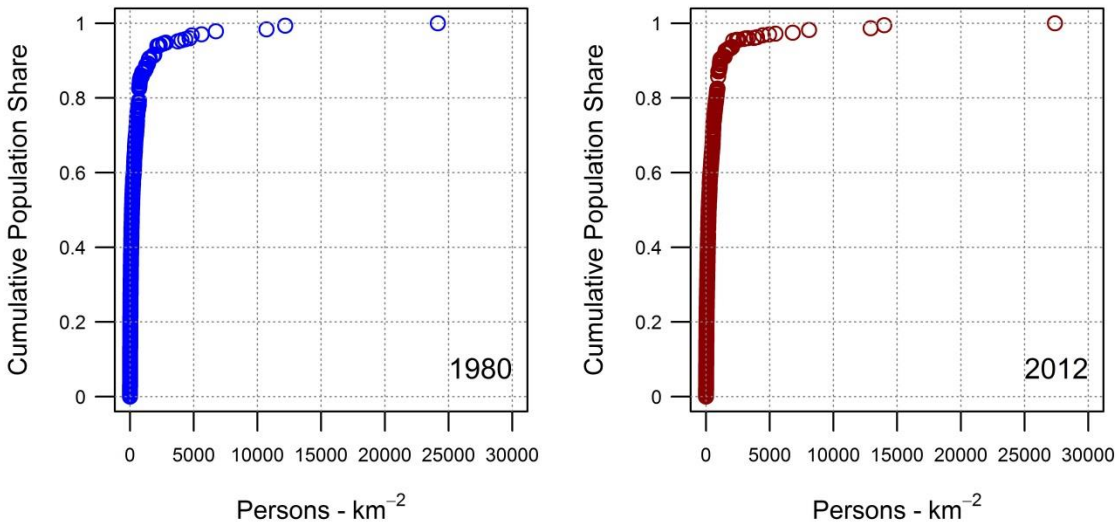

Figure B7. Cumulative population as share of U.S. total vs. population density for U.S. counties in 1980 (left) compared to in 2012 (right). Over 85% of the U.S. population resided in counties with densities less than 1,000 persons-km^{-2} in 2012. Population growth in low-density counties in the South and Central U.S. has resulted in the urbanization of small- and medium-sized cities with population densities that are typically associated with high per-capita transportation energy consumption and related carbon emissions. As a consequence, despite the overall growth in urban populations since 1980, the total distribution U.S. population by density has not substantially shifted towards the denser urban core counties.

Public Transit and Emissions

To investigate the potential influence of transit ridership on per-capita on-road CO_2 emissions we made use of decadal Census long-form survey responses on the percentage of workers who commute by private vehicle, carpool, public transit, or other modes (cycling, walking, motorcycle). For the years 1990, 2000

and 2010, this data is available at the Census Designated Place level of geography (U.S. Census Bureau 1990; U.S. Census Bureau 2010) (Figure B8 and Fig 8C in the main text). Trends in per-capita emissions as a function of transit commuters per person (Figure 8C) and the share of workers over the age of 16 who commute by public transit (Figure B8) show similar trends, although we observe differences in the magnitude of change in transit shares when we only consider the mode choice of commuter trips. Per-capita emissions appear to decrease somewhat slower with increasing transit use by commuters, however as commuting only comprises ~28% of national VMT on average (FHWA 2011), this is not surprising. Cities with high population density are also the cities with the highest per-capita transit mode share, and these cities tend to have lower per-capita on-road CO_2 emissions. For the cities with lower population density and lower transit mode share, we observed higher per-capita emissions in the more recent data (2000 and 2010). The results in Figure 8C and Figure B8 provide evidence for a modest correlation between population density, public transit usage and per-capita emissions, and for cities that are already relatively dense the correlation appears be negative over time. However, due to the limited sample size available, it is difficult to rigorously quantify the transit-emissions relationship, particularly in

the low density cities and counties that have experienced the greatest amount of population growth across the past decade.

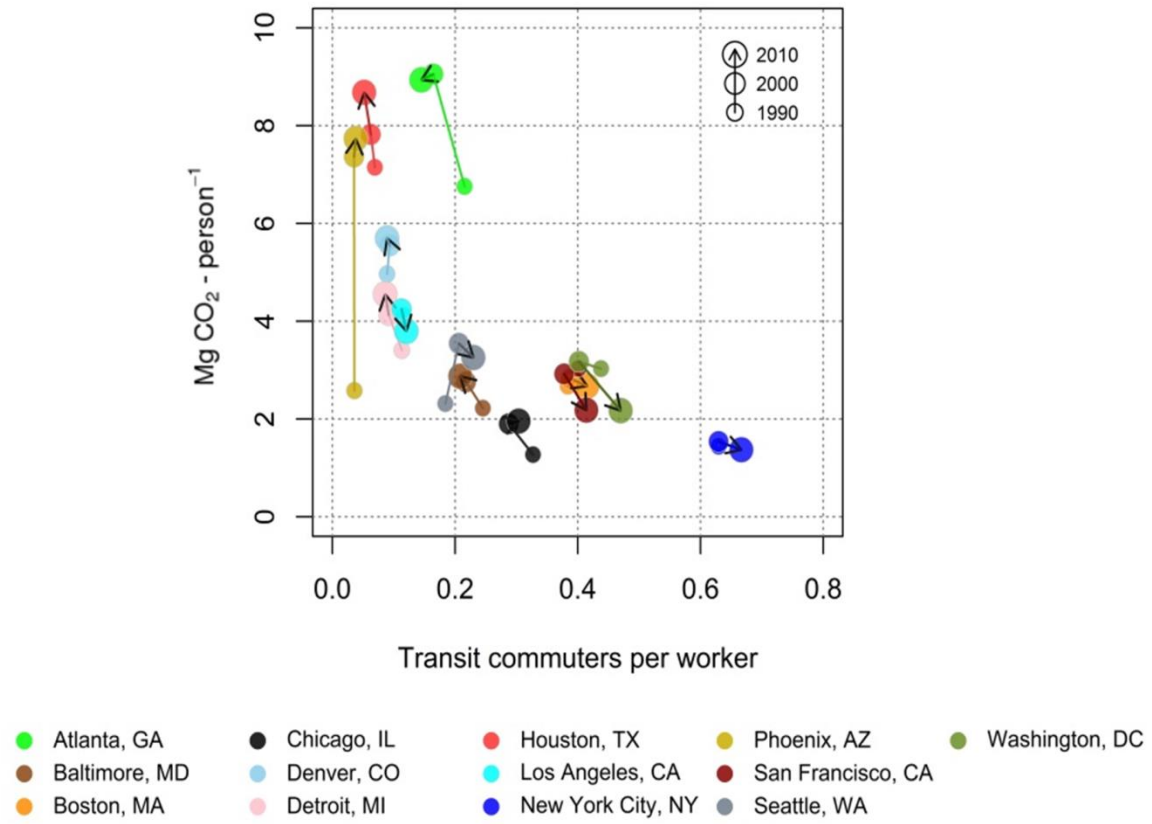

Figure B8. Plot of on-road CO_2 emissions per person vs. the share or workers over the age of 16 who commute by public transit, in 1990, 2000 and 2010 for a sample of U.S. cities.

Note, we were not able to include data on ridership levels from different transit systems as part of our regression modeling analysis due to limitations in

data collection by public transit agencies across the United States.The National Transit Database maintained by the Federal Transit Administration is the best data source for systematic transit ridership, however the data is aggregated by agency and by Census Urbanized Area Disaggregating data from the Urbanized Area scale to the county scale would have introduced significant bias, as many transit systems in large cities span multiple counties, and there is no information available on the distribution of ridership across the system.

8. Ranking of counties by emissions

Over 50% of U.S. on-road CO_2 emissions occur in just 7% of counties. In 2012 the top 10 highest emitting counties were responsible for 10% of all national emissions (Table B5). Compared to the rest of the U.S., the top ten counties have lower per-capita emissions for both gasoline and diesel vehicle CO_2, but have both higher road densities and higher emissions per kilometer of road than the rest of the country, offsetting the below-average per-capita emissions and contributing to their large total emission levels. With the exception of San Bernardino County, CA, all of these counties have population densities higher than the national average, and in most cases they contain large urban areas where population densities are even significantly higher. Despite the high

densities and below-average per-capita emissions rates, the sheer number of people residing and driving in these counties means that their total level of on-road emissions is high.

County	Tons CO_2	Pop. Density (per km^2)	Road Density (km / km^2)	CO_2 per capita (tons)			CO_2 per road-km (tons)			CO_2 per VMT (grams)		
				Total	*Gasoline*	*Diesel*	*Total*	*Gasoline*	*Diesel*	*Total*	*Gasoline*	*Diesel*
1. Los Angeles, CA	39,447,761	947.9	4.7	4.0	3.4	0.6	799.6	679.5	120.0	497.6	422.9	74.7
2. Harris, TX	19,354,340	964.1	7.4	4.6	3.6	0.9	590.1	469.3	120.9	560.0	445.3	114.7
3. Cook, IL	17,679,211	2,136.7	10.9	3.4	2.6	0.7	663.6	519.3	144.2	491.4	384.6	106.8
4. Maricopa, AZ	16,179,572	165.4	1.9	4.1	3.4	0.7	358.7	295.8	62.9	480.7	396.4	84.3
5. San Diego, CA	13,965,639	291.6	2.4	4.4	3.6	0.8	530.9	438.3	92.6	504.9	416.8	88.1
6. Orange, CA	13,178,336	1509.2	7.6	4.3	3.7	0.6	842.9	723.8	119.1	495.3	425.3	70.0
7. Dallas, TX	12,878,332	1087.4	7.8	5.2	4.2	1.1	727.6	580.3	147.3	559.3	446.0	113.3
8. San Bernardino, CA	11,013,708	40.1	0.9	5.3	4.1	1.2	229.7	179.5	50.1	522.0	408.0	113.9
9. Riverside, CA	10,548,353	121.6	1.4	4.6	3.7	1.0	393.5	312.7	80.9	517.0	410.8	106.2
10. Miami-Dade, FL	9,071,230	527.2	3.0	3.5	3.0	0.5	617.3	535.5	81.9	452.4	392.4	60.0
Rest of U.S.	*1,386,722,431*	*99.7*	*1.8*	*8.2*	*5.5*	*2.7*	*125.4*	*92.8*	*32.6*	*550.2*	*389.8*	*160.4*

Table B5. Top ten highest-emitting counties in 2012. These counties also comprise 10% of the U.S. population, but have lower per-capita emissions and higher road and population densities than the average of the remaining 3,094 counties. Total and average emissions reflect contributions from both diesel and gasoline vehicles.

9. Uncertainty of VMT

Vehicle miles travelled estimates in HPMS are derived from a combination of PTRs and short-term traffic counts conducted with portable sensors. PTRs provide year-round data on traffic activity and are considered to measure total volumes with 95%-99% accuracy (Batelle Institute 2004). These data are used to derive seasonal and day-of-week factors to convert short-term counts into annualized average daily traffic (AADT) values. For roads whose traffic is not directly measured, AADT is imputed from similar roads nearby that have been directly measured (FHWA 2005). FHWA requires all AADT estimates submitted to HPMS to meet precision and accuracy standards that vary by roadway functional class: Freeways and larger roads are required to be accurate within 5%, while local rural road AADT must be within 15% (FHWA 2005).

Total emissions for each road class in each county were assigned to the TIGER/Line road network by dividing the total emissions on functional class *f*, in county *c*, by the total length of roads of functional class *f* in county *c*, and then applying the resulting per-kilometer emissions factor to all roads of class *f* in county *c*. This procedure averaged out the local variation in per-kilometer emissions across roadway segments within each functional class. To estimate the potential uncertainty associated with this process we calculated the coefficient of

variation (CV) for VMT on each functional class within each county for each year using roadway-level VMT from the HPMS archive. We then averaged the annual CVs across all years in the dataset and plotted them on a national map (Figure B9). We found that for most U.S. counties, the within-county variation in VMT was low for rural freeways and for urban roads in general. The largest variation was seen on rural non-freeway road classes, with Indiana, Alabama, Vermont and Idaho showing the largest within-county variation on these roads. Rural non-freeway road segments are typically the least-sampled roads in HPMS, and are held to lower standards of precision according to the guidelines in the HPMS Field Manual (FHWA 2005). This would account for the overall larger values of CV on these roads, but there are also clear state-specific deviations that suggest data from certain states may be less precisely collected than in others. Rural non-freeways only accounted for 17% of total VMT (and 17% of total CO_2 emissions) in 2012, so while the spatial uncertainty of emissions from these roads is larger than other functional class roads, the overall contribution to total emissions uncertainty is relatively small.

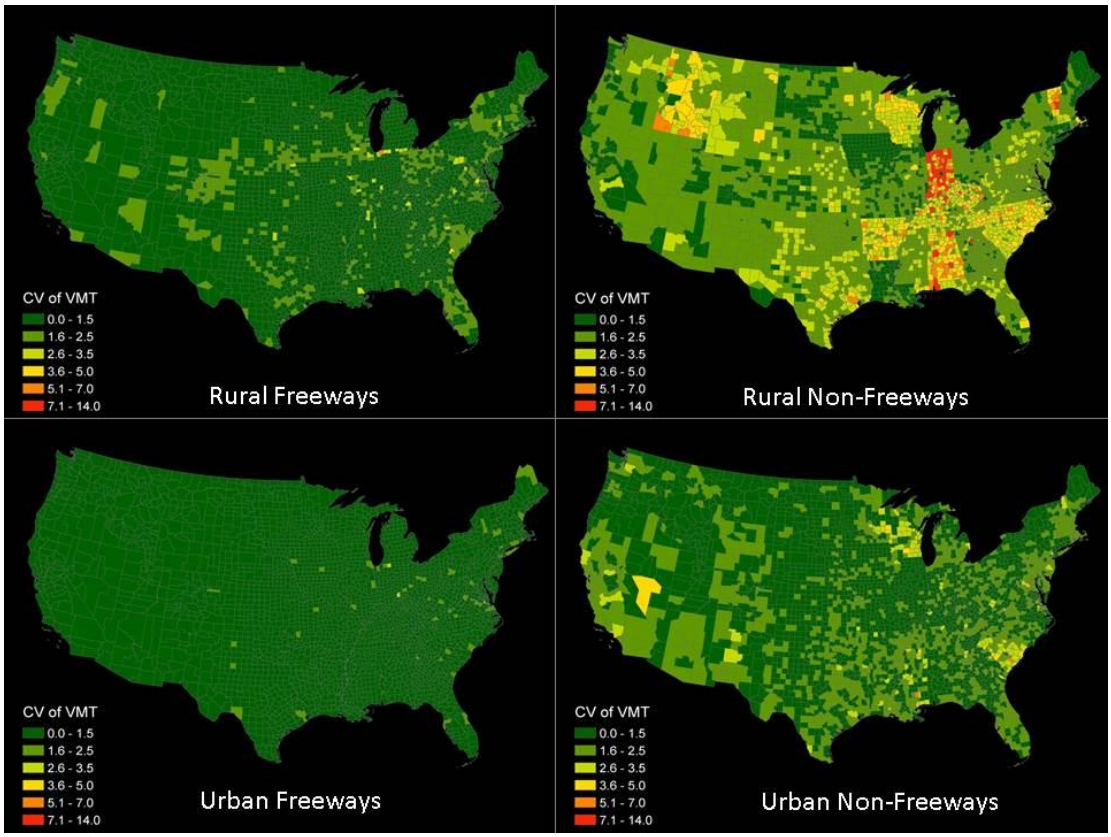

Figure B9. Within-county coefficient of variation (CV) of vehicles miles travelled by functional class, averaged over all years in the HPMS database.

At county and state scales the spatial imputation of AADT for roads that are not directly measured is another important source of uncertainty for VMT estimates. The imputation procedure consists of assigning traffic volumes to roads of similar functional class and urban/rural context using traffic counts measured on nearby roads. Large amounts of high resolution traffic data are needed to directly estimate the magnitude of this uncertainty. We calculated the

within-state (between-county) coefficients of variation of VMT as a proxy measure of this spatial uncertainty. The CV of urban VMT ranged from 0.5 to 4.0 across all states and years, while rural VMT ranged more narrowly from 0.75 to 1.75 (Figure B10).The large variation in the state-level CVs of urban VMT reflects the broader range of urban area sizes at state scales, as small and large cities with different levels of vehicle activity fall into the same category of 'urban VMT' despite their inherent differences. The within-state CVs of emissions intensity (CO_2 / VMT) were small, ranging from 0.1 – 0.2 on average. Low variation in emissions relative to VMT is consistent with previous findings that uncertainty in vehicle fleet and fuel economy characteristics are a minor contributor to the overall uncertainty in emissions estimates from the on-road sector (Mendoza et al. 2013).

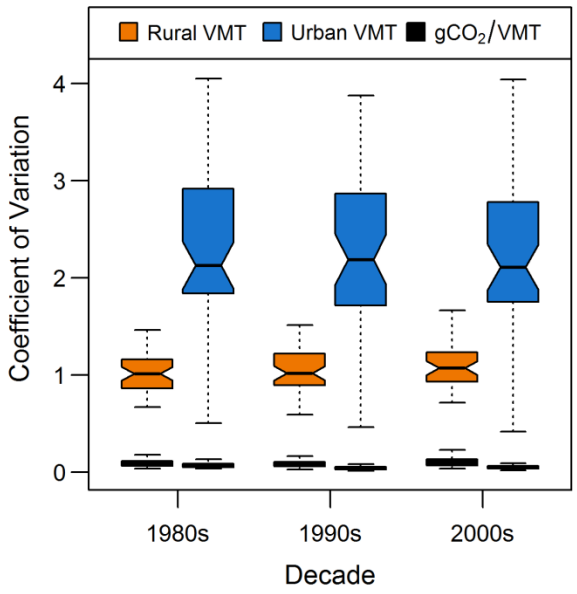

Figure B10. Coefficient of variation (CV) of intrastate VMT and emissions intensity (CO_2 per VMT) by decade. Each boxplot represents the distribution of CVs across all states. The CV for each state was calculated on the distribution of values for VMT and emissions intensity across all urban or rural roads in a state over each decade.

APPENDIX C

Calculating relative humidity

To satisfy the format of the MOVES model emissions factors, we needed to obtain relative humidity values for the ambient atmospheric conditions on each road segment and for each hour of the year. The NLDAS-2 data fields do not contain estimates of relative humidity, but do contain values for air temperature, air pressure, and specific humidity at a height of 2m above the surface. We can use these variables to calculate relative humidity as shown below.

Relative humidity is the ratio of the mass mixing ratios of water vapor at actual and saturation values, while specific humidity is the mass mixing ratio of water vapor in air, defined as:

$$q \equiv m_v / (m_v+m_d) = w / (w+1) \approx w$$

Relative humidity can be expressed as the ratio of the water vapor mixing ratio to the saturation water vapor mixing ratio, w/w_s, where:

$$w_s \equiv m_{vs} / m_d = (e_s * R_d) / (R_v * (p-e_s)) \approx 0.622 * e_s / p$$

Using the Clausius-Clapeyron equation we can calculate the saturation vapor pressure (e_s) at temperature T:

$$e_s(T) = e_{s0} * \exp[(L_v(T) / R_v) * (1/T_0-1/T)] \approx 611 * \exp[(17.67 * (T-T_0) / (T-29.65)]$$

Combining the above equations, relative humidity can then be expressed as:

$$RH = 100 * w / w_s \approx 0.263 * p * q * [\exp(17.67*(T-T_0)*T-29.65)]^{-1}$$

Where:

q is specific humidity or the mass mixing ratio of water vapor to total air (dimensionless)

m_v is specific mass of water vapor (kg)

m_{vs} is specific mass of water vapor at equilibrium (kg)

m_d is specific mass of dry air (kg)

w is mass mixing ratio of water vapor to dry air (dimensionless)

w_s is mass mixing ratio of water vapor to dry air at equilibrium (dimensionless)

$e_s(T)$ is saturation vapor pressure (Pa)

e_{s0} is saturation vapor pressure at T_0 (Pa)

R_d is specific gas constant for dry air (J kg−1 K−1)

R_v is specific gas constant for water vapor (J kg−1 K−1)

p is pressure (Pa)

$L_v(T)$ is specific enthalpy of vaporization (J kg−1)

T is temperature (K)

T_0 is reference temperature (273.16 K) (K)

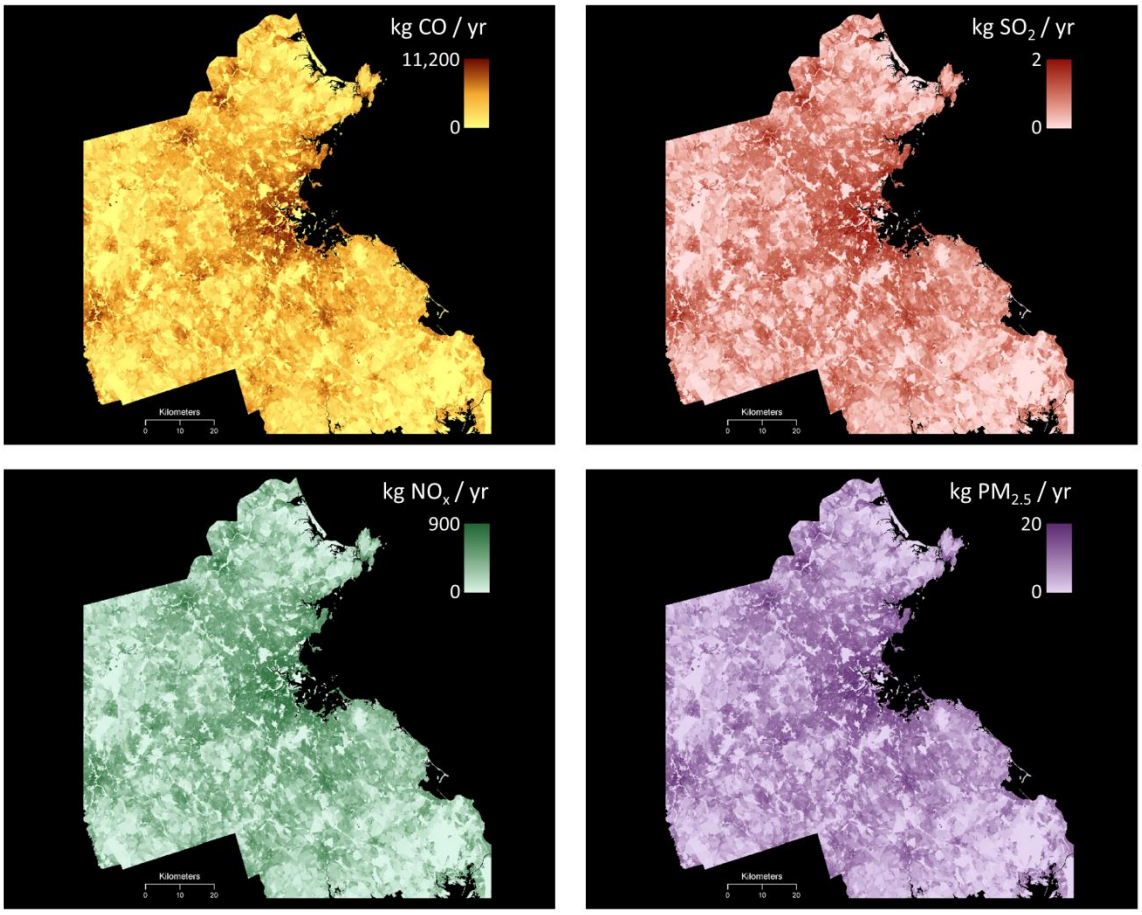

Figure C1. Annual emissions of CO, SO_2, NO_x, and $PM_{2.5}$ from passenger vehicle cold starts. The spatial distribution of starts is determined by the average number of trips per household as reported by the 2010 Massachusetts Travel Survey (Massachusetts Department of Transportation 2012).

BIBLIOGRAPHY

1. Andres R, Marland G, Fung I, Matthews E, 1996. A 1° × 1° Distribution of Carbon Dioxide Emissions from Fossil Fuel Consumption and Cement Manufacture, 1950–1990. Global Biogeochemical Cycles, 10, (3), 10.1029/96GB01523.
2. Andres RJ, et al., 2012. A Synthesis of Carbon Dioxide Emissions from Fossil-fuel Combustion. Biogeosciences, 9, (5), 10.5194/bg-9-1845-2012.
3. Asefi-Najafabady S, et al., 2014. A multiyear, global gridded fossil fuel CO_2 emission data product: Evaluation and analysis of results, Journal of Geophysical Research: Atmosphere 119, 10.1002/2013JD021296.
4. Batelle Institute, 2004. Traffic Data Quality Measurement – Final Report. Prepared by Batelle Institute in association with Cambridge Systematics Inc. and Texas Transportation Institute for the Office of Highway Policy Information, Federal Highway Administration, U.S. Department of Transportation, Washington, DC, September 15, 2004.
5. Bento AM, Cropper ML, Mobarak AM, Vinha K, 2005. The Effects of Urban Spatial Structure on Travel Demand in the United States. Review of Economics and Statistics, 87, (3), 466-478.

6. Blasing TJ, Broniak C, Marland G, 2005. State-by-state carbon dioxide emissions from fossil-fuel use in the United States 1960–2000, Mitigation and Adaptation Strategies for Global Change, 10, 10.1007/s11027-005-6471-9.
7. Brenkert AL, 1998. Carbon Dioxide Emission Estimates From Fossil-Fuel Burning, Hydraulic Cement Production, and Gas Flaring for 1995 on a One Degree Grid Cell Basis, Carbon Dioxide Information Analysis Center, Oak Ridge National Laboratory, Oak Ridge, Tennessee.
8. Brondfield M, Hutyra LR, Gately CK, Raciti S, Peterson S, 2012. Modeling and validation of on-road CO_2 emissions inventories at the urban regional scale. Environmental Pollution, 170, 113-123.
9. Brownstone D, Golob TF, 2009. The impact of residential density on vehicle usage and energy consumption. Journal of Urban Economics, 65, 91-98.
10. California AB-32 – California Global Warming Solutions Act, Health & SC § 38500–38598, 2006; http://www.arb.ca.gov/cc/docs/ab32text.pdf
11. Cao X, Mokhtarian PL, Handy SL, 2009. Examining the Impacts of Residential Self-Selection on Travel Behaviour: A Focus on Empirical Findings. Transportation Review, 29, (3), 359-395.

12. Cervero R, Kockelman K, 1999. Travel Demand and the 3Ds: Density, Diversity, and Design. Transportation Research: Part D, 2, (3), 199-219.
13. Cervero R, Hansen M, 2002. Induced Travel Demand and Induced Road investment. Journal of Transport Economics and Policy, 36, (3), 469-490.
14. Cervero R, Murakami J, 2009. Effects of built environments on vehicle miles traveled: evidence from 370 US urbanized areas. Environment and Planning A, 42, 400-418.
15. Ciais P, Paris JD, Marland G, Peylin P, Piao SL, Levin I, Pregger T, et al., 2010. The European Carbon Balance, Part 1: Fossil Fuel Emissions. Global Change Biology, 16, (5), 1395–1408. doi:10.1111/j.1365-2486.2009.02098.x.
16. City of Boston, 2010. City of Boston Climate Action Plan, Boston MA; http://www.cityofboston.gov/climate/bostonsplan/
17. Cohen AJ, et al., 2005. The global burden of disease due to outdoor air pollution. Journal of Toxicology and Environmental Health A, 68, 1301-1307.
18. DeCicco J, Fung F, An, F, 2006. Global Warming of the Road: The Climate Impact of America's Automobiles. Environmental Defense Fund, New York.

19. Duranton G, Turner MA, 2011. The Fundamental Law of Road Congestion: Evidence from US Cities. American Economic Review, 101, (6), 2616-52.

20. Energy Information Administration, 2007. Documentation for Emissions of Greenhouse Gases in the U.S. 2005, Table 6-1. DOE/EIA-0638 (2005), U.S. Department of Energy, Washington, DC.

21. European Commission, Joint Research Centre (JRC)/Netherlands Environmental Assessment Agency (PBL), 2011a. Emission Database for Global Atmospheric Research (EDGAR), release version 4.2; http://edgar.jrc.ec.europa.eu

22. European Commission, Joint Research Centre (JRC)/Netherlands Environmental Assessment Agency (PBL), 2011b. Emission Database for Global Atmospheric Research (EDGAR), Factsheet - Energy: Combustion in 1A3b; http://edgar.jrc.ec.europa.eu/factsheet_1a3b.php

23. Ewing R, Cervero R, 2010. Travel and the Built Environment. Journal of the American Planning Association, 76, (3), 265–294.

24. Federal Highway Administration, 1980-2012. Highway Statistics Series, Table VM-1, Table VM-2, Table VM-4, Table MF-21, Table HM-20. U.S.

Department of Transportation, Washington, DC; http://www.fhwa.dot.gov/policyinformation/statistics.

25. Federal Highway Administration, 2005. Highway Performance Monitoring System Field Manual, Washington, DC; http://www.fhwa.dot.gov/ohim/hpmsmanl/hpms.cfm
26. Federal Highway Administration, 2009. Archived data from the Highway Performance Monitoring System. Made available by Robert Rozycki, U.S. Department of Transportation, Washington, DC.
27. Federal Highway Administration, 2011. Summary of Travel Trends: 2009 National Household Travel Survey, Table 6. U.S. Department of Transportation, Washington, DC; http://nhts.ornl.gov/2009/pub/stt.pdf
28. Gadda S, Magoon A, Kockelman KM, 2007. Estimates of AADT: Quantifying the uncertainty. Proceedings of the 86th Annual Meeting of the Transportation Research Board, Washington DC.
29. Gately CK, Hutyra LR, Sue Wing I, Brondfield MN, 2013. A bottom-up approach to on-road CO_2 emissions estimates: Improved spatial accuracy and applications for regional planning. Environmental Science and Technology, 47, (5), 2423-2430.

30. Gregg J, Losey L, Andres R, Blasing T, Marland G, 2009. The temporal and spatial distribution of carbon dioxide emissions from fossil fuel use in North America. Journal of Applied Meteorology and Climatology, 48, 2528-2542.

31. Glaeser EL, Kahn ME, 2010. The greenness of cities: Carbon dioxide emissions and urban development. Journal of Urban Economics, 67, 404–418.

32. Gurjar BR, et al., 2010. Human health risks in megacities due to air pollution. Atmospheric Environment, 44, 4606-4613.

33. Gurney K, Mendoza D, Zhou Y, Fischer M, Miller C, Geethakumar S, de la Rue de Can S, 2009. High resolution fossil fuel combustion CO_2 emission fluxes for the United States. Environmental Science and Technology, 43, 5535-5541.

34. Gurney KR, Mendoza D, Geethakumar S, Zhou Y, Chandrasekaran V, Miller C, Godbole A, Sahni N, Seib B, Ansley W, Peraino S, Chen X, Maloo U, Kam J, Binion J, Fischer M, de la Rue du Can S, 2010. Vulcan Science Methods Documentation, Version 2.0; http://vulcan.project.asu.edu/pdf/Vulcan.documentation.v2.0.online.pdf

35. Gurney KR, Zhou Y, Mendoza D, Chanrdasekaran V, Geethakumar S, Razlivanov I, Song Y, Godbole A, 2011. Vulcan and Hestia: High Resolution quantification of fossil fuel CO_2 emissions. MODSIM 2011 - 19th International Congress on Modeling and Simulation - Sustaining Our Future: Understanding and Living with Uncertainty, 1781-1787.

36. Gurney KR, Razlivanov I, Song Y, Zhou Y, Benes B, Abdul-Massih M, 2012. Quantification of fossil fuel CO_2 emissions on the building/street scale for a large U.S. City. Environmental Science and Technology, 46, (21), 12194-12202.

37. Harley RA, McKeen SA, Pearson J, Rodgers MO, Lonneman WA, 2001. Analysis of motor vehicle emissions during the Nashville/Middle Tennessee ozone study. Journal of Geophysical Research, 106, (D4), 3559–3567

38. Hutyra LH, et al., 2014. Urbanization and the carbon cycle: Current capabilities and research outlook from the natural sciences perspective. Earth's Future, doi: 10.1002/2014EF000255.

39. Hymel KM, Small KA, Van Dender K, 2010. Induced demand and rebound effects in road transport. Transportation Research: Part B, 44, (10), 1220-1241.

40. IPCC SRES (2000), Nakićenović, N, Swart R, ed., Special Report on Emissions Scenarios: A special report of Working Group III of the Intergovernmental Panel on Climate Change (book), Cambridge University Press, ISBN 0-521-80081-1.
41. International Energy Agency, 2013. Policy Pathways: A Tale of Renewed Cities. International Energy Agency, Paris, 98 pp.
42. Jacob DJ, Winner DA, 2009. Effect of climate change on air quality. Atmospheric Environment, 43, (1), 51–63.
43. Jones C, Kammen DM, 2014. Spatial Distribution of U.S. Household Carbon Footprints Reveals Suburbanization Undermines Greenhouse Gas Benefits of Urban Population Density. Environmental Science and Technology, 48, (2), 895-902.
44. Kim J, Brownstone D, 2013. The impact of residential density on vehicle usage and fuel consumption: Evidence from national samples. Energy Economics, 40, (1), 196–206. doi:10.1016/j.eneco.2013.06.012
45. Lelieveld J, Evans JS, Fnais M, Giannadaki D, Pozzer A, 2015. The contribution of outdoor air pollution sources to premature mortality on a global scale. Nature, 525, 367-371.

46. Lu X, Salovaara J, McElroy MB, 2012. Implications of the recent reductions in natural gas prices for emissions of CO_2 from the US power sector. Environmental Science and Technology, 46, (5), 3014-3021.

47. Massachusetts Department of Environmental Protection, 2010. Massachusetts Greenhouse Gas Emissions Inventory: Preliminary 2006-2008; http://www.mass.gov/dep/air/climate/ghg08inv.pdf

48. Massachusetts Department of Revenue, 2012. Municipal Databank; http://www.mass.gov/dor/local-officials/municipal-data-and-financial-management/data-bank-reports/socioeconomic.html

49. Massachusetts Department of Transportation, 2009. Road Inventory File; http://www.massdot.state.ma.us/planning/Main/MapsDataandReports/Data/GISData.aspx

50. Massachusetts Department of Transportation, 2012. Massachusetts Travel Survey, Final Report, Appendices. Prepared for the Massachussets Department of Transportation by Nustats Research Solutions, Austin, TX. Available at: www.mass.gov/massdot/travelsurvey

51. Massachusetts Department of Transportation, 2013. Road Inventory File; http://www.massdot.state.ma.us/planning/Main/MapsDataandReports/Data/GISData.aspx

52. Massachusetts Department of Transportation, 2014. Traffic Volume Counts; http://www.massdot.state.ma.us/highway/TrafficVolumeCounts.aspx

53. McDonald BC, Gentner DR, Goldstein AH, Harley RA, 2013. Long-Term Trends in Motor Vehicle Emissions in U.S. Urban Areas. Environmental Science and Technology, 47, 10022-10031.

54. McDonald BC, McBride ZC, Martin EW, Harley RA, 2014. High-resolution mapping of motor vehicle carbon dioxide emissions. Journal of Geophysical Research: Atmosphere, 119, 5283-5298.

55. McKain K, Wofsy SC, Nehrkorn T, Eluszkiewicz J, Ehrlinger JR, Stephens BB, 2012. Assessment of ground-based atmospheric observations for verification of greenhouse gas emissions from an urban region. Proceedings of the National Academy of Sciences 109, (22), 8423-8428.

56. Mendoza D, Gurney KR, Geethakumar S, Chandrasekaran V, Zhou Y, Razlivanov I, 2013. Implications of uncertainty on regional CO_2 mitigation policies for the U.S. onroad sector based on a high-resolution emissions estimate. Energy Policy, 55, 386–395. doi:10.1016/j.enpol.2012.12.027

57. National Research Council, 2009. Driving and the Built Environment : the Effects of Compact Development on Motorized Travel, Energy Use, and

CO_2 Emissions. Committee for the Study on the Relationships Among Development Patterns and Vehicle Miles Traveled, Transportation Research Board, and National Research Council Board on Energy and Environmental Systems, Washington, DC..

58. National Research Council, 2010. Verifying greenhouse gas emissions: method to support international climate agreements. Committee on Methods for Estimating Greenhouse Gas Emissions, National Academy Press, Washington, DC.
59. Newman P, Kenworthy J, 1989. Cities and Automobile Dependence: An International Sourcebook. Gower, Aldershot, UK.
60. Noland RB, 2001. Relationships between Highway Capacity and Induced Vehicle Travel. Transportation Research: Part A, 35, 47-72.
61. Peters W, Jacobson AR, Sweeney C, Andrews AE, Conway TJ, Masarie K, Miller JB, 2007. An atmospheric perspective on North American carbon dioxide exchange: CarbonTracker. Proceedings of the National Academy of Sciences, 104, (48), 18925-18930.
62. Peylin P, Houweling S, Krol MC, Karstens U, Rödenbeck C, Geels C, Vermeulen A, et al., 2011. Importance of Fossil Fuel Emission Uncertainties over Europe for CO_2 Modeling: Model Intercomparison.

Atmospheric Chemistry and Physics, 11, (13), 6607–6622. doi:10.5194/acp-11-6607-2011.

63. Pope CA, et al., 2002. Lung cancer, cardiopulmonary mortality, and long-term exposure to fine particulate air pollution. Journal of the American Medical Association, 287, 1132-1141.
64. Rayner PJ, Raupach MR, Paget M, Peylin P, Koffi, E, 2010. A New Global Gridded Data Set of CO_2 Emissions from Fossil Fuel Combustion: Methodology and Evaluation. Journal of Geophysical Research, 115, 10.1029/2009JD013439.
65. Ritchie SG, 1986. A statistical approach to statewide traffic counting. Transportation Research Record No. 1090, pp14-21 Transportation Research Board, Washington, DC.
66. Rosenzweig C, Solecki W, Hammer SA, Mehrotra S, 2010. Cities lead the way in climate-change action. Nature, 467, 909-911.
67. Russell AG, Brunekreef BA, 2009. A focus on particulate matter and health. Environmental Science and Technology, 43, 4620-4625.
68. Schuh AE, Denning AS, Corbin KD, Baker IT, Uliasz M, Parazoo N, Andrews AE, Worthy DEJ, 2010. A Regional High-resolution Carbon Flux

Inversion of North America for 2004. Biogeosciences, 7, (5), 1625–1644. doi:10.5194/bg-7-1625-2010.

69. Shrank D, Lomax T, Eiselle B, 2011. The 2011 Urban Mobility Report. Texas Transportation Institute, Texas A&M University, College Station, TX; http://mobility.tamu.edu/ums/

70. Shrank D, Lomax T, Eiselle B, 2012. The 2012 Urban Mobility Report. Texas Transportation Institute, Texas A&M University, College Station, TX; http://mobility.tamu.edu/ums/

71. Shu Y, Lam N, Reams M, 2010. A new method for estimating carbon dioxide emissions from transportation at fine spatial scales. Environmental Research Letters, 5, 1-9.

72. Sims R, et al., 2014. Climate Change 2014: Mitigation of Climate Change. Contribution of Working Group III to the Fifth Assessment Report of the Intergovernmental Panel on Climate Change [Edenhofer, O., et al. (eds.)]. Cambridge University Press, Cambridge, United Kingdom and New York, NY, USA.

73. Sjodin A, Persson K, Andreasson K, Arlander B, Galle B, 1998. On-road emission factors derived from measurements in a traffic tunnel. International Journal of Vehicle Design, 20, 147-158.

74. Small KA, Van Dender K, 2007. Fuel efficiency and motor vehicle travel: The declining rebound effect. Energy Journal, 28, (1), 25-51.

75. Solomon S, Qin D, Manning M, Chen Z, Marquis M, Avery KB, Tignor M, Miller HL, Eds., 2008. Climate Change 2007: The Physical Science Basis. Contribution of Working Group I to the Fourth Assessment Report of the Intergovernmental Panel on Climate Change. Cambridge University Press, Cambridge, United Kingdom and New York, NY, USA, pp 996.

76. Steiner AL, Tonse S, Cohen RC, Goldstein AH, Harley RA, 2006. Influence of future climate and emissions on regional air quality in California. Journal of Geophysical Research, 111, (D18), D18303. http://doi.org/10.1029/2005JD006935

77. Thurston GD, et al., 2013. In National Particle Component Toxicity (NPACT) Initiative: Integrated Epidemiologic and Toxicologic Studies of the Health Effects of Particulate Matter Components (eds Lippmann, M. et al.), 127-166. Health Effects Institute Research Report 177, Boston, 2013.

78. Tuomisto JT, Wilson A, Evans JS, Tainio M, 2008. Uncertainty in mortality response to airborne fine particulate matter: Combining European air pollution experts. Reliability Engineering and System Safety, 93, (5), 732-744.

79. United Nations, Department of Economic and Social Affairs, Population Division, 2014. World Urbanization Prospects: The 2014 Revision, CD-ROM Edition.

80. U.S. Census Bureau, 1982-2002. Vehicle Inventory and Use Survey, Washington, DC; https://www.census.gov/svsd/www/vius/products.html

81. U.S. Census Bureau, 1990. Commuting and Journey to Work Data, 1990 Travel to Work Characteristics for the 50 Largest Cities in the United States by Population, Washington, DC; https://www.census.gov/hhes/commuting/data/commuting.html

82. U.S. Census Bureau, 2002. Census 2000 Urban and Rural Classification, Washington, DC; https://www.census.gov/geo/reference/ua/urban-rural-2000.html

83. U.S. Census Bureau, 2010. American Community Survey 5-year Estimates, Table S0802; 2000 Census SF3 Sample Data, Table P030; factfinder2.census.gov.

84. U.S. Census Bureau, 2012. TIGER/Line shapefiles, Washington DC;

    a. http://www.census.gov/geo/maps-data/data/tiger-line.html

85. U.S. Department of Energy, 2011. Transportation Energy Data Book, 30th Edition, Energy Efficiency and Renewable Energy, Washington, DC; http://cta.ornl.gov/data/index.shtml

86. U.S. Environmental Protection Agency, 2008. National Emissions Inventory 2008, Washington, DC; http://www.epa.gov/ttn/chief/net/2008inventory.html.

87. U.S. Environmental Protection Agency, 2010a. Motor Vehicle Emission Simulator (MOVES 2010b), Washington, DC; http://www.epa.gov/otaq/models/moves/index.htm

88. U.S. Environmental Protection Agency, 2010b. MOVES2010 Highway Vehicle Temperature, Humidity, Air Conditioning, and Inspection and Maintenance Adjustments. EPA-420-R-10-027 Washington DC, December 2010; http://www3.epa.gov/otaq/models/moves/420r10027.pdf

89. U.S. Environmental Protection Agency, 2011a. Inventory of U.S. greenhouse gas emissions and sinks: 1990 – 2009, Washington, DC.

90. U.S. Environmental Protection Agency, 2011b. National Multipollutant Emissions Comparison by Source Sector. http://www.epa.gov/air/emissions/multi.htm

91. Environmental Protection Agency, 2011c. State and County Emissions Summaries. http://www.epa.gov/air/emissions/where.htm

92. U.S. Environmental Protection Agency, 2014a. Inventory of U.S. Greenhouse Gas Emissions and Sinks: 1990-2012., Report No. EPA 430-R-14-003, Washington, DC.

93. U.S. Environmental Protection Agency, 2014b. Motor Vehicle Emission Simulator (MOVES 2014), Washington, DC; http://www.epa.gov/otaq/models/moves/index.htm

94. U.S. Environmental Protection Agency, 2014c. Near Roadway Pollution and Health. http://www.epa.gov/otaq/documents/nearroadway/420f14044.pdf

95. West B, McGill R, Sluder S, 1999. Development and validation of light-duty vehicle modal emissions and fuel consumption values for traffic models. Report No. FHWA-RD-99-068, Federal Highway Administration, McLean, VA.

96. Xia Y, Mitchell K, Ek M, Sheffield J, Cosgrove B, Wood E, et al., 2012. Continental-scale water and energy flux analysis and validation for the North American Land Data Assimilation System project phase 2 (NLDAS-2): 1. Intercomparison and application of model products. Journal of

Geophysical Research, 117, (D3), D03109. http://doi.org/10.1029/2011JD016048

97. Zhou Y, Gurney KR, 2011. Spatial Relationships of Sector-specific Fossil Fuel CO_2 Emissions in the United States. Global Biogeochemical Cycles, 25, (3), GB3002, pp 13: DOI 10.1029/2010GB003822.

98. Zhu Y, Hinds WC, Kim S, Shen S, Sioutas C, 2002. Study of ultrafine particles near a major highway with heavy-duty diesel traffic. Atmospheric Environment, 36, 4323-4335.

99. Zwack LM, Paciorek CJ, Spengler JD, Levy, JI, 2011a. Modeling Spatial Patterns of Traffic-Related Air Pollutants in Complex Urban Terrain. Environmental Health Perspectives 119:852–859

100. Zwack LM, Paciorek CJ, Spengler JD, Levy, JI, 2011b. Characterizing local traffic contributions to particulate air pollution in street canyons using mobile monitoring techniques. Atmospheric Environment, 45, 2507-2514